Cincotta, Joseph John

PROXIMATE CHARGE CATALYSIS

City University of New York PH.D. 1983

PLEASE NOTE:

In all cases this material has been filmed in the best possible way from the available copy. Problems encountered with this document have been identified here with a check mark __✓__.

1. Glossy photographs or pages _____
2. Colored illustrations, paper or print _____
3. Photographs with dark background _____
4. Illustrations are poor copy _____
5. Pages with black marks, not original copy __✓__
6. Print shows through as there is text on both sides of page _____
7. Indistinct, broken or small print on several pages __✓__
8. Print exceeds margin requirements _____
9. Tightly bound copy with print lost in spine _____
10. Computer printout pages with indistinct print _____
11. Page(s) _____ lacking when material received, and not available from school or author.
12. Page(s) _____ seem to be missing in numbering only as text follows.
13. Two pages numbered _____. Text follows.
14. Curling and wrinkled pages __✓__
15. Other _____

PROXIMATE CHARGE CATALYSIS

by

JOSEPH JOHN CINCOTTA

A dissertation submitted to the Graduate Faculty in Chemistry in partial fulfillment of the requirements for the degree of Doctor of Philosophy, The City University of New York.

1983

This manuscript has been read and accepted for the Graduate Faculty in Chemistry in satisfaction of the dissertation requirement for the degree of Doctor of Philosophy.

3/8/83
date

Chairman of Examining Committee

8 March 83
date

Executive Officer

Howard Hendrickson

Herman E. Zieger
Supervisory Committee

The City University of New York

Abstract

The aminolysis rate constants have been determined for the esters p-nitrophenyl-γ-trimethylammonium butyrate fluoborate (IV) and p-nitrophenyl hexanoate(VI), with the amines tetra-n-butylammonium taurinate, TBAT(V), and benzylamine in both 95.3 mole % dioxane-water (D-W) and water at 25 °C. Second order hydrolysis rate constants (solv. H_2O) were also determined for each ester in the presence of hydroxide ion.

The aminolysis reactions which involved at least one uncharged reactant followed second order kinetics (rate = k[ester][amine]) in D-W. The reaction of charged ester (IV) with TBAT(V) in D-W was found to obey the following two term rate law: rate = k_1[RIP] + k_2[RIP][TBAT]. Pre-equilibrium formation of a reacting ion pair (RIP) between IV and V, is proposed to occur prior to the formation of the tetrahedral intermediate. The value of this ion pair equilibrium constant was determined to be 1.4. The rate determining breakdown of the tetrahedral intermediate was observed to occur by either of two pathways. One pathway (k_1) involved direct breakdown of the intermediate to its corresponding amide and p-nitrophenol, while the other pathway (k_2) involved proton transfer from the intermediate to a second molecule of amine prior to its breakdown (this accounts for dependence of k_2 on the TBAT concentration). The individual rate constants k_1 and k_2 for this

special case were found to be 1.880 ($\pm$ 0.20) x 10^{-2} sec^{-1} and 41.15 $\pm$ 0.75 liter $mole^{-1}sec^{-1}$ respectively. The catalytic influence, of pre-equilibrium complex formation between the charged reactant molecules (via electrostatic attraction) in D-W has been estimated to be > 10^2.

In Part II of this work, the equilibrium expression associated with the proton transfer from p-nitrophenol to TBAT(V) in 95.3 mole % dioxane-water was found to consist of two distinct equilibria (K and K_d). The initial equilibrium (K) involved proton transfer to the amine, and formation of a small ion aggregate. The subsequent equilibrium (K_d) involved the dissociation of this ion aggregate into p-nitrophenoxide-tetra-n-butylammonium ion pair and taurine (zwitterion). The equilibrium constants for K and K_d were evaluated and found to be 3.5727 $\pm$ 0.0746 liter $mole^{-1}$ and 1.7304 ($\pm$ 0.168) x 10^{-7} mole $liter^{-1}$ respectively.

To Clarissa, whose love, patience,
and support, was one constant I
could always depend on.

Acknowledgments

I would like to express my sincere thanks to Professor Paul Haberfield for his guidance, acessibility, understanding, and patience throughout the course of this work. I am proud to have worked under such a fine research chemist, and his lessons will never be forgotten.

I further wish to thank Mr. Steven Greenberg for making available both his time and expertise with "Unix" text editing during the preparation of this manuscript; and Dr. Russell Selzer for making available his expertise in the stopped-flow measurements used in this work.

SUBJECT PAGE

Part I

SUBJECT PAGE

SUBJECT PAGE

SUBJECT PAGE

SUBJECT PAGE

Part II

SUBJECT PAGE

Appendix

PAGE

List of Tables

Part I

PAGE

Part II

PAGE

List of Figures, Schemes, and Graphs

Part I

Part II

Introduction

Enzymatic Reactions

A typical enzymatic reaction is generally considered to proceed through formation of an enzyme-substrate (ES) complex, which further reacts to products and free enzyme (equation 1) (1).

$$E + S \;\langle\!=\!=\!=\rangle\; ES \;\longrightarrow\; E + P \qquad \text{(eqn 1)}$$

The ES complex involves the substrate being held in close proximity to key functional groups comprising the enzyme active site. Proximity and orientation effects of these functional groups have been thought to be a major factor in the efficiency of enzymes (2-5).

The only means of determining the kinetic importance of the juxtaposition of functional groups at the active site is through the study of reactions occurring intramolecularly or via pre-equilibrium complex formation.

Intramolecular Catalysis

Systems designed to assess the kinetic importance of intramolecular participation of acidic and basic groups in ester and amide hydrolysis have been considered simple models of hydrolytic enzymes (6,7). These intramolecular models mimic enzymatic systems in their ability to bring together reactive functionalities within a single molecule (Proximity effect).

Intramolecular nucleophilic attack on esters and amides by various nucleophiles has been extensively studied (1,8-15). The efficiency of a nucleophile in an intramolecular reaction is often expressed as the "effective molarity" of the neighboring group (15). The effective molarity can be calculated by dividing the first order rate constant (sec^{-1}) determined for the intramolecular reaction, by the second order rate constant ($1mole^{-1}sec^{-1}$) for the analogous bimolecular reaction (which follows the same mechanism). The ratio of rate constants has the units of molarity and is described as the hypothetical concentration of nucleophile necessary in the bimolecular reaction to give a pseudo-first order rate constant equivalent to the true rate constant for the intramolecular reaction. The effective molarity is a measure of the rate enhancement due to the juxtaposition of the nucleophile to the carbonyl group of the ester or amide. A few examples of the magnitudes of these effective molarities are given below.

Intramolecular nucleophilic attack by a neighboring carboxylate ion on phenyl esters gives rate enhancements of 10^7-10^8 M (14).

The amino group of phenyl N-(2-aminophenyl)-N-methylcarbamate I (equation 2) has an effective molarity of 3×10^8 M when compared to the bimolecular attack of amine on phenyl N-(4-aminophenyl)-N-methylcarbamate (15).

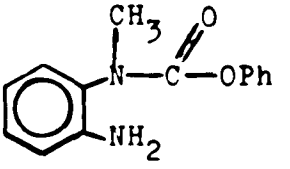

(I)

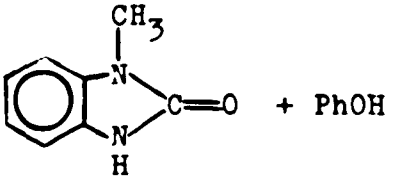

(eqn 2)

The effective molarity determined for the neutral amine nucleopnile was 5 x 10^3 M in the case of the dimethylamino group of p-nitrophenyl-γ-dimethylamino butyrate (II) (7).

$$(CH_3)_2NCH_2CH_2CH_2COOC_6H_4NO_2\text{-}p$$

(II)

These results along with numerous others cited in the references above give an indication of the dramatic acceleration possible due to the proximity of reactive functionalities.

Electrostatic Catalysis

Pre-equilibrium complex formation of substrates by enzyme models (molecules or polymers containing functional groups similar to those found at the enzyme active site) has come under investigation in the last twenty years (16-36). Of particular interest to me was substrate binding to polymeric catalysts by electrostatic interaction. It was shown by Letsinger (19) that a partially protonated poly (4-vinyl pyridine) in ethanol-water served as an effective catalyst, relative to 4- picoline, non-protonated

polymer, or highly protonated polymer, for the solvolysis of 3-nitro-4-acetoxy benzenesulfonate ion (an anionic ester). The rate enhancement found for the polymer catalyzed reaction was rationalized on the basis that protonated nitrogen sites were available to catalyze the solvolysis. He estimated the solvolytic rate at $\alpha = 0.6$ (α is the fraction of nitrogen present as the free base) to be enhanced by a factor of eighty as a consequence of electrostatic association.

Overberger (20,21,26,28,30,31,33,34) found similar electrostatic catalysis was possible for a variety of other polymers and copolymers. One such example of electrostatic catalysis was found using the copolymer of 4(5)-vinyl imidazole and acrylic acid (0.77 : 1 molar ratio, respectively) in 25.8 % ethanol-water (28,33). The esterolytic action of the polymer was tested with neutral, negatively and positively charged esters. They were p-nitrophenyl acetate, 4-acetoxy-3-nitrobenzoic acid, and 3-acetoxy-N-trimethylanilinium iodide, respectively. At high pH the copolymer showed marked selectivity toward the positively charged ester. These results were explained on the basis of electrostatic attraction of the cationic ester to the negatively charged sites of the copolymer, which allowed the imidazole groups to catalyze the solvolysis. Strong electrostatic replusion between the copolymer and the ester carboxylate anion depressed the rate of

imidazole catalysis.

From the two examples above, one can get an indication of how pre-equilibrium complex formation via electrostatic interactions can accelerate reactions.

Aminolysis Reactions in Aprotic Solvents

Enzymes exist in aqueous solution, but recent X-ray crystallographic studies clearly demonstrate the active sites of hydrolytic enzymes contain hydrophobic regions (36,37). Since rather low concentrations of water exist at these catalytic centers, the medium of enzyme catalyzed nucleophilic reactions of carboxylic acid derivatives may be apolar in nature (38).

Aminolysis reactions of simple alkyl esters in aprotic organic solvents have been studied in detail in the last 15 years (39-47). A unifying mechanistic theory proposed by Menger and his coworkers suggests the operation of the mechanism shown in scheme I (39,40)

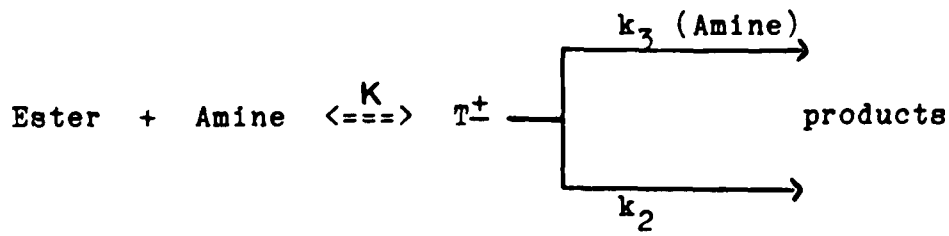

Scheme I

Scheme I accounts for the two term rate law (equation 3) usually observed for primary and secondary amines under pseudo first order conditions.

$$\text{rate} = k_2\,(\text{ester})(\text{amine}) + k_3\,(\text{ester})(\text{amine})^2 \qquad \text{(eqn 3)}$$

Menger proposed that the breakdown of the dipolar tetrahedral intermediate ($T^{\pm}$) was the rate-limiting step of ester aminolysis in aprotic solvents from the following evidence.

1) The reactions of esters with amines in aprotic solvents such as chlorobenzene and acetonitrile were more sensitive to substituents on the leaving group of the ester (ρ = 4-6), than to substituents on the acyl portion (ρ = 1-2). This was the reverse order of sensitivity found in reactions of esters with hydroxide ion in water.

2) Tetra-n-hexylammonium benzoate (THAB) catalyzes aminolysis reactions of esters by piperidine in hydrocarbon solvents (in toluene, benzoate ion is a 10^3 better proton acceptor than piperidine (pK_b = 2.88)). Menger claims that this acceleration arises from removal of a proton residing on the nitrogen of the dipolar tetrahedral intermediate by benzoate ion, which facilitates its collapse to products. As the concentration of THAB in the reaction mixture was increased the observed rate of aminolysis increased steadily, until at high THAB concentrations the rate leveled off and no longer increased with increased

concentrations of THAB. This leveling off of observed rate at high THAB concentrations indicated a change in the rate determining step. The collapse of the tetrahedral intermediate is so fast at high THAB concentrations that formation of the intermediate becomes rate determining.

A possible structure for this intermediate would be (III).

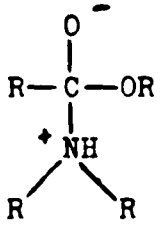

(III)

A second molecule of amine could assist in transfer of the proton in (III), thereby leading to the third order rate constant (k_3).

In this work I plan to examine the influence that complex formation via electrostatic attraction (ion-pair formation) will have on the reaction of other functional groups within the reactant molecules in solvents of low dielectric constant. As far as I know, no similar work has been undertaken.

The Effects of Electrostatic Interaction of Reactant Molecules on Reaction Rates.

Objective

The purpose of this investigation is to gather evidence in support of our supposition that, complex formation via electrostatic interaction (ion pair formation) between reactant molecules will facilitate any subsequent reaction between them. The structural prerequisites of these reactant molecules call for each to consist of a charged functional group (non-reactive) connected indirectly to a second functional group (reactive). In order to maximize the electrostatic interaction between reactant molecules, the reaction will be run in a solvent of low dielectric constant. A general scheme proposed for this type of reaction can be found in scheme 2.

$$A^+ + B^- \quad \overset{K}{\langle ==\!=\rangle} \quad A^+ \text{---} B^- \quad \overset{k}{\text{---}\rangle} \text{ Products}$$

Scheme 2.

The initial step in Scheme 2 is the equilibrium for ion pair formation (A^+---B^-) between reactant molecules. Once formed the ion pair can react to yield products.

Selection of Reactants and Solvent

In order to gather kinetic evidence in support of our hypothesis, I chose to study the aminolysis of p-nitrophenyl-γ-trimethylammonium butyrate fluoborate (IV)

by tetra-n-butylammonium taurinate (TBAT, V).

$$BF_4^- \ (CH_3)_3N^+CH_2CH_2CH_2COOC_6H_4NO_2\text{-}p$$

(IV)

$$Bu_4N^+ \ ^-O_3SCH_2CH_2NH_2$$

(V)

The solvent in which I chose to carry out this reaction in was 95.3 mole % dioxane-water, which has a dielectric constant (D) of 2.53 at 25 °C (48). This solvent was ideal because of its ability to dissolve sufficient amounts of each salt (for kinetic analysis) at such an extremely low dielectric constant.

From Menger's (39,40) work in aprotic organic solvents (see introduction for details), aminolysis reactions were found to obey a two term rate law (equation 3.1).

$$\text{rate} = k_2(\text{ester})(\text{amine}) + k_3(\text{ester})(\text{amine})^2 \quad \text{(eqn. 3.1)}$$

Since 95.3 mole % dioxane-water contains a fairly high concentration of water (0.556 M), the third order term in equation 3.1 (the second molecule of amine assists in proton transfer in the tetrahedral intermediate) should be negligible, and aminolysis reactions proceed through simple second order kinetics.

Control Reactions

Control reactions utilizing an uncharged ester and amine were also studied in 95.3 mole % dioxane-water, in order to form a basis for comparison. It was decided that p-nitrophenyl hexanoate (VI) and benzylamine (VII) would be suitable for this purpose.

$$CH_3CH_2CH_2CH_2CH_2COOC_6H_4NO_2\text{-}p$$

(VI)

$$C_6H_5CH_2NH_2$$

(VII)

This decision was based on structural similarities in the former case, and comparable pK_bs in water (benzylamine = 4.65 (49); taurinate = 4.94 (50)) for the latter case.

In order to determine aminolysis rates of each ester (IV and VI) in the absence of ion pairing, each reaction was carried out in a polar solvent. The solvent chosen for this purpose was water. At this point I will discuss the results I obtained in water, followed immediately, by my results and discussion in 95.3 mole % dioxane-water.

Results of Rate Constant Determinations for Aminolysis Reactions in Water

In order to determine the aminolysis rates in the absence of possible ionic interactions between reactants

(ion pair formation), each aminolysis reaction was studied in water. Investigation of the literature concerning aminolysis of esters in water (7), along with my kinetic results and product analyses, led me to use the following two term rate law.

$$\text{rate} = k_{am}[\text{ester}][\text{amine}] + k_{OH}[\text{ester}][OH^-] \qquad \text{(eqn 4)}$$

A study of the reaction rate data reveals that competition is occurring between both aminolysis (k_{am}) and hydrolysis (k_{OH}) of ester. The overall rate of consumption of ester was measured spectrophotometrically (400 nm) by the appearance of p-nitrophenoxide ion. The experimental data however, proved to be insufficient for the proper evaluation of each rate constant (k_{am} and k_{OH}). It therefore became necessary to determine the hydrolysis rate constant (k_{OH}) in a separate experiment (independent of aminolysis).

Hydrolysis rate constants were determined for each ester (IV and VI) in an aqueous Na_2CO_3 buffer solution, as a source of hydroxide ion. The second order hydrolysis rate constants were evaluated using equation 4.1, and listed in Table 1.

$$\text{rate} = k_{OH}[\text{ester}][OH^-] \qquad \text{(eqn 4.1)}$$

Once the hydrolysis rate constant was determined for each ester, the aminolysis rate constant was evaluated using

equation 4 (see experimental for details). The results are also listed in Table 1.

TABLE 1 Second Order Rate Constants for Aminolysis and Hydrolysis of Esters IV and VI in Water (25 °C)

Ester	Nucleophile	second order rate constant ($l mole^{-1} sec^{-1}$)[h]
IV	OH^-	60 ± 2.4[a]
IV	Benzylamine	2.84 ± 0.14[b]
IV	Taurinate [g]	1.54 ± 0.12[c]
VI	OH^-	5.50 ± 0.20[d]
VI	Benzylamine	1.26 ± 0.04[e]
VI	Taurinate [g]	0.383 ± 0.004[f]

a) average of 5 runs at Na_2CO_3 conc. of 4.449×10^{-4} - 9.323×10^{-3} M.

b) average of 6 runs at amine conc. of 2.008×10^{-4} - 1.136×10^{-3} M.

c) average of 4 runs at amine conc. of 3.183×10^{-4} - 2.122×10^{-3} M.

d) average of 3 runs at Na_2CO_3 conc. of 4.449×10^{-3} - 4.449×10^{-2} M.

e) average of 6 runs at amine conc. of 5.679×10^{-4} - 5.02×10^{-3} M.

f) average of 4 runs at amine conc of 1.302×10^{-3} - 1.061×10^{-2} M.

g) as the sodium salt.

h) uncertainties given as standard deviation of the mean

The results in Table 1 show an eleven fold increase in the hydrolysis rate constant (k_{OH}) when the quaternary ammonium group is present in the molecule (charged ester IV). Aminolysis rate constants (k_{am}) however, are accelerated by a factor of only 2.3 for benzylamine and 4 for the taurinate runs in the presence of the quaternary ammonium group.

Since the through bond inductive effects of the quaternary ammonium group will be identical for aminolysis and hydrolysis of charged ester IV, the disparity between the magnitudes of the rate enhancements for hydrolysis and aminolysis must be due to an electrostatic interaction.

Intramolecular Electrostatic Catalysis in Water

I propose that this rate acceleration is due to intramolecular electrostatic catalysis, as found in structure VIII.

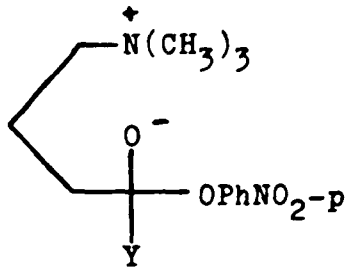

(VIII)

Y = Nucleophile

The six member cyclic intermediate VIII, depicts charge stabilization of the tetrahedral intermediate formed during nucleophilic attack. Electrostatic interaction between the positively charged quaternary ammonium group and the developing negative charge on the carbonyl oxygen is responsible for the rate acceleration. The magnitude of this acceleration should be identical for both aminolysis and hydrolysis reactions, unless the formation of the cyclic intermediate is sterically hindered.

When molecular models (Fisher-Taylor-Hirshfelder) were constructed for each tetrahedral intermediate VIII (where Y = OH, $H_2NCH_2C_6H_5$, and $H_2NCH_2CH_2SO_3^-$), they showed that relative to hydroxide, the benzylamine and taurinate groups sterically hindered the approach of the quaternary ammonium group to the negatively charged carbonyl oxygen (benzylamine >> taurinate). Since formation of the cyclic intermediate VIII was highly strained when benzylamine was the nucleophile, the 2.3 fold rate enhancement of charged ester IV over p-nitrophenyl hexanoate (VI) must be assumed to be substantially due to through-bond induction of the quaternary ammonium group, with little if any through-space electrostatic interaction. Thus, the rate enhancement estimated for charged ester IV owing to a purely inductive effect, is only a maximum of 2.3 fold. This is a reasonable conclusion since the quaternary ammonium group contributes an approximately 5 fold rate enhancement for

the alkaline hydrolysis of acetylcholine (IX) (51).

$$(CH_3)_3^+NCH_2CH_2OOCCH_3$$

(IX)

If one assumes the inductive effect of the quaternary ammonium group in charged ester IV, to increase the rate of nucleophilic attack on the carbonyl carbon by a maximum of 2.3 fold (through-bond induction), then the through-space electrostatic catalysis contributes a 1.7 fold rate enhancement for aminolysis by taurinate, and a 4.8 fold rate enhancement for hydrolysis. These rate enhancements may seem small, but one must realize that to witness any through-space electrostatic interaction in water is exciting. Other studies involving charge stabilization of a tetrahedral intermediate in protic and aprotic solvents have been found in the literature. Some examples are reviewed in the following section.

Charge Stabilization of a Tetrahedral Intermediate in Protic and Aprotic Solvents

Rate enhancement due to charge stabilization of the tetrahedral intermediate formed during nucleophilic attack by a neighboring quaternary ammonium group has been previously observed in polar protic and dipolar aprotic solvents.

Lazarus and Benkovic (52) demonstrated, that in-

tramolecular electrostatic catalysis had occurred in water for the alkaline hydrolysis of the phosphotriester (X) when compared to (XI).

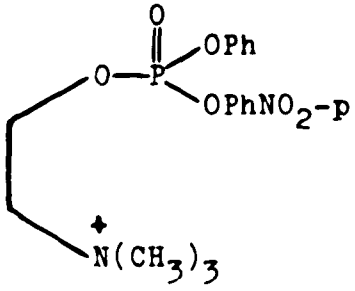

(X)

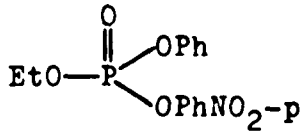

(XI)

After compensating for the through-bond induction, there remained a 3 fold rate enhancement for hydrolysis of (X) which was attributed to the juxtaposition of the positive charge to the developing negative charge on the oxygen. This deduction was supported by the observation, that the rate of nucleophilic attack by anions on (X) was markedly accelerated by increasing the dioxane content in the aqueous solvent, whereas (XI) remained unchanged or slightly decreased.

While measuring rates of alkaline hydrolysis of a series of meta- and para- substituted ethyl-β-phenylpropionates in 87.8% ethanol-water, Fuchs and Caputo (53) found that the m-$(CH_3)_3N^+$ ester yielded an unexpectedly higher rate constant than would be attributed to the slightly shorter inductive pathway (compared to para iso-

mer). They attributed this to the high reactivity of a few molecules that exist in conformation XII at any given time, and would allow stabilization of the transition state formed from hydroxide attack (XIII).

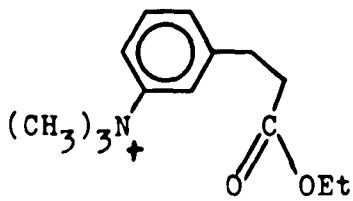

(XII)

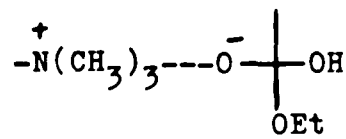

(XIII)

P.Y. Bruice and H. Mautner (54) found rate enhancement during hydrolysis of benzoylcholine (XIV) in aqueous buffer solution (pH > 11).

$$C_6H_5COOCH_2CH_2N^+(CH_3)_3$$

(XIV)

They also claim that this phenomenon is due to electrostatic interaction between the positive charge on the nitrogen and the developing negative charge on the carbonyl oxygen, which results in transition state stabilization.

Hajdu and Smith (55) presented evidence for considerable electrophilic activation (approximately 1000 fold) of the carbonyl group by the quaternary ammonium group of 2-[(p-nitrophenoxy)carbonyl]benzyl- trimethylammonium bromide (XV) in acetonitrile.

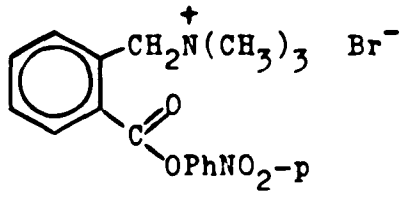

(XV)

Aprotic organic solvents allow considerably greater electrostatic interactions than aqueous solvent systems.

Results of Rate Constant Determinations for Aminolysis Reactions in 95.3 Mole % Dioxane-Water

The kinetic data obtained in 95.3 mole % dioxane-water (0.556 M in water), at amine concentrations at least 10 times less than the ambient water concentration, have shown the rate equation to consist of a single second order term (with exception of the reaction of IV and V).

$$\text{Rate} = k_2 \text{ (Ester)(Amine)} \qquad \text{(eqn 5)}$$

These results were verified at two amine concentrations and by separate product analysis runs which yielded 100% recovery of product amides. Table 2 contains second order aminolysis rate constants for each ester (with the exception of charged ester IV and TBAT (V)).

TABLE 2 Second Order Rate Constants (k_2) for Aminolysis Reactions in 95.3 Mole % Dioxane-Water (25°C).

Ester	Amine	k_2 ($lmole^{-1}$ sec^{-1})[d]
IV	Benzylamine(VII)	0.242[a] ± 0.008
VI	TBAT(V)	0.682[b] ± 0.024
VI	Benzylamine(VII)	0.00421[c] ± 0.00024

a) average of six runs determined over amine conc. range of 2.52×10^{-3} - 3.0×10^{-2} M.

b) average of five runs determined over amine conc. range of 1.53×10^{-3} - 1.400×10^{-2} M.

c) average of five runs determined over amine conc. range of 5.00×10^{-3} - 5.00×10^{-2} M.

d) uncertainties given as the standard deviation of the mean

The aminolysis of charged ester IV by TBAT (V) was found to be too fast for conventional kinetic measurement, and initial rates were therefore determined by the stopped-flow technique. This special case did not follow simple second order kinetics, and is throughly discussed in the following section.

The Aminolysis of p-Nitrophenyl-γ-Trimethylammonium Butyrate Fluoborate (IV) by Tetra-n-Butylammonium Taurinate (TBAT,V) in 95.3 Mole % Dioxane-Water

I propose that the reaction of charged ester IV with TBAT (V) in 95.3 mole % dioxane-water (D = 2.53, 25 °C) proceeds through the route depicted in Scheme 3.

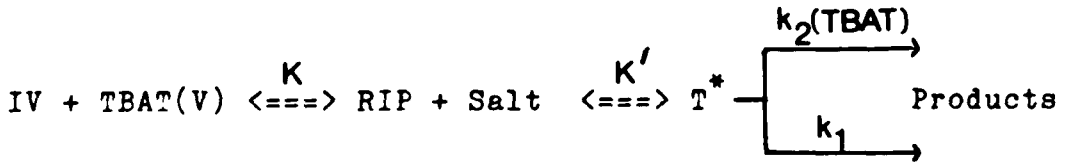

Scheme 3

RIP = p-nitrophenyl-γ-trimethylammonium butyrate - taurinate ion pair

Salt = tetra-n-butylammonium fluoborate ion pair

T^* = quadrupolar tetrahedral intermediate

Each pathway (k_1 or k_2) in Scheme 3 leads to formation of identical products (N-(2-ethylsulfonate)-γ-trimethylammonium butyramide ($(CH_3)_3N^+CH_2CH_2CH_2CONHCH_2CH_2SO_3^-$), p-nitrophenoxide ion, taurine ($H_3^+NCH_2CH_2SO_3^-$) and p-nitrophenol).

The mechanism I proposed in Scheme 3, is quite similar to the one proposed by Menger (39,40) for aminolysis of esters in aprotic organic solvents. Since both mechanisms include a rate determining step in which a second

molecule of amine assists in proton removal from the tetrahedral intermediate, I will consider the breakdown of the tetrahedral intermediate in my mechanism to be rate determining as does Menger in his (see introduction for evidence Menger used in forming this conclusion). The only difference in the mechanism that I propose from that of Menger's is the counterion exchange equilibrium (K) which precedes formation of my tetrahedral intermediate (T^*). This equilibrium is responsible for the formation of the reacting ion pair (RIP).

From the results of a separate investigation of the p-nitrophenol-p-nitrophenoxide equilibrium constant (see Part II of this work) in the presence of TBAT (V), I found that "free" ions or large ion aggregates do not exist as independent kinetic species in 95.3 mole % dioxane-water. In accord with my derived equilibrium expression, every ionic species exists as a member of an ion pair, and therefore, ion pairs are treated as single kinetic species.

The reacting ion pair (RIP) will therefore be treated as a single kinetic species throughout all further kinetic evaluations.

Derivation of RIP Concentration

An equation can now be written expressing K (Scheme 3) as a function of the initial charged ester (IV) and amine (V) concentrations, and the equilibrium concentration

of RIP (assuming that during the initial stages of the reaction [RIP] = [Salt]).

$$K = \frac{[RIP]^2}{[E_{stoi} - RIP][A_{stoi} - RIP]} \qquad \text{(eqn 5.1)}$$

RIP = reacting ion pair concentration

E_{stoi} = initial concentration of charged ester (IV)

A_{stoi} = initial concentration of TBAT (V)

The concentration of RIP at any given value of K, can be expressed by equation 5.2.

$$[RIP] = \frac{-K[E_{stoi} + A_{stoi}]}{2(1 - K)} \pm \frac{\sqrt{K^2[E_{stoi} + A_{stoi}]^2 + 4K(1 - K)(E_{stoi})(A_{stoi})}}{2(1 - K)}$$

(eqn 5.2)

For the special case when K equals one, equation 5.1 reduces to the following simple expression for the RIP concentration.

$$[RIP] = \frac{[E_{stoi}][A_{stoi}]}{[E_{stoi} + A_{stoi}]} \qquad \text{(eqn 5.3)}$$

The Tetrahedral Intermediate

Scheme 3 proceeds through equilibrium formation of the quadrupolar tetrahedral intermediate found in figure 1.

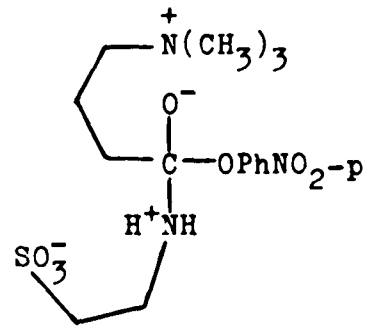

Figure 1

One stable conformation of this quadrupolar tetrahedral intermediate would allow through-space electrostatic interactions between the negatively charged carbonyl oxygen and the quaternary ammonium group. In addition a second interaction can occur simultaneously which involves a hydrogen bond between a sulfonate oxygen and a hydrogen bond to the secondary ammonium group. Both of these interactions occur through formation of stable six member ring structures.

Through-space electrostatic interactions have been previously shown to accelerate both aminolysis (1.7 fold) and hydrolysis (4.8 fold) of charged ester IV in water (see preceding sections). We therefore must assume a strong likelihood of this interaction occurring in 95.3 mole % dioxane-water. The contribution to the rate ac-

celeration due solely to this type of elecrostatic catalysis (Figure 1) can not be separated from other types of catalysis present during these aminolysis reactions in 95.3 mole % dioxane-water. Other factors contributing to rate acceleration (when charged reactants are present) will therefore be briefly discussed.

There exists a through-bond inductive effect of the quaternary ammonium group which will accelerate the aminolysis of charged ester IV (over uncharged ester VI) with either amine. The magnitude of this effect in 95.3 mole % dioxane-water can not be assumed equal to its magnitude previously estimated in water.

Formation of a dipolar tetrahedral intermediate from neutral reactants necessitates the formation of charge from uncharged reactants. Therefore, this process will not be favorable in solvents of low dielectric constant. In the cases where charge is already present (on either reactant) in the reaction mixture, the reactants are at a higher energy level than in corresponding neutral cases, thereby, lowering the activation energy of the process. A conclusion that can be drawn from this reasoning is that when charge is present in either reactant (or both), the rate of reaction will be faster than when charge is not present. The magnitude of the rate acceleration due to the presence of a charged amine in the reaction mixture is not necessarily equal to that of a charged ester. From the

data available, it therefore becomes impossible to separate the catalysis due to electrostatic interaction (Figure 1), through-bond induction, and lowering of the activation energy of the process in the presence of charged reactants.

At the present time there are no data bearing on the merits of a two step mechanism involving a tetrahedral intermediate over a direct displacement mechanism in aprotic organic solvents. However, the existence of addition intermediates are common in acyl transfer reactions in water (69-72). Mechanisms involving tetrahedral intermediates for ester aminolysis and methanolysis in hydroxylic solvents have been detailed by Jencks (73-76). From these observations Menger and others favor the existence of a tetrahedral intermediate in aprotic organic solvents (39, 40, 77, 78).

Determination of the Rate Expression for Aminolysis of Charged Ester IV by TBAT (V) in 95.3 Mole % Dioxane-Water

The reaction pathway depicted in Scheme 3, in which breakdown of the tetrahedral intermediate (T^*) is rate determining, would correspond to the following rate law.

$$\text{rate} = k[T^*] + k'[T^*][\text{TBAT}] \qquad \text{(eqn 6)}$$

(where [TBAT] is the free amine concentration; [TBAT] = $[\text{TBAT}_{\text{stoi}} - \text{RIP}]$)

The second order term k' in equation 6 involves a second molecule of amine accepting the proton from the nitrogen of T^* (Figure 1), thereby impairing the back reaction of the intermediate.

The equilibrium expression for K' (equilibrium for formation of T^*) in Scheme 3 can be written in the following form

$$K' = \frac{[T^*]}{[\text{RIP}]} \qquad \text{(eqn 6.1)}$$

Equation 6.1 can be rearranged to yield an expression for the T^* concentration.

$$[T^*] = K'[\text{RIP}] \qquad \text{(eqn 6.2)}$$

If we now substitute equation 6.2 into equation 6, the rate expression can be written as a function of k, k', K' and the concentrations of RIP and TBAT(V).

$$\text{rate} = kK'[RIP] + k'K'[RIP][TBAT] \qquad \text{(eqn 6.3)}$$

On combining the constants in equation 6.3, a rate expression is derived for my proposed mechanism (Scheme 3), in which the RIP concentration is crucial to the evaluation of both rate constants.

$$\text{rate} = k_1[RIP] + k_2[RIP][TBAT] \qquad \text{(eqn 6.4)}$$

Since the RIP is treated as a single kinetic species (whose concentration is a function of K and the initial ester and amine concentrations (eqn 5.2)), the k_1 rate constant has the units of sec^{-1} (first order), while the k_2 rate constant has the units of 1 $mole^{-1}sec^{-1}$ (second order).

Determination of the Counterion Exchange Equilibrium Constant (K)

Scheme 3 contains three constants (K, k_1, and k_2) that must be evaluated in order to fully explain the kinetic behavior of this reaction. This section contains two methods which we derived to evaluate the counterion exchange equilibrium constant (K). The first method consists of an empirical derivation, while the second is purely speculative.

Method 1

Comparison of the kinetic behavior of the reaction found in Scheme 3 at both extremes of amine concentration led to some interesting observations. At high amine concentrations (SF1 and SF2), doubling the amine concentration yielded only a 7.8 % difference in rate constants (assuming K = 1.4 for the time being) determined by simple second order kinetics (rate = k_2[RIP][TBAT]), while for the same runs first order kinetics (rate = k_1[RIP]) yielded rate constants that differed by 87 % (Table 3). These facts indicate that at high amine concentrations (high "free" amine concentrations), a fair approximation of the reaction rate can be calculated using a single term bimolecular rate law.

TABLE 3 First[b] and Second[a] Order Rate Constants Determined at High and Low Amine Concentrations

Run #	Ester Conc. (10^5)	Amine Conc. (10^3)	2nd Order Rate Const[a,d]	1st Order Rate Const[b,d]
SF1	4.9208	5.5322	44.58[c]	0.2444
SF2	4.9208	2.7661	48.07[c]	0.1306
K174	1.1463	0.011540	3.584×10^3	1.902×10^{-2}
K163	1.6160	0.021276	1.699×10^3	1.927×10^{-2}

a) rate = k_2 (RIP)(TBAT)

b) rate = k_1 (RIP)

c) Eight percent difference in second order rate constants due primarily to small amount of unimolecular reaction which is occurring.

d) Based on total rates calculated at K = 1.4. In each case above, K163 was the only one in which experimentally determined rates differed from calculated rate by greater than 3.2 %.

At low amine concentrations (K174 and K163) doubling the initial amine concentration yielded only a 1% difference in rate constants determined by first order kinetics (rate = k_1[RIP]), while for the same runs, second order kinetics (rate = k_2[RIP][TBAT]) yielded rate constants that differed by 110 % (Table 3). These facts clearly indicate that at very low amine concentrations (low "free" amine concentrations), the reaction rate can be approximated quite accurately using a single term unimolecular rate law. From the observations above the following generalizations can be derived.

At low amine concentrations the two term rate law proposed for the reaction in Scheme 3 can be simplified to the following single term expression.

$$\text{rate}_L = k_1[RIP_L] = k_1 f(K, A_L, E_L) \qquad \text{(eqn 7)}$$

(subscript L signifies a "low" amine concentration run (K174))

In equation 7, RIP_L is expressed as a function of the

equilibrium constant K, and the initial amine (A_L) and the ester (E_L) concentrations. The first order rate constant (k_1) can therefore be expressed as

$$k_1 = \frac{rate_L}{f(K, A_L, E_L)} \qquad \text{(eqn 7.1)}$$

At high amine concentrations the two term rate law for the proposed reaction in Scheme 3 can be simplified to the following single term expression.

$$rate_H = k_2[RIP_H][a_H] = k_2 f(K, A_H, E_H)[a_H] \qquad \text{(eqn 7.2)}$$

(subscript H signifies a "high" amine concentration run (SF5))

In equation 7.2, a_H is the "free" amine concentration. Therefore, the second order rate constant (k_2) can be expressed as

$$k_2 = \frac{rate_H}{[a_H] f(K, A_H, E_H)} \qquad \text{(eqn 7.3)}$$

At some intermediate amine concentration the two term rate law for the proposed reaction in Scheme 3 can not be simplified, and is therefore expressed as follows

$$rate_I = k_1[RIP_I] + k_2[RIP_I][a_I] \qquad \text{(eqn 7.4)}$$

(subscript I signifies some "intermediate" amine concentration run)

On substituting equations 7.1 and 7.3 into equation 7.4,

the following expression for the intermediate rate can be derived.

$$\text{rate}_I = \frac{\text{rate}_L \times f(K, A_I, E_I)}{f(K, A_L, E_L)} + \frac{\text{rate}_H \times f(K, A_I, E_I) \times a_I}{a_H \times f(k, A_H, E_H)}$$

(eqn 7.5)

Equation 5.2 (pg 22) has already been derived , which expresses the RIP concentration as a function of K and the initial amine and ester concentrations.

Attempts to solve equation 7.5 for K are fruitless due to the quadratic nature of all the functions above. However, we can calculate values of rate_I over a wide range of K values for each intermediate amine concentration run, and compare these calculated rates to the experimentally determined rates. This method would allow us to determine the best K value, by finding the minimum in the mean percent difference in calculated rate_I values from the experimentally determined rates, over all the intermediate amine concentration runs (Table 4).

TABLE 4 Mean Percent Difference [a,b] at Various K Values

K	Mean % Difference
0.05	11.3
0.2	8.54
0.8	4.63
1.1	4.29
1.3	4.15
1.4	4.09
1.5	4.11
2.0	4.22
3.0	4.63
6.0	5.48
10.0	6.14

a) $\% \text{ Diff} = \frac{\text{calc. rate}_I - \text{exper. rate}_I}{\text{exper. rate}_I} \times 100\ \%$

b) Mean of 9 intermediate amine concentration runs.

The mean % differences determined above reached a minimum at K = 1.4. Therefore, throughout the entirety of this work the value of the counterion exchange equilibrium constant (K) will be 1.4.

Method 2

A second method to determine the magnitude of K was derived from information gathered from the literature concerning dissociation constants of quaternary ammonium salts in solvents of low dielectric constant.

The equilibrium denoted by K (in Scheme 3) is merely an exchange of counterions. I will be therefore more explicit and redefine K as K_{exch} (exch = exchange) for the purposes of this derivation. Since only initial rates will be determined for this reaction, the equilibrium equation for K_{exch} can be written

$$RN^+(CH_3)_3\text{---}BF_4^- + R'SO_3^-\text{---}Bu_4N^+ \overset{K_{exch}}{\langle\!=\!=\!=\!\rangle} RN^+(CH_3)_3\text{---}R'SO_3^- + Bu_4N^+\text{---}BF_4^-$$

(eqn 8)

$$K_{exch} = \frac{[RN^+(CH_3)_3\ R'SO_3^-][Bu_4N^+\ BF_4^-]}{[RN^+(CH_3)_3\ BF_4^-][R'SO_3^-\ Bu_4N^+]}$$

(eqn 8.1)

R = p-$O_2NC_6H_5OOC(CH_2)_3$-

R' = $H_2NCH_2CH_2$-

This exchange equilibrium is only valid during the initial stages of the reaction, when product concentrations are insignificant. As product concentrations increase and compete with reactants for ion pairing sites, equation 8.1 is no longer valid. The individual dissociation equations for each ion pair found in equation 8 are

$$RN^+(CH_3)_3\text{---}R'SO_3^- \overset{K_{d1}}{\langle=\!=\!=\rangle} RN^+(CH_3)_3 + R'SO_3^- \quad \text{(eqn 9)}$$

$$Bu_4N^+\text{---}BF_4^- \overset{K_{d2}}{\langle=\!=\!=\rangle} Bu_4N^+ + BF_4^- \quad \text{(eqn 10)}$$

$$RN^+(CH_3)_3\text{---}BF_4^- \overset{K_{d3}}{\langle=\!=\!=\rangle} RN^+(CH_3)_3 + BF_4^- \quad \text{(eqn 11)}$$

$$Bu_4N^+\text{---}R'SO_3^- \overset{K_{d4}}{\langle=\!=\!=\rangle} Bu_4N^+ + R'SO_3^- \quad \text{(eqn 12)}$$

with corresponding expressions for each equilibrium constant.

$$K_{d1} = \frac{[RN^+(CH_3)_3][R'SO_3^-]}{[RN^+(CH_3)_3\text{---}R'SO_3^-]}$$

(eqn 13)

$$K_{d2} = \frac{[Bu_4N^+][BF_4^-]}{[Bu_4N^+\text{---}BF_4^-]}$$

(eqn 14)

$$K_{d3} = \frac{[RN^+(CH_3)_3][BF_4^-]}{[RN^+(CH_3)_3\text{---}BF_4^-]}$$

(eqn 15)

$$K_{d4} = \frac{[Bu_4N^+][R'SO_3^-]}{[Bu_4N^+\text{---}R'SO_3^-]}$$

(eqn 16)

On substituting equations 13, 14, 15, and 16 into equation 8.1, an expression is derived which relates K_{exch} to all the individual dissociation constants.

$$K_{exch} = \frac{(K_{d3})(K_{d4})}{(K_{d1})(K_{d2})}$$

(eqn 17)

A comparison of ion pair dissociation constants (K_d) of quaternary ammonium salts in a variety of solvents is found in Table 5.

TABLE 5 K_d Values for Ion Pair Dissociation of Quaternary Ammonium Salts in Various Organic Solvents (25 °C).

Solvent (D)[b]	Salt	K_d (M^{-1})	Reference
Anisole	$Bu_4N^+Pi^-$[c]	1.09×10^{-9}	56
(4.30)	$Et_4N^+Pi^-$	9.55×10^{-10}	56
Ethylene-	$Am_4N^+Pi^-$	2.40×10^{-4}	59
Chloride (10.23)	$Bu_4N^+Pi^-$	2.28×10^{-4}	58
	$AcChol^+Pi^-$[e]	1.96×10^{-4}	57
	$Et_4N^+Pi^-$	1.59×10^{-4}	59
	$Et_4N^+NO_3^-$	0.74×10^{-4}	59
	$Bu_4N^+NO_3^-$	1.18×10^{-4}	59
o-Dichloro-	$Bu_4N^+Pi^-$	1.92×10^{-5}	60
benzene (9.94)	$Et_4N^+Pi^-$	1.23×10^{-5}	60
Acetone (20.7)	$Me_4N^+Pi^-$	1.12×10^{-2}	61
	$Et_4N^+Pi^-$	2.23×10^{-2}	61
	$Bu_4N^+Pi^-$	1.75×10^{-2}	62
Nitrobenzene	$Me_4N^+Pi^-$	4.00×10^{-2}	63
(34.8)	$Et_4N^+Pi^-$	3.02×10^{-2}	56
	$Bu_4N^+Pi^-$	7.67×10^{-2}	56
Triphenyl-	$Me_4N^+Tos^-$[d]	0.267×10^{-8}	64
phosphite (3.75)	$Et_4N^+Tos^-$	38.64×10^{-8}	64
	$Pr_4N^+Tos^-$	37.27×10^{-8}	64
	$Bu_4N^+Tos^-$	33.36×10^{-8}	64

a) K_d corresponds to the reaction $R_4N^+X^- \langle===\rangle R_4N^+ + X^-$.

b) D signifies the dielectric constant of the solvent given by authors in reference.

c) Pi signifies Picrate.

d) Tos signifies p-toluenesulfonate.

e) AcChol = acetylcholine (IX)

A generalization that can be drawn from Table 5 is that the relative difference between dissociation constants of tetra-ethyl and tetra-n-butyl quaternary ammonium picrates decreases as you move to lower dielectric constant solvents. A comparison of Bu_4N^+, acetylcholine (IX), and Et_4N^+ picrates in ethylene chloride (D = 10.23) yields dissociation constants (K_d) of 2.28×10^{-4}, 1.96×10^{-4}, and 1.59×10^{-4} M^{-1} respectively.

$$(CH_3)_3N^+CH_2CH_2OOCCH_3$$

(IX)

There exists a 43% difference between K_d values for Bu_4N^+ and Et_4N^+ picrates, with acetylcholine picrate lying approximately midway between the two. In anisole (D = 4.30), Bu_4N^+ and Et_4N^+ picrates have dissociation constants of 1.10×10^{-9} and 9.55×10^{-10} M^{-1}, respectively. The difference between K_d values has now dropped to only 15%.

Since acetylcholine (IX) picrate has structural similarities to charged ester IV (with IV having slightly more

hydrophobic character because of the presence of the benzene ring). I therefore propose that the cation of charged ester IV will have similar electrostatic effects on a counterion as Bu_4N^+ ion, in solvents of low dielectric constant.

From this assumption the ion pair dissociation constants of Bu_4N^+ and charged ester IV salts of identical counterions should be quite similar in identical solvent systems.

This relationship between dissociation constants of each fluoborate (K_{d2} and K_{d3}) and each taurinate (K_{d1} and K_{d4}) salt can be expressed mathematically by equations 18 and 18.1, respectively.

$$K_{d2} = mK_{d3} \qquad \text{(eqn 18)}$$

$$K_{d4} = nK_{d1} \qquad \text{(eqn 18.1)}$$

Each of the above expressions include a factor m or n, which are equal to the quotients of their respective dissociation constants. From the assumptions we made above, the ratios of the dissociation constants of the fluoborate (K_{d2}/K_{d3}) and taurinate (K_{d4}/K_{d1}) salts in identical solvents should be approximately equal. Therefore, the factors m and n should be approximately equal. Substitution of equations 18 and 18.1 into equation 17 yields a K_{exch} value of 1 (eqn 19).

$$K_{exch} = \frac{K_{d3} \times nK_{d1}}{K_{d1} \times mK_{d3}} = \frac{n}{m} = 1$$

(eqn 19)

It is therefore reasonable to assume from the derivation above, that $K = 1$ is a good approximation of the counterion exchange equilibrium constant.

Determination of Rate Constants (k_1 and k_2)

Since we have determined the counterion exchange equilibrium constant K to be 1.4, this leaves only the determination of both rate constants to complete our investigation of the reaction in Scheme 3. Equation 6.4 can be rewritten in the form

$$\text{initial rate} = [RIP]\,(k_1 + k_2[TBAT]) \qquad \text{(eqn 20)}$$

(where [TBAT] = the "free" amine concentration)

By rearranging equation 20 into the form of $y = mx + b$, one can now evaluate both k_1 and k_2 from the initial ester and amine concentrations, the initial rate (determined by stopped-flow method), and the free amine concentration ($[TBAT] = TBAT_{stoi} - RIP$).

$$\frac{\text{initial rate}}{RIP} = k_2[TBAT] + k_1$$

(eqn 21)

A plot of initial rate/RIP versus the free amine con-

centration [TBAT], yields a slope of k_2 and a y-intercept of k_1. Table 6 contains experimentally determined initial rates (stopped-flow method) and calculated RIP concentrations for my kinetic runs at K = 1.4.

TABLE 6 Initial Rates of Aminolysis Reaction of Charged Ester IV by TBAT (V) in 95.3 Mole % Dioxane-Water (25 °C)

Run #	E_{stoi} (M)[e] (10^5)	A_{stoi} (M)[e] (10^3)	RIP (M)[d] (10^5)	Initial Rate[a] $Msec^{-1}$ (10^6)
SF1[b]	4.9206	5.5322	4.8896	11.947
SF2[b]	"	2.7661	4.8587	6.2773
SF3[b]	"	1.1064	4.7674	2.9964
SF4[b]	"	0.5532	4.6200	1.8870
SF5[b]	5.3332	5.9957	5.2994	13.930
SF6[b]	"	0.5996	5.0073	2.1943
SF7[b]	5.2269	2.2877	5.1424	5.9810
SF8[b]	"	3.8222	5.1761	8.7871
SF9[b]	"	1.1438	5.0596	3.5511
SF10[b]	"	1.9111	5.1260	5.2420
SF11[b]	"	0.7644	4.9791	2.0477
SF12[b]	"	0.5719	4.8991	1.4211
K174[c]	1.1463	0.01154	0.6233	0.1149
K163[c]	1.6160	0.02127	0.9938	0.2157

a) corrected for p-nitrophenol - p-nitrophenoxide equilibrium in the presence of TBAT (see equation 42 in part II of this work).

b) initial rates determined by stopped-flow method at 400 nm.

c) rates determined on Cary 17 at 310 nm over first 20% reaction.

d) RIP concentration determined at K = 1.4

e) E_{stoi} = initial charged ester IV concentration

A_{stoi} = initial TBAT (V) concentration

When K = 1.4, the values determined from a least square fit of the experimental data (equation 21) for k_2 and k_1 are 41.15 $\pm$ 0.75 l $mole^{-1}sec^{-1}$, and 1.880 $\pm$ 0.20 x 10^{-2} sec^{-1}, respectively. The error in slope and y-intercept are expressed as their standard deviation. A plot of this data can be found in Graph 1.

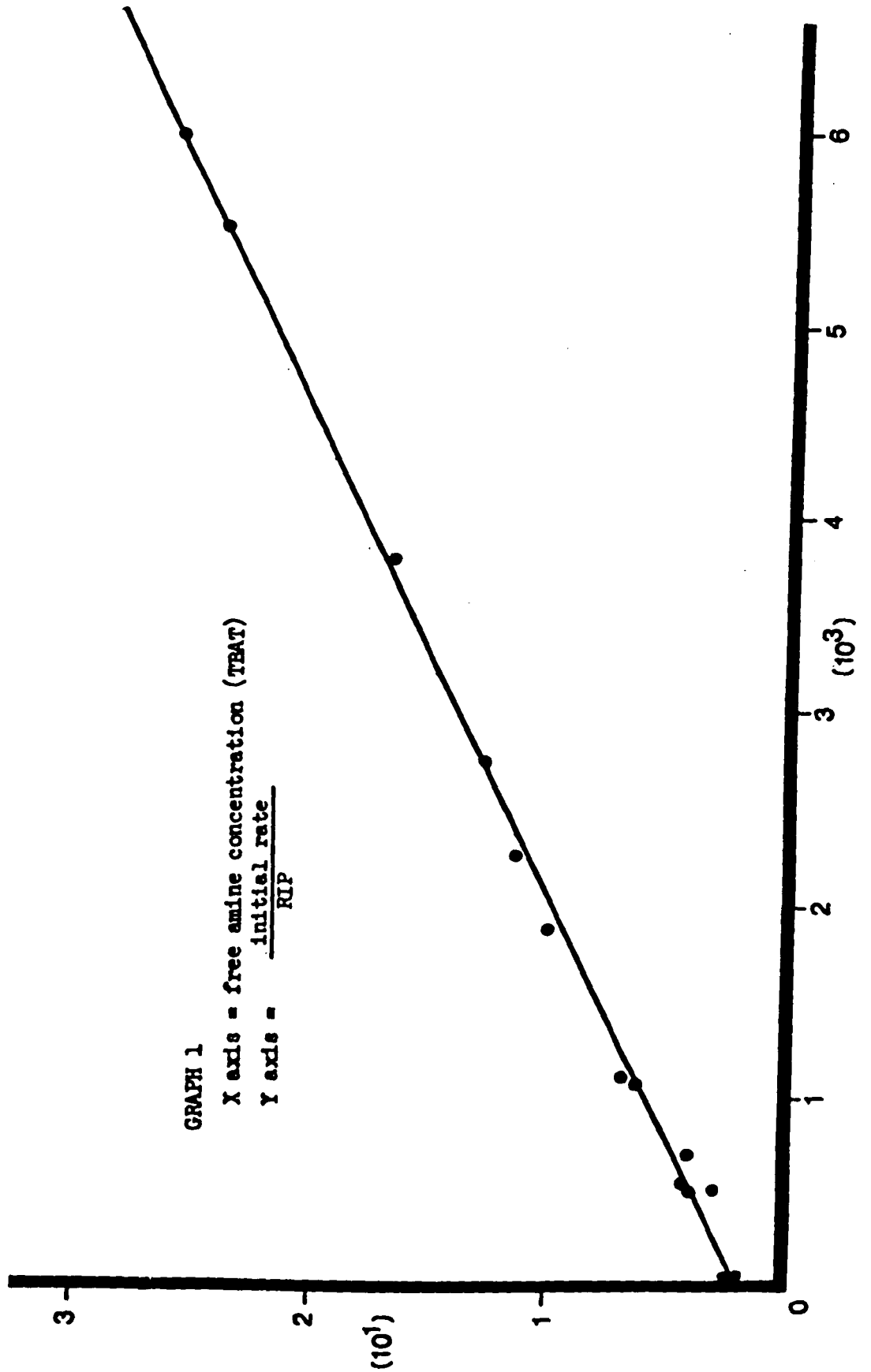
GRAPH 1
X axis = free amine concentration (TBAT)
Y axis = initial rate / RIP
0
1
2
3
4
5
6
(10³)
(10¹)

If we now recalculate k_1 and k_2 for values of K from 0.1 - 10 (Table 7), it turns out that k_2 changes only 2% over this range, while k_1 changes by a factor of 2.5.

TABLE 7 Variations in k_2 and k_1 at Various K Values.

K	$k_2^{a,b}$ ($1mole^{-1}$ sec^{-1})	$k_1^{a,b}$ (sec^{-1})(10^2)
0.10	40.82 $\pm$1.09	3.913 $\pm$0.29
1.4	41.16 $\pm$0.75	1.880 $\pm$0.20
10.0	41.53 $\pm$0.74	1.592 $\pm$0.20

a) rate = k_2 [RIP][TBAT] + k_1 [RIP]

b) k_2 and k_1 were determined by plotting initial rate / RIP verses the free amine concentration. Uncertainties given as the standard deviations of slope and y-intercept.

The apparent lack of sensitivity of k_2 to a change in K is a consequence of the second order term (k_2[RIP][TBAT]). As the RIP concentration increases (with increasing K), the TBAT concentration decreases. Therefore, each of these influences counteract the other and the k_2 term remains constant.

The 2.5 fold decrease in k_1 as we change K from 0.1 - 10 is a consequence of the first order term (k_1[RIP]). From the k_1 term the RIP concentration is expected to have a recipocal relationship to the rate constant (k_1).

Therefore, the 2.5 fold change in k_1 is approximately the average change in RIP concentration over all my runs.

In order to determine the kinetic importance of each term in equation 6.4 on the overall rate of reaction, I compared calculated rates (from calculated rate constants) of each term with the total rate (Table 8).

TABLE 8 Comparison of Single Term Rates Versus Total Calculated Rates for the Reaction of Charged Ester IV and TBAT V in 95.3 Mole % Dioxane-Water (25°C)

Run #	E_{stoi} (10^5)	A_{stoi} (10^3)	Rate k_1 term (10^7)	Rate k_2 term (10^6)	Total[a] Rate (10^6)	k_1 term as % of Total Rate
SF1	4.9206	5.5322	9.1926	11.034	11.953	7.30
SF2	"	2.7661	8.627	5.1370	5.9997	14.4
SF3	"	1.1064	8.963	2.0772	2.9735	30.1
SF4	"	0.5532	8.686	0.9640	1.8326	47.4
SF5	5.3332	5.9957	9.963	12.961	13.957	7.14
SF6	"	0.5996	9.414	1.1323	2.0738	45.4
SF7	5.2269	2.2877	9.668	4.7327	5.6995	16.7
SF8	"	3.8222	9.731	8.0318	9.0049	10.8
SF9	"	1.1438	9.512	2.2763	3.2276	29.5
SF10	"	1.9111	9.637	3.9235	4.8867	19.7
SF11	"	0.7644	9.361	1.4643	2.4004	39.0
SF12	"	0.5719	9.210	1.0543	1.9753	46.6
K174	1.1463	0.01154	1.172	0.00136	0.11856	98.9
K163	1.6160	0.02127	1.868	0.00463	0.1915	97.6

a) This is not the observed rate, but the total rate calculated from the k_1 and k_2 values determined from all the observed rates.

The results in Table 8 clearly demonstrate that the major contributing term in my proposed rate law (equation 6.4) continuously shifts toward the first order term (k_1) as the ratio of initial amine to ester concentration approaches one.

When large disparities exist between the initial amine and ester concentrations (ie. SF 1, 5, and 8), the major contributing term to the overall rate is k_2. Therefore, the reaction appears to be second order.

When the initial amine and ester concentrations are approximately equal (K174 and K163) the major contributing term is now the first order term k_1.

The Effects of an Added Salt on the Reacting Ion Pair (RIP) Concentration.

In order to substantiate the existence of a reacting ion pair (RIP), an experiment was carried out to determine the effect that an added salt would have on the rate of reaction of charged ester IV and TBAT V (K122). My assumption was that the addition of a non-reactive salt with a comparable ion pair dissociation constant to charged ester IV would adversely effect the initial equilibrium K (Scheme 3) and thereby decrease the rate of reaction. This

competition for ion pairing sites will exert its maximum influence on the equilibrium constant when the initial ester and amine concentrations are approximately equal. The salt chosen for this purpose was N-Benzyl-γ-Trimethylammonium Butyramide Fluoborate (XVI) (see experimental for preparation).

$$BF_4^- \ (CH_3)_3N^+CH_2CH_2CH_2CONHCH_2C_6H_5$$

(XVI)

When XVI was present as a 3.5 fold excess over the initial ester concentration in the reaction mixture, the observed rate over the first twenty seven percent reaction was found to be 7.570×10^{-8} M sec^{-1} (dp/dt). The initial rate calculated from the experimentally determined k_1 and k_2 at the same initial concentrations of ester and amine was 2.087×10^{-7} M sec^{-1} (assuming no competion for ion pairing sites).

If the formation of the RIP was not important, we should have observed a slight increase in the rate of reaction in the presence of added salt. This increase would be due to stabilization of the dipolar intermediate III proposed by Menger for aminolysis reactions (see introduction) when the ionic strength of the solvent is increased. The fact that the rate is suppressed indicates that ion pair formation (RIP) is a crucial step in the reaction of charged ester IV and TBAT (V) in 95.3 mole %

dioxane-water.

The Efficiency of the Ion Pair Reaction

In order to adequately determine the magnitude of the catalysis present in the ion pair reaction (charged ester IV and TEAT(V)), a method had to be found which would allow us to compare the first order rate constant (k_1) obtained in the ion pair reaction, to the various second order aminolysis rate constants determined in this work. Since no direct comparison of first and second order rate constants is possible, the method of calculating effective molarities used by Bruice and Benkovic (7) became my only alternative.

Effective molarity was utilized by Bruice as a simple method of determining the efficiency of intramolecular aminolysis reactions over analogous bimolecular reactions. The value calculated for the effective molarity was considered the hypothetical concentration of amine necessary in the bimolecular reaction, to give a pseudo-first order rate constant equivalent to the true rate constant for the intramolecular reaction (see introduction for examples). A rough approximation of the efficiency of the ion pair reaction may be calculated by dividing the first order rate constant determined in the ion pair reaction, by each second order rate constant of its bimolecular analogs (Table 8.1).

TABLE 8.1 Determination of Effective Molarities of the Ion Pair Reaction by Comparison to Bimolecular Analogs.

Bimolecular Analog	Effective Molarity (M)
1) PNPH[a] + Benzylamine(VII)	4.5
2) PNPB[b] + Benzylamine(VII)	7.8×10^{-2}
3) PNPH[a] + TBAT(V)	2.8×10^{-2}

a) PNPH = p-nitrophenyl hexanoate (VI)

b) PNPB = charged ester (IV)

Cases 1, 2, and 3 in Table 8.1 yield effective molarities for each amine of 4.5, 7.8×10^{-2}, and 2.8×10^{-2} M respectively. This can be considered the hypothetical concentration of amine necessary in bimolecular reaction, to give roughly equal rates to the ion pair reaction. Comparison of these effective concentrations of amine for each bimolecular analog to the amine concentration present in the reacting ion pair (RIP), which has a maximum of approximately 5×10^{-5} M, leads to rough estimates of the catalysis due to the ion pair mechanism (Scheme 3). The magnitudes of these rate enhancements are 9×10^4, 1.6×10^3, and 560 for cases 1, 2, and 3 respectively. No decision will be made concerning which case in Table 8.1 is the best bimolecular model of the ion pair reaction. However, the results clearly demonstrate that in all cases, large rate enhancements are occurring due to pre-equilibrium complex formation of reactant molecules

via electrostatic attraction.

Single Term Rate Laws

The data up to this point strongly indicate that the kinetic species represented as the reacting ion pair (RIP) is essential to correct kinetic evaluations. Single term rate laws of the type:

(A) rate = $k'(RIP)$

(B) rate = $k''(RIP)(amine)$

(C) rate = $k'''(RIP)(amine)^2$

were evaluated using the experimental data. Rate laws (A) and (B) above gave good results at only one extreme of the amine-ester concentration ratio. Rate law (C) gave totally absurd results over the entire concentration range.

The two term rate law (eqn 6.4) seems to best explain my experimental results at either extreme in amine concentration.

Comparison of Charged Ester IV to Acetylcholine

Acetylcholine (IX) is synthesized in biological systems and stored in membrane bound vesicles, termed synaptic vesicles. When a potential gradient traveling along the surface of an axon reaches these synaptic vesicles, the vesicles rupture, releasing acetylcholine molecules. The acetylcholine diffuses across the synapse to receptor sites located in the post synaptic membrane. The presence of acetylcholine causes an influx of sodium ions through

the axon membrane, followed by an outflux of potassium ions (65). This produces a small potential gradient which is propagated along the surface of the axon. Along with its importance as a neural transmitter, the speed at which acetylcholine is deactivated after its function has been completed is also crucial. This degradation is accomplished by the enzyme acetylcholine esterase along with other enzymes (66). The speed at which complete hydrolysis of all the acetylcholine molecules occurs (in the presence of enzyme) is less than one hundred microseconds, faster than any neural event.

The electrostatic binding action (ion pair formation) of taurinate (V) anion to charged ester IV, can be roughly compared to the action of the enzyme acetylcholine esterase. This enzyme is known to have an active site in which the cationic end of the acetylcholine interacts with a negative charge (carboxylate group) found at the enzyme active site, while the ester function is positioned for attack by a nucleophile (imidazole) also contained at the enzyme active site (26, 28, 67).

During the enzymatic reaction, intimate contact between enzyme and acetylcholine can only occur if there exists a closely defined spacing between interacting groups (68). If one now compares the spacing between the quaternary ammonium group and the carbonyl group of acetylcholine to that of charged ester IV (and its 2-

ethylsulfonate (XVII) and benzyl (XVI) amides), then each can be considered an analog of acetylcholine.

Because of these structural similarities, charged ester IV and its 2-ethylsulfonate (XVII) and benzyl (XVI) amides, may possess some inhibitory action on the enzyme acetylcholine esterase in vitro (with possible biological significance).

$$(CH_3)_3N^+ CH_2CH_2CH_2CONHCH_2CH_2SO_3^-$$

(XVII)

Product Analysis Runs

The products and their yields formed in various aminolyses, were checked by conducting preparative scale reactions whose concentrations simulated as far as possible those of the kinetic experiments. The reactions were allowed to sit for several half-lives (determined from kinetic runs) to insure that each went to completion.

Each product amide was synthesized and purified in order that standard solutions could be prepared. Analyses were carrried out by reversed phase high pressure liquid chromatography (see experimental for details). No hydrolysis of product amides was detected when controls containing known amounts of amide in aqueous amine solutions were worked up in a similar manner to product determination runs.

TABLE 9 Recovery of Product Amides From Aminolysis Reactions

Ester	Amine	Solvent[d]	Recovery (%)
IV	TBAT	D-W	100
IV	Sodium taurinate	Water	--- [a]
IV	Benzylamine	D-W	100
IV	Benzylamine	Water	19 [b]
VI	TBAT	D-W	100
VI	Sodium taurinate	Water	--- [a]
VI	Benzylamine	D-W	97
VI	Benzylamine	Water	78 [c]

a) HPLC analysis useless in presence of large amounts of Sodium taurinate.

b) Theoretical percent amide in product mixture from calculated rate constant equals 23.

c) Theoretical percent amide in product mixture from calculated rate constant equals 77.

d) D-W = 95.3 mole % dioxane-water

Conclusion

The following conclusions can be drawn from the experimental results found in this work concerning aminolysis reactions in water and 95.3 mole % dioxane-water.

1) There exists a rate enhancement for both aminolysis and hydrolysis of charged ester IV in water, due to intramolecular charge stabilization of its dipolar tetrahedral intermediate by the neighboring quaternary ammonium group (VIII, pg 13).

2) The aminolysis of charged ester IV by TBAT (V) was found to proceed through the route depicted in Scheme 3 (pg 20). The first step of this reaction consists of equilibrium formation of a reacting ion pair (RIP). The kinetics provide evidence of its existence as a viable kinetic species. This equilibrium constant was evaluated and found to be 1.4. The next step in the reaction was equilibrium formation (from RIP) of a tetrahedral intermediate (Figure 1, pg 23), whose breakdown was considered rate determining. This breakdown was found to occur by either of two pathways. One pathway involved direct breakdown of the tetrahedral intermediate to products, while the other involved a second molecule of amine, which assisted in proton removal from the tetrahedral intermediate prior to its breakdown. At low amine concentrations this reaction appeared to go exclusively by first order kinetics (rate = k_1[RIP]), while at very high amine con-

centrations appeared to proceed mainly by second order kinetics (rate = k_2[RIP][TBAT]). At intermediate amine concentrations the reaction of charged ester IV and TBAT (V) was found to obey the following two term rate law.

$$\text{rate} = k_1[\text{RIP}] + k_2[\text{RIP}][\text{TBAT}]$$

3) The magnitude of the catalytic influence of reacting ion pair formation was estimated by calculating effective molarities (k_1 of the ion pair reaction divided by k_2 of the various bimolecular aminolysis reactions). This technique enables us to estimate rate enhancements of $> 10^2$ due to pre-equilibrium complex formation of reactant molecules via electrostatic attraction. The presence of a reacting ion pair (RIP) was recognized as an important kinetic species, essential to correct kinetic evaluations.

Experimental

Solvents

Water was deionized and filtered through a Milli-Q water purification system (Millipore Corp.), and then deaerated by bubbling nitrogen gas through it for twenty minutes. Purification of 1,4-dioxane (Baker Analyzed Reagent) was accomplished by passing solvent through a 40 cm. (height) by 4 cm. (diameter) column of activated alumina (Alcoa), and collecting under nitrogen. The dioxane was tested at one liter intervals for peroxides (2% aq. KI), n_D^{20} = 1.4229 (lit (79): n_D^{20} = 1.4224). The 95.3 mole % dioxane-water was prepared by weight and deaerated for twenty minutes with nitrogen. Acetonitrile (Aldrich) was extracted with saturated aqueous K_2CO_3 and distilled over P_2O_5, bp 80.0-80.5 °C (lit(80): bp 81.6 °C). The dioxane, 95.3 mole % dioxane-water, and acetonitrile were stored in brown glass containers under nitrogen, and used within three days. Acetone, diethyl ether, methanol, benzene, methylene chloride, hexane, petroleum ether, absolute ethanol and ethyl acetate were reagent grade and were used as obtained without further purification.

Materials

Melting and boiling points are uncorrected. Taurine (Aldrich), was recrystallized from water and dried at 100 °C in vacuo. Benzylamine (Eastman) was purified by drying

over KOH and then distilled from KOH in a glass apparatus under nitrogen bp 180-181 °C (lit (81): bp 184.6-185.2 °C (771 mm Hg)), n_D^{20} = 1.5441 (lit (82): n_D^{20} = 1.5438). Sodium taurinate was prepared from recrystallized taurine in the following manner. Taurine, 8.9952 g (7.18775×10^{-2} moles) was dissolved in 67.81 ml of 1.060 N NaOH (7.187×10^{-2} moles). Water was removed by vacuum distillation at 50 °C. The remaining oil was triturated with acetone until it was completely crystalline, and collected. The crystals were dried in vacuo at 100 °C. The equivalent weight determined by titration with 0.0515 N HCl to bromocresol green endpoint (pH = 4.5) was 148.42 g/equiv. (calc 147.14). p-Nitrophenol (Fisher) was recrystallized from 2% aq. HCl and dried at 78 °C in vacuo, mp 113-114 °C (lit (83): mp 114 °C). Crystals were stored in the dark under nitrogen. Tetra-n-butylammonium bromide (Eastman) was recrystallized twice from a 3:1 by volume ethyl acetate-ether solution and dried at 78 °C in vacuo, mp 118-119 °C (lit (84): mp 118.0 °C). Butyramide (Eastman) was recrystallized from benzene and dried at room temperature in vacuo, mp 115-116 °C (lit (85): mp 115.5-116 °C). The 2-chloro-5-hydroxy toluene (Kodak) was recrystallized from petroleum ether and dried at room temperature in vacuo, mp 65-67 °C (lit (86): mp 66 °C). Tetra-n-butylammonium hydroxide (Aldrich and Eastman) 40% w/v in water and 0.4 M in water were used without purification. The following

commercial reagents were used without further purification: anhyd. sodium carbonate (Fisher cert. ACS), ammonium nitrate (Baker Analyzed Reagent), silver(I)oxide (Baker Analyzed Reagent), anhyd. calcium chloride (Baker purified), magnesium sulfate, anhyd. (Baker Analyzed Reagent), sodium hydroxide (J.T. Baker), potassium carbonate (Baker Analyzed Reagent), Norite-A (Matheson Coleman and Bell).

Micro analyses were done by Schwarzkopf Microanalytical Laboratory, Woodside N.Y. and MicAnal Microanalytical Laboratory, Tucson, Arizona.

Spectra

NMR spectra were determined on a Varian Associates model T-60 spectrometer. All chemical shifts are given in terms of δ scale relative to tetramethylsilane. IR spectra were obtained with a Perkin-Elmer model 267 spectrophotometer.

Computations

Kinetic calculations were carried out on an IBM 360-50 computer and PL/C compiler.

Preparation of p-Nitrophenyl-γ-Trimethylammonium Butyrate Chloride and Fluoroborate Salts

A sample of γ-butyrolactone $CH_2COOCH_2CH_2$ (Antara Chem., GAF) was dried over anhydrous $MgSO_4$ and distilled, bp 203-205 °C (lit(87): bp 204 °C). A solution of 70 ml (0.92 moles) of γ-butyrolactone and 150 ml of absolute ethanol was placed in a flask that was fitted with a dropping funnel and a reflux condenser equipped with an anhyd. $CaCl_2$ drying tube, leading to a conc. aq. NaOH trap. To this solution 90 ml (1.125 moles) of redistilled thionyl chloride (Aldrich) was added dropwise with occasional swirling of the entire apparatus. Upon addition of all the thionyl chloride the mixture was heated at reflux for sixteen hours (trap was removed after 4 hours). The resulting solution was distilled, and 110 g (80% yield) of ethyl-γ-chlorobutyrate was collected, bp 184.5-185.5 °C (lit (88): bp 186 °C). To 50 ml (0.357 moles) of ethyl-γ-chlorobutyrate in a two liter roundbottom flask was added 750 ml (2.47 moles) of 3.833 M aq. trimethylamine (Aldrich). Acetone was added to the two phase system until a homogeneous solution was obtained. The roundbottom was fitted with a condenser and allowed to stand at room temperature for three days in the dark.

The acetone, trimethylamine, and water were removed by vacuum distillation (10 mm Hg) at 100 °C until the volume was reduced by approximately two-thirds. Further

vacuum distillation (1 mm Hg) was carried out at 50 °C. The white solid that remained was triturated with two 100 ml portions of anhyd. ether whereupon it became crystalline. A total of 52.4 g of white crystals were isolated. H^1 NMR analysis showed that the product was a mixture of the chloride salts of γ-trimethylammonium butyric acid and its ethyl ester ($(CH_3)_3N^+CH_2CH_2CH_2COOH$ and $(CH_3)_3N^+CH_2CH_2CH_2COOCH_2CH_3$).

The product mixture was dissolved in 60 ml of 1 N HCl and heated overnight on a steam bath. The water and HCl were removed by vacuum distillation (1 mm Hg) at 50 °C, and a white solid was isolated. The solid was triturated with two 50 ml portions of anhyd. acetone whereupon it became crystalline. The crystals were dried in vacuo at 100 °C, and 45.4 g (100% yield) of the chloride salt of γ-trimethylammonium butyric acid were collected, mp 208-212 °C (lit (89): mp 207-210 °C).

H^1 NMR (D_2O): 3.6 (2H,t), 3.4 (9H,s), 2.8 (2H,t), 2.4 (2H,m).

IR (KBr): $\nu_{C=O}$ = 1721 cm^{-1}.

To 6.7 g (0.037 moles) of the dry chloride salt of γ-trimethylammonium butyric acid was added 0.6 ml (0.082 moles) of redistilled thionyl chloride. The acid dissolved completely within a few seconds. The roundbottom flask was fitted with an anhyd. $CaCl_2$ drying tube and the mixture was stirred for sixteen hours at room temperature.

The excess thionyl chloride was removed by vacuum distillation (10 mm Hg) at 30 °C until a viscous brown oil remained. A 6.2 g (0.044 moles) sample of recrystallized p-nitrophenol and 2 ml of nitrobenzene (Fisher Cert. Reagent) were added to the oil and the homogeneous mixture was stirred (with a magnetic stirring bar) for 3.5 hours at 80 °C. The nitrobenzene was removed by vacuum distillation (1 mm Hg) at 100 °C. The dark brown solid that remained was triturated with anhyd. ether and (while still beneath the ether layer) crushed into a fine powder with a glass stirring rod. The ether layer was decanted and the crude product, p-nitrophenyl-γ-trimethylammonium butyrate chloride, was immediately dried in vacuo at room temperature. At this point the product was noticed to be quite hygroscopic, and exposure to air was kept to a minimum.

A) Purification of p-Nitrophenyl-γ-Trimethylammonium Butyrate Chloride

Crude p-nitrophenyl-γ-trimethylammonium butyrate chloride was recrystallized twice from purified acetonitrile. Pale yellow crystals were collected in a dry box (nitrogen atmosphere) and dried at 78 °C in vacuo, mp 205-207 °C (dec.).

H^1 NMR (D_2O): 7.8 (2H,d), 6.9 (2H,d), 3.17 (2H,t), 2.87 (9H,s), 2.50 (2H,t), 1.90 (2H,m).

The molar absorptivity in water at 270 nm (λ_{max}) was 8,569.0 1 $mole^{-1}$. The equivalent weight determined by a

potentiometric chloride titration was 302.99 g/equiv. (calc: 302.77 g/equiv.). p-Nitrophenoxide ion produced upon hydrolysis of a known weight of p-nitrophenyl ester with 0.1 N NaOH (visible absorbance at 400 nm) gave an equivalent weight of 299 g/equiv. The molar absorptivity of p-nitrophenoxide ion in water at 400 nm was determined separately by dilution of a weighed amount of p-nitro phenol with 0.1 N NaOH. Its value was 18,276 1 $mole^{-1}$.

B) Preparation and Purification of p-Nitrophenyl-γ-Trimethylammonium Butyrate Fluoborate

An 8 g sample of the crude chloride salt above, was dissolved in 130 ml of cold absolute ethanol. To this solution was added 9.0 ml of 48% aq. Fluoboric acid (Matheson, Coleman, and Bell), whereupon a purple precipitate formed immediately. The precipitate was collected and washed with cold absolute ethanol. The crude fluoborate salt was dissolved in 100 ml of hot acetone and decolorized twice with Norite. The solution was cooled (at -10 ^{o}C) and 4.2 g (45% yield) of pale yellow crystals were collected. The crystals were again dissolved in acetone and this time upon addition of an equal volume of ether a liquid phase separated, and gradually solidified. These crystals were next triturated with ether, collected and dried at room temperature in vacuo, mp 132-133 ^{o}C. The molar absorptivity of the fluoborate salt in water at 270 nm was 8,524.9 1 $mole^{-1}$. This value was only .5 % less

than its pure chloride salt analog. The equivalent weight determined from p-nitrophenoxide ion produced upon hydrolysis of a weighed amount of this fluoborate salt ester was 352 g/equiv. (calc: 354 g/equiv.).

Anal. Calcd. for $C_{13}H_{19}N_2O_4BF_4$: C, 44.10; H, 5.41; N, 7.91 Found: C, 44.35; H, 5.49; N, 7.65.

Preparation of Hexanoyl Chloride

A 50 ml (0.4 moles) sample of distilled hexanoic acid (Eastman), bp 205-206 °C (lit(93): bp 205.4 °C) was added dropwise to 33 ml (0.45 moles) of redistilled thionyl chloride at 80 °C (oil bath). Upon addition of all the acid the resulting solution was heated for 30 minutes at 80 °C. The reaction mixture was distilled, and 51 g (95% yield) of hexanoyl chloride was collected between 150-152 °C (lit (90): bp 152.6 °C) and sealed under nitrogen.

Preparation of p-Nitrophenyl Hexanoate

Hexanoyl chloride, 10 g (0.1334 moles) was added to an equimolar amount of p-nitrophenol (18.6 g) and 21.6 ml (2 equiv.) of pyridine (dried over KOH pellets) in a roundbottom flask. The flask was fitted with a condenser and $CaCl_2$ filled drying tube, and heated for 30 minutes on a steam bath. The product mixture was poured into a separatory funnel along with 30 ml of hexane, and the hexane layer was repeatedly extracted with 30 ml portions of 5% aq. Na_2CO_3 until the aqueous layer no longer turned

yellow. The hexane layer was extracted with three 30 ml portions of water, dried over anhyd. $CaCl_2$, and filtered. The filtrate was vacuum distilled (through a micro distillation apparatus equipped with a Vigreux column) and 8 g (25% yield) of p-nitrophenyl hexanoate was collected between 142-143 °C at 2.4 mm Hg. (lit (91): bp 123-124 °C (1 mm Hg)); n_D^{20} = 1.5185 (no lit value found). The distillate was redistilled, collected, and sealed under nitrogen.

p-Nitrophenoxide ion produced upon hydrolysis of a known weight of p-nitrophenyl hexanoate by 0.1 N NaOH (absorbance at 400 nm) gave an equivalent weight of 237.1 (calc: 237.26).

Preparation of N-Benzyl-γ-Trimethylammonium Butyramide Fluoborate

A) Preparation of Ethyl-γ-Trimethylammonium Butyrate Chloride ($Cl^- (CH_3)_3N^+CH_2CH_2CH_2COOCH_2CH_3$)

A 14 g (0.077 moles) sample of actinine hydrochloride ($Cl^- (CH_3)_3N^+CH_2CH_2CH_2COOH$) and 0.9 g of p-toluenesulfonic acid (Eastman, recry. from benzene) were added to 100 ml of benzene in a 500 ml roundbottom flask fitted with a Dean-Stark trap. The reactants and solvent were dried by an azeotropic distillation (benzene-water) of the reaction mixture into the Dean-Stark trap. The trap was drained and 150 ml of absolute ethanol was added to the reaction

mixture. The resulting solution was heated at reflux and the first 25 ml of distillate collected in the Dean-Stark trap was discarded. Twenty-five ml of distillate was drained from the trap every half hour for 2.5 hours. The solvent that remained was removed by vacuum distillation (1 mm Hg) at 30 °C and the solid residue was triturated with a single 100 ml portion of ether, and four 50 ml portions of acetone. The white crystals that remained, 14 g (87% yield), were dried at 78 °C in vacuo, mp 135-137 °C (no lit value found for chloride salt). NMR and IR analysis showed product to be ethyl-γ-trimethylammonium butyrate chloride of fairly high purity.

H^1 NMR (D_2O): 4.4 (2H,q), 3.6 (2H,t), 3.4 (9H,s), 2.7 (2H,t), 2.3 (2H,m), 1.4 (3H,t).

IR (KBr): $\nu_{C=O}$ = 1738 cm^{-1}.

B) Preparation of N-(Benzyl)-γ-Trimethylammonium Butyramide Fluoborate

$(BF_4^- \ (CH_3)_3N^+CH_2CH_2CH_2CONHCH_2C_6H_5)$

An 11.0 g (0.052 moles) sample of the ethyl ester prepared in part (A), and 176.3 mg (1.228×10^{-3} moles) of benzylamine hydrochloride were added to 30 ml (0.275 moles) of benzylamine in a roundbottom flask fitted with a condenser and a $CaCl_2$ filled drying tube. The solution was heated at reflux for three hours and the excess benzylamine was removed by vacuum distillation (1 mm Hg) at 80 °C. The slurry that remained behind was dissolved in 80 ml of

water and 142.4 mg (6.145×10^{-4} moles) of Ag_2O was added. The mixture was stirred for three hours in the dark, filtered, and the water removed by vacuum distillation (1 mm Hg) at 30 °C. The residue (still a slurry) was dissolved in 80 ml of ice cold absolute ethanol, and 20 ml of 48% aq. Fluoboric acid was added. A white solid immediately precipitated and was collected and washed with ice cold ethanol (8 g, 48% yield). A 4 g sample of the crude product was dissolved in 150 ml of hot acetone and the solution was allowed to cool to room temperature. No crystallization was observed, so product was precipitated (a white solid) by addition of an equal volume of ether. The product, 2.5 g, was collected and dissolved in 90 ml of hot methanol (some solid remained undissolved). The hot methanol solution was filtered (through a hot Buchner funnel) and the filtrate was allowed to crystallize at -10 °C for one hour. The crystals, 1.5 g (38% yield) were washed with cold methanol and dried at 78 °C in vacuo, mp 185-186 °C.

IR (KBr): $\nu_{C=O}$ = 1640 cm^{-1}; ν_{N-H} = 3250 cm^{-1}.

H^1 NMR: (d_6 DMSO) 8.5 (1H,broad), 7.4 (5H,s), 4.4 (2H,d), 3.4 (2H,t), 3.15 (9H,s), 2.2 (2H,t), 2.2-1.8 (2H,m).

Anal. Calc. for $BC_{14}F_4H_{23}N_2O$: C, 52.20; H, 7.20; N, 8.69 Found: C, 52.48; H, 7.35; N, 8.46.

Preparation of N-(2-Ethyl Sulfonate)-γ-Trimethylammonium Butyramide

$((CH_3)_3N^+CH_2CH_2CH_2CONHCH_2CH_2SO_3^-)$

To a 3.4g (0.019 moles) sample of actinine hydrochloride, Cl^- $(CH_3)_3N^+CH_2CH_2CH_2COOH$, (see pp 60 and 61 for preparation) in a 100 ml roundbottom flask was added 3 ml (0.04 moles) of redistilled thionyl chloride. The flask was fitted with a $CaCl_2$ filled drying tube and the mixture was stirred overnight at room temperature. The excess thionyl chloride was removed by vacuum distillation (10 mm Hg) at 30 °C, until a brown oil (the acid chloride) remained in the flask. To the acid chloride was added 3.0 g (0.020 moles) of sodium taurinate (Na^+ $^-O_3SCH_2CH_2NH_2$), 1.0 g (0.010 moles) of Na_2CO_3 , and 5 ml of nitrobenzene. The mixture was stirred for one hour at 90 °C, and the residue triturated (with vigorous stirring) with one 50 ml portion of ether, and two 50 ml portions of acetone.

The solid that remained behind was dissolved in 150 ml of hot methanol , decolorized with Norite, filtered, and allowed to crystallize at -10 °C overnight. The crystals were collected, washed with cold methanol and again added to 70 ml of hot methanol. Since the product did not completely dissolve in methanol, water was added dropwise to the hot methanolic solution until the solution became homogeneous. The solution was decolorized with Norite, filtered, and allowed to crystallize at -10 °C. This re-

crystallization procedure from aqueous methanol was repeated three times until white crystals were obtained. The crystals were dried in vacuo at 100 °C; yield 1.5 g (32% yield), mp 285-87 °C.

H^1NMR(D_2O): 3.35(9H,s), 2.8-2.0(4H,m), 4-3.4(6H,m).

IR(KBr): $\nu_{C=O}$ = 1670 cm^{-1}; ν_{N-H} = 3340 cm^{-1}.

Anal. Calcd. for $C_9H_{20}N_2O_4S$: C, 42.84; H, 7.99; N, 11.10 Found: C, 41.80; H, 8.05; N, 11.00.

Preparation of N-Benzyl Hexanamide

A 5.0 g (0.037 moles) sample of hexanoyl chloride was added to 50 ml of anhydrous ether in a roundbottom flask. A solution of 9.5 g (0.089 moles) of benzylamine dissolved in 60 ml of anhydrous ether was also prepared. The benzylamine solution was added dropwise to the hexanoyl chloride solution in an ice water bath with constant stirring. An immediate white precipitate formed. Upon addition of all the benzylamine solution, the product mixture was allowed to warm to room temperature. The mixture was poured into a separatory funnel and extracted with an equal volume of 0.1 N HCl. The ether layer was extracted with an equal volume of water, then dried over $CaCl_2$, and filtered. The ether was removed by evaporation at room temperature under a constant flow of nitrogen, and 7 g (92% yield) of a pale yellow powder was isolated.

IR analysis showed a band at 1632 cm^{-1} corresponding to the presence of amide. A 5.0 g sample of the crude

amide was dissolved in 40 ml of hot methanol. The solution was decolorized with Norite and filtered. The filtrate was heated on a steam bath and water was added dropwise until the solution became turbid. A homogeneous solution was again obtained on addition of hot methanol. The solution was allowed to cool to room temperature and stored at -10 ^{o}C overnight. White crystals were collected and again crystallized from aqueous methanol. The crystals were dried in vacuo at room temperature over P_2O_5, mp 54-55 ^{o}C.

H^1NMR($CDCl_3$): 7.4(5H,s), 6.5(1H,s), 4.4(2H,d), 2.2(2H,t), 1.9-0.8(9H,m).

IR(KBr): $\nu_{C=O}$ = 1632 cm^{-1}; ν_{N-H} = 3300 cm^{-1}.

Preparation of Sodium N-(2-Ethylsulfonate) Hexanamide

($CH_3CH_2CH_2CH_2CH_2CONHCH_2CH_2SO_3^-$ Na^+)

To a 5.0 g (0.0372 equiv.) sample of hexanoyl chloride dissolved in 100 ml of anhydrous ether was added 4.0 g (0.075 equiv.) of Na_2CO_3. A 5.47 g (0.0372 equiv.) sample of sodium taurinate was added to the ether solution in small portions with constant stirring. The product mixture was heated at reflux for 15 minutes, and then allowed to cool to room temperature. The solid collected on filtering the product mixture was found to have an IR band at 1640 cm^{-1}, which corresponded to the formation of an amide bond.

The crude amide was added to 100 ml of hot methanol, stirred for 10 minutes, and suction filtered. The methanol

was removed from the filtrate by vacuum distillation (1 mm Hg) at room temperature and yielded 3.6 g of a yellow powder. The powder was dissolved in 100 ml of hot methanol, decolorized twice with Norite, and filtered by suction. The methanol was removed by vacuum distillation (1 mm Hg) at room temperature and the product , 3.4 g (37% yield) was dried in vacuo at 100 °C, mp 240 °C (dec.).

H^1NMR(D_2O): 3.8(2H,t), 3.3(2H,t), 2.5(2H,t), 2-1.3(6H,m), 1.1(3H,t).

IR(KBr): $\nu_{C=O}$ = 1642 cm^{-1}; ν_{N-H} = 3310 cm^{-1}.

Preparation of N,N,N-Trimethyl-γ-Butyrobetaine (Actinine) $(CH_3)_3N^+CH_2CH_2CH_2COO^-$

To a 5.0 g (0.0275 equiv.) sample of actinine hydrochloride (see pp 60 and 61 for preparation) dissolved in 50 ml of water, was added 4.0 g (0.0346 equiv.) of Ag_2O. The mixture was stirred for one hour in the dark and was basic to litmus. The aqueous mixture was filtered, and the water removed from the filtrate by vacuum distillation (1 mm Hg) at room temperature. The solid residue was dissolved in 25 ml of absolute ethanol. This solution was decolorized with Norite and filtered. A second layer precipitated as an oil from the filtrate on addition of 150 ml of ether, and on standing the oil crystallized. The crystallization procedure was repeated, and the crystals collected and dried in vacuo at 78 C; yield 3.0 g (75% yield), mp 222 °C (lit(92): mp 222 °C).

IR(KBr): $\nu_{C=O}$ = 1575 cm^{-1}.

Preparation of Tetra-n-Butylammonium Taurinate (TBAT)

($Bu_4N^+ \ ^-O_3SCH_2CH_2NH_2$)

A 7.408 g (2.299×10^{-2} equiv.) sample of tetra-n-butylammonium bromide was dissolved in 95 ml of water. To this solution a 2.9497 g (2.546×10^{-2} equiv.) sample of Ag_2O was added. The mixture was stirred for twenty minutes (in the dark) and filtered. The filtrate (aqueous tetra-n-butylammonium hydroxide) was poured into a 100 ml volumetric flask and diluted to the mark with water. A 5 ml aliquot of this solution was removed and diluted to 100 ml. A 10 ml aliquot of this second solution was titrated to the bromothymol blue endpoint with 0.0515 N HCl. The normality of the original tetra-n-butylammonium hydroxide (TBAH) solution was found to be 2.0243×10^{-1} N.

To the 95 ml of 2.0243×10^{-1} N aqueous TBAH solution (1.923×10^{-2} moles TBAH) was added 2.4562 g (1.9615×10^{-2} moles) of taurine. The excess water was removed by vacuum distillation (1 mm Hg) at room temperature.

The brown solid that remained behind was dissolved in 50 ml of methylene chloride, decolorized at room temperature, and filtered. The methylene chloride was removed from the filtrate by vacuum distillation (1 mm Hg) at room temperature, and a white oil was isolated. The oil was triturated with four 100 ml portions of hexane, whereupon it crystallized into a white solid; 5.5 g, 78% yield. The

TBAT was dried in vacuo at room temperature over P_2O_5, mp 116-118 °C (sealed tube), and was found to be extremely hygroscopic.

The equivalent weight was determined by titration to bromothymol blue endpoint with 0.0515 N HCl, E.W. = 377.0 (calc: 366.6 g/equiv.).

Kinetic Measurements

Kinetic measurements were made with either a Cary 17 or Perkin-Elmer Model 202 UV-Visible spectrophotometer. Both were equipped with a thermostated cuvette holder through which water was circulated at 25.00 ± 0.05 °C. Product formation was followed at one wavelength as a function of time. Aminolysis rates were determined at two different amine concentrations. Pseudo first order and second order rate constants were calculated with the aid of a PL/C computer program and the following equations:

$kt = \ln(A_o/(A_o - x))$,

$kt = (B_o - A_o)^{-1} \ln(A_o(B_o - x)/B_o(A_o - x))$. In each case a plot of kt versus time(t) yielded a slope (determined by least square fit) which was the desired rate constant.

Fast reaction kinetics were determined by stopped-flow technique using a Morrow Stopped-Flow apparatus (American Instrument Co.), a Beckman Model DU Quartz spectrophotometer, and a Type 549 storage oscilloscope. The stopped-flow apparatus was equipped with a value block through which water was circulated at 25.0 ± .1 °C. Rates

were determined from the initial slope (d(product)/dt). See section on stopped-flow for a more detailed description of technique.

Kinetic Measurement of Aminolysis Rates in 95.3 mole % Dioxane-Water. Benzylamine Runs.

The following procedure is typical of that used throughout my experimental runs (K128). A 2.272 x 10^{-4} M solution of p-nitrophenyl-γ-trimethylammonium butyrate fluoborate, and 5.042 x 10^{-3} M solution of benzylamine were prepared by weight and successively diluted with 95.3 mole % dioxane-water. Separate solutions of ester and amine were equilibrated at 25 ^{o}C in a thermostated bath. The spectrophotometer was adjusted to zero absorbance at 310 nm (λ_{max} of p-nitrophenol in 95.3 mole % dioxane-water) with pure solvent, and the absorbance of each solution was measured separately. After each use the quartz spectrophotometer cell was flushed with water and then solvent. As 10 ml aliquots of each solution were mixed in a clean, dry 50 ml Erlenmeyer flask, the initial time was recorded.

The one centimeter spectrophotometer cell was rinsed with this solution , and the filled cell was stoppered and placed in the thermostated spectrophotometer cell compartment. The spectrophotometer was then switched to record mode (time noted), and a continuous trace of absorbance (at 310 nm) was recorded as a function of time. As the trace was being recorded the remainder of the reaction

mixture was sealed under nitrogen in a brown glass container, and stored overnight in the dark at room temperature.

The increase in absorbance at 310 nm was due to the production of p-nitrophenol. Since both ester (E^{310} = 1,142 l $mole^{-1}$) and p-nitrophenol (E^{310} = 10,694.5 l $mole^{-1}$) absorb at 310 nm (benzylamine solution has negligible absorbance), the actual concentration of p-nitrophenol at any particular point in the trace was calculated by equation 23.

$$C_{pnp} = \frac{A^{310}_{obs} - (C_{est} \times E^{310}_{est})}{(E^{310}_{pnp} - E^{310}_{est})} \qquad \text{(eqn 23)}$$

C_{pnp} = actual concentration of p-nitrophenol
A^{310}_{obs} = observed absorbance at 310 nm
C_{est} = initial conc. of ester
E^{310}_{est} = molar absorptivity of ester at 310 nm
E^{310}_{pnp} = molar absorptivity of p-nitrophenol at 310 nm

The absorbance at infinity was recorded the following day, and was in good agreement with absorbance calculated for 100% reaction. A second order rate constant was calculated utilizing at least twelve points between twenty and eighty percent reaction.

The same procedure was followed for the reaction of p-nitrophenyl hexanoate (E^{310} = 1,391.4 l $mole^{-1}$) and benzylamine. In each case no p-nitrophenoxide ion was found

to be produced during the reaction. The molar absorptivity of p-nitrophenol at 310 nm was evaluated separately by dilution of a recrystallized sample of p-nitrophenol in 95.3 mole % dioxane-water.

Kinetic Measurement of Aminolysis Rates in Water.
Benzylamine and Sodium Taurinate Runs.

The following proceedure is typical of that used throughout my experimental runs (K139). A 8.010×10^{-5} M solution of p-nitrophenyl-γ-trimethylammonium butyrate fluoborate and 2.270×10^{-3} M solution of benzylamine were prepared by weight and successively diluted with water. Separate solutions of ester and amine were equilibrated at 25.0 °C in a thermostated bath. The spectrophotometer was adjusted to zero absorbance at 400 nm (λ_{max} of p-nitrophenoxide ion in water) with pure solvent, and the absorbance of each solution was measured separately. Neither reactant solution had any measurable absorbance at 400 nm. After each use the spectrophotometer cell was flushed with water. As ten ml aliquots of each solution were mixed in a clean, dry 50 ml Erlenmeyer flask, the initial time was recorded. The one centimeter spectrophotometer cell was rinsed with this solution, and the filled cell was stoppered and placed in the thermostated spectrophotometer cell compartment. The spectrophotometer was then switched to record mode (time noted), and a continuous trace of the absorbance (400 nm) was recorded as a

function of time. The remainder of the reaction mixture was sealed under nitrogen and stored overnight at room temperature. The increase in absorbance at 400 nm was due to the production of p-nitrophenoxide ion. The absorbance at infinity was recorded the following day, and was in good agreement with absorbance calculated for 100% reaction. The molar absorptivity of p-nitrophenoxide ion at 400 nm was determined separately by addition of an aqueous p-nitrophenol solution to aqueous sodium hydroxide or to benzylamine or to sodium taurinate solutions. All gave a similar value of 18,276 l $mole^{-1}$.

The concentration of p-nitrophenoxide ion at any particular point in the trace was calculated by equation 24.

$$C_{phenox} = \frac{A^{400}_{obs}}{E^{400}_{phenox}} \qquad \text{(eqn 24)}$$

C_{phenox} = conc. of p-nitrophenoxide ion
A^{400}_{obs} = observed absorbance at 400nm
E^{400}_{phenox} = molar absorptivity of p-nitrophenoxide ion at 400 nm

Bruice (94) found earlier that aminolysis of esters in water follow a two term rate law.

$$\text{rate} = k_{am}(\text{ester})(\text{amine}) + k_{OH}(\text{ester})(OH^-) \qquad \text{(eqn 25)}$$

One term corresponded to aminolysis (k_{am}), and the other

hydrolysis (k_{OH}) of the ester.

This rate law was found to be applicable to my kinetic runs in water. It was confirmed by agreement of calculated aminolysis rate constants at two amine concentrations, as well as by product analysis.

Since both rate constants could not be determined from the available data, it was therefore decided to determine the hydrolysis rate constant (k_{OH}) of each ester in a separate experiment (see pp 80). Once the value of k_{OH} for each ester was determined this allowed evaluation of k_{am} from the available data.

The hydroxide ion concentration at any particular amine concentration was determined by equation 26.

$$(OH^-) = \frac{-K_b \pm \sqrt{K_b^2 + 4K_b(\text{Amine})}}{2} \qquad \text{(eqn 26)}$$

(K_b = base dissociation constant of the respective amine in water at 25 °C (see page 10)).

Once the amine and hydroxide ion concentrations were determined for each point in time within a kinetic run, the quotient of the hydroxide conc. divided by the amine concentration yielded a factor f. This factor, f, was found to vary only 1% at high amine concentrations and approximately 7% at the lowest amine concentrations throughout all the kinetic runs. The mean f value found within a kinetic run was used in all subsequent calculations for that run. The hydroxide ion concentration was

from then on expressed as the product of f multiplied by the available amine concentration.

$$(OH^-) = f \times (\text{Amine}) \qquad \text{(eqn 26.1)}$$

This simplified the rate law found in equation 25 to:

$$\text{rate} = k_{am}(\text{ester})(\text{amine}) + k_{OH}(\text{ester})f(\text{amine}) \qquad \text{(eqn 27)}$$

where,

$$\frac{\text{Rate}}{(\text{Amine})} = (\text{ester})(k_{am} + fk_{OH}) \qquad \text{(eqn 27.1)}$$

The aminolysis rate constant was evaluated by calculating the rate between every data point ($d(\text{product}_{n,n+1})/dt_{n,n+1}$), as well as the mean ester, amine, and hydroxide ion concentrations between each of these points. A plot of the rate/(amine) versus the ester concentration for each point, yielded a slope (calculated graphically or by least square fit) which when subtracted by the product of f k_{OH}, yielded the aminolysis rate constant.

$$k_{am} = \text{slope} - f\,k_{OH} \qquad \text{(eqn 28)}$$

Exactly the same procedure was followed in all aminolysis runs determined in water. In no case was p-nitrophenol found to be present in the product mixture.

Kinetic Measurement of Hydrolysis in Water. Sodium Carbonate Buffer Runs.

The following procedure is typical of that used throughout my experimental runs (K166). p-Nitrophenyl hexanoate, 70.31 mg , was dissolved in 100 ml of dioxane. The dioxane was successively diluted with water until a final concentration of 6.707×10^{-5} M in ester was achieved. The final solution contained 1.1 mole % dioxane. An aqueous solution of 8.890×10^{-2} M Na_2CO_3 was prepared by weight with water. From this point the procedure follows exactly that of aminolysis measurements in water (see pp 72 for procedure). The base dissociation constant (K_b) of Na_2CO_3 was calculated from the acid dissociation constant (K_a) of HCO_3^- ion (95) and the ionization constant of water (K_w) as in equation 29.

$$K_b = \frac{[HCO_3^-][OH^-]}{[CO_3^{-2}]} = \frac{K_w}{K_{a(HCO_3^-)}} \qquad \text{(eqn 29)}$$

The base dissociation constant (K_b) of Na_2CO_3 was calculated to be 1.7825×10^{-4} in water. The hydroxide ion concentration at any particular carbonate concentration was calculated using equation 30.

$$OH^- = \frac{-K_b \pm \sqrt{K_b^2 + 4K_b(Na_2CO_3)}}{2} \qquad \text{(eqn 30)}$$

Calculations showed the hydroxide ion concentration to remain essentially (within 0.3%) constant throughout

the kinetic run. Second order hydrolysis rate constants (k_{OH}) were calculated using the following rate law:

$$\text{rate} = k_{OH}(\text{ester})(OH^-) \qquad \text{(eqn 31)}$$

The rate constant (k_{OH}) was determined by calculating the slope of the rate/OH^- conc. versus the ester conc. for at least ten points between twenty and eighty percent reaction. The absorbance of p-nitrophenoxide ion (λ_{max} = 400 nm) at infinity was measured the following day, and was in good agreement with calculated values for 100% reaction. The molar absorptivity of p-nitrophenoxide ion at 400 nm was calculated separately, by dilution of a 5 ml aliquot of a 2.4448×10^{-4} M aqueous p-nitrophenol solution with 45 ml of a 1.8646×10^{-1} M solution of aqueous Na_2CO_3. Its value was 18,276 l $mole^{-1}$.

Product Analysis Runs

Product analyses were undertaken to determine the amount of amide produced during aminolysis runs in 95.3 mole % dioxane-water and water. They were necessary as a verification of the rate laws. Quantitative analysis of amide produced during the aminolysis reactions by both hydroxamic acid-ferric chloride complex titrations and by IR spectroscopy proved inadequate. Liquid chromatography was the only alternative. Analyses were performed on a Waters Assoc. Liquid Chromatograph with a model 6000A solvent delivery system, and a R400 differential refractometer detector.

A reversed phase Waters Microbondapak C_{18} column (30 cm x 3.9 mm ID) was employed, and various mixtures of methanol and water were tested to determine the appropriate mobile phase for each amide separation. The mobile phase was chosen for its ability to give a clean separation of the amide peak from all other components in the product mixture. Retention times were cataloged at flow rates of 1 ml/minute and pressures of approximately 1000 psi. Internal standards were selected for each individual separation with retention times well clear of any product peaks. In the case of N-benzylhexanamide, no adequate internal standard was found. Amide concentrations in the product mixtures were therefore determined by comparison to standard amide solutions of equal volume.

A) Product Analysis Runs in Water

Since a change in amine concentration alters the aminolysis-hydrolysis product ratio for each ester, product analysis runs were prepared at initial concentrations of ester and amine comparable to those used during actual kinetic runs. In order that suitable amounts (40 mg) of amide would be obtained for analysis, the volume of water in the final reaction mixture was two liters. The general procedure followed for each ester-amine pair is as follows: Both ester and amine were weighed into separate containers and each dissolved, in succession, in 2 liters of deaerated water. The aqueous solution was sealed under nitrogen, and allowed to react for several half-lives (from kinetic runs) at room temperature.

Water (and excess benzylamine, if any) was removed by vacuum distillation at 50 ^{o}C. A control containing a known amount of amide and amine was also vacuum distilled (to dryness) to determine whether during distillation any hydrolysis of amide was occuring. HPLC analysis of the solid residue from the control run showed that all the amide initially added was still present, and therefore, the method was good. Once the solid residue from the product analysis run was dried in vacuo at r.t. the appropriate internal standard was weighed and carefully transfered into the flask containing the residue. Both solids were dissolved in 5 ml of the appropriate mobile phase. A standard solu-

tion was separately prepared which contained known concentrations of amide and internal standard. A standard solution of amide and internal standard was necessary in order that a relative response factor (f_i) could be calculated.

Five microliter sample volumes of each solution were injected into the injection port of the system. Product and standard solutions were analyzed consecutively by a differential refractometer detector after separation on a microbondapak C_{18} column. Both amide and internal standard peaks were traced on heavy-weight paper, cut out and weighed, to determine the area ratio. The relative response factor (f_i) was calculated from the area ratio and known concentrations of amide and internal standard in the standard solution (eqn 32).

$$f_i = \frac{conc_i}{conc_{st}} \times \frac{Area_{st}}{Area_i} \qquad \text{(eqn 32)}$$

The subscript "st" was used for the internal standard and "i" for the component of interest. Once the relative response factor (f_i) was determined, the concentration of component i (amide) in the product residue could be determined by the area ratio of amide to internal standard by equation 33.

$$conc_i = \frac{Area_i}{Area_{st}} \times conc_{st} \times f_i \qquad \text{(eqn 33)}$$

The high concentration of sodium taurinate necessary to

give adequate yields of amide, along with the fact that the taurinate salt is not removed by vacuum distillation (vis-a-vis benzylamine), caused serious problems during product analysis. A large excess of sodium taurinate seemed to saturate (swamp) the entire chromatograph and make analysis of peaks impossible. Therefore, the ester-benzylamine runs were the only runs in water in which product analyses were determined.

B) Product Analysis Run in 95.3 Mole % Dioxane-Water

Runs were typically prepared by weighing 50 mg of ester and an appropriate amount of amine (approx. the same ratio of amine to ester as used in kinetic runs) in 50 ml of 95.3 mole % dioxane-water. The solution was sealed under nitrogen and allowed to sit at room temperature (with stirring when necessary) in the dark for several half-lives. Dioxane and water were removed by vacuum distillation at room temp. The analysis and calculations to determine the amount of amide in the product residue were exactly analogous to those used in product analysis in water (experimental pp 83).

TABLE 10 Parameters and Retention Times for HPLC Product Analysis

Amide	Mobile Phase	Internal Standard
XVII[a] rt.= 319 sec.	H_2O - 0.1 M NH_4NO_3	Butyramide rt.= 621.3 sec
XVI[b] rt.= 269 sec	50% by vol MeOH-H_2O- 0.1 M NH_4NO_3	2-chloro-5-hydroxy-toluene rt.= 798.4 sec
XVIII[c] rt.= 685 sec	20% by vol MeOH-H_2O- 0.1 M NH_4NO_3	Na^+ $SO_3^-C_6H_4Cl$-p rt.= 536.2 sec
XIX[d] rt.= 401.6 sec	66% by vol MeOH-H_2O- 0.1 M NH_4NO_3	---[e]

a) XVII = $(CH_3)_3N^+CH_2CH_2CONHCH_2CH_2SO_3^-$

b) XVI = $BF_4^-(CH_3)_3N^+CH_2CH_2CH_2CONHCH_2C_6H_5$

c) XVIII = $CH_3(CH_2)_4CONHCH_2CH_2SO_3^-$ Na^+

d) XIX = $CH_3(CH_2)_4CONHCH_2C_6H_5$

e) No suitable internal standard found, amide concentrations determined by comparison to standard amide solutions.

Stopped-Flow Measurements of Initial Rates in 95.3 Mole % Dioxane-Water. p-Nitrophenyl-γ-Trimethylammonium Butyrate Fluoborate (IV) and TBAT (V).

In order that initial rates could be determined for the reaction of charged ester IV and TBAT (V) in 95.3 mole % dioxane-water, the stopped-flow technique was employed.

Initial rates were necessary because of the expeditious nature of this reaction, along with the fact that competition for ion pairing between products and reactants (when product concentration becomes significant) would complicate the rate equation.

The following general procedure is typical of that used throughout my experimental runs. A solution of charged ester IV was prepared by addition of approximately 50 mg of ester to 80 ml of 95.3 mole % dioxane-water, and the mixture was shaken for 30 minutes under a nitrogen atmosphere. The mixture was filtered into a 100 ml volumetric flask, and diluted to the mark with solvent. The final concentration of ester was determined by reaction with a 5.0×10^{-2} M benzylamine solution (prepared by weight). The concentration of p-nitrophenol (λ_{max} = 310 nm) produced at infinity was calculated, and the initial concentration of ester determined. A solution of TBAT (V) was prepared by weight and successive dilution with solvent.

The spectrophotometer was adjusted with solvent to

register 100% transmittance on the oscilloscope screen at 400 nm (samples of ester and amine solutions were transparent at this wavelength). Since the major observable product of the reaction was p-nitrophenoxide ion, its molar absorptivity at 400 nm was determined in a separate experiment.

Each reactant solution was injected into the thermostated value block of the stopped-flow apparatus. As both solutions were simultaneously injected into the mixing chamber, a recording of the % transmittance versus time was traced on the oscilloscope screen (which was previously calibrated at both 0 and 100% transmittance). A photograph of the screen which contained the trace was taken, and the initial rate was determined from the initial slope of p-nitrophenoxide ion concentration versus time (d(product)/dt).

The Determination of the p-Nitrophenol-p-Nitrophenoxide Equilibrium Constant in 95.3 Mole % Dioxane-Water in The Presence of Tetra-n-butylammonium Taurinate.

Introduction

Acid-base behavior in solvents of low dielectric constant has been reviewed quite throughly by Davis (1) and King (2). I will present a summary of the features which have a direct influence on my work.

Acid-base reactions in relatively inert solvents (solvents which are not sufficiently basic to remove protons from acids) of low dielectric constant, were found to conform to the general equations 1 and 2 (3,4).

$$HA(\text{the acid}) + B(\text{the base}) \overset{K}{<==>} BH^{+}---A^{-} \qquad (\text{eqn } 1)$$

$$K = \frac{[BH^{+}---A^{-}]}{[HA][B]} \qquad (\text{eqn } 2)$$

Ionization leads to the production of a hydrogen bonded ion pair ($BH^{+}---A^{-}$) which undergoes negligible dissociation to free ions, and can therefore be treated as a single kinetic species. The equilibrium constant (K) possesses the units of recipocal molarity.

This behavior was demonstrated by Pearson (3) in heptane, benzene, dioxane, chloroform, chlorobenzene, ethylacetate, and ethylene dichloride for 2,4-dinitrophenol and a variety of amines. The amines include mono-, di-,

and tri- substituted methyl, ethyl, or n-butyl amines, as well as n-hexylamine.

Davis (4) also demonstrated that acid-base reactions in benzene conform to the general pattern of equations 1 and 2. She studied the reaction of triethylamine with each of the six isomeric di-nitrophenols. The acid strengths of the isomers in benzene, with triethylamine as the reference base, followed the order 2,6 > 2,3 > 3,4 > 2,4 > 3,5 > 2,5 dinitrophenol. The stronger the proton donor, the larger was the equilibrium constant.

The Effects of Added Water on the Acid-Base Equilibrium in Dioxane

On addition of small amounts of water to dioxane, Pearson (3) discovered that only a relatively small change in equilibrium constant occurred for 2,4-dinitrophenol and n-hexylamine (Table 1). This indicated that the n-hexylammonium-2,4-dinitrophenolate ion pair is quite sufficiently stabilized by dioxane molecules. The equilibrium expression in equation 2 was still applicable in the aqueous dioxane solvent systems investigated.

TABLE 1 The Effects of Adding Small Amounts of Other Solvents on the Equilibrium, 2,4-Dinitrophenol + n-Hexylamine = n-Hexylammonium 2,4-Dinitrophenolate in Dioxane and Chloroform at 25 °C

1. Dioxane

mole % Water	K (1 mole^{-1})
0.00	4300
0.72	5400
1.25	5800
2.25	7180
5.52	15,300

2. Chloroform

mole % Ethanol	K (1 mole^{-1})
0.00	53
1.49	360
3.42	1490

The Effects of Added Salts on the Acid-Base Equilibrium in Benzene and Chloroform

In order to substantiate the existence of the hydrogen bonded ion pair BH^+---A^- as found in equation 1. Pearson (3) noted that on addition of salts of a common cation (n-hexylammonium tosylate) to benzene and chloroform solutions of 2,4-dinitrophenol and n-hexylamine, an increase

rather than a decrease in equilibrium constant occurred. He stated that this was good evidence that equation 1 is correct, rather than equation 3.

$$HA + B \overset{K}{<===>} BH^+ + A^- \qquad \text{(eqn 3)}$$

Addition of BH^+ would drive the equilibrium in equation 3 to the left, but would have no direct effect on the equilibrium in equation 1. The small increase in equilibrium constant is primarily due to the favoring of charge formation in solvents of higher ionic strength.

The Self-Association of Phenols in Aprotic Solvents

Many investigators (7,8,9,10) found that in several aprotic solvents, self-association of phenol is a very important reaction. Most favored the assumption of a monomer-dimer equilibrium ($K_{1,2}$) at the lowest concentrations studied.

$$2\ ArOH \overset{K_{1,2}}{<==>} (ArOH)_2 \qquad \text{(eqn 4)}$$

If an allowance is not made for this behavior, equilibrium constants obtained from equation 2 will not remain constant as concentrations are changed. Davison (11) determined $K_{1,2}$ values for some substituted phenols in benzene cryoscopically. The relative values follow the same order as the acidities, that is o-Me = p-Me < m-NO_2 << p-NO_2.

Philbrick (7) measured self association constants for substituted phenols in various solvents, and found that

groups like NO_2 which reduce association when present in the solvent, increase it when present in the solute. The exceptions were o-nitro and o-halophenols (or any ortho substituent capable of accepting a hydrogen bond).

Ortho-nitro and ortho-halophenols form intramolecularly H-bonded structures even in highly polar solvents (12). The tendency toward intramolecular H-bonding is especially strong in o-nitrophenol because of resonance, as well as favorable geometry. Therefore, intramolecular H-bonding must occur at the expense of intermolecular H-bonding. For these reasons, Pearson (3) and Davis (4) did not need to take into account self-association when evaluating equilibrium constants of o-nitro substituted phenols. Davis did note that equilibrium constants determined for 3,4 and 3,5 dinitrophenols were corrected (apparently for self-association). She did not elaborate on just how this correction was evaluated.

Studies of the IR spectra of p-nitrophenol in carbon tetrachloride by Cardinaud (13) suggested that it tends to form dimers by "head-to-tail" association, in which a nitro group is bonded to a hydroxy group.

Results and Discussion

The Ionization of p-Nitrophenol in the Presence of Tetra-n-butylammonium Taurinate (TBAT)

Spectrophotometric analysis of the product mixture at "infinity", for the aminolysis of each ester with tetra-n-butylammonium taurinate (TBAT) in 95.3 mole % dioxane-water, showed that p-nitrophenol (λ_{max}= 308 nm) and p-nitrophenoxide (λ_{max}= 408 nm) were both present. The ratio of p-nitrophenol to p-nitrophenoxide favored the ion at high amine concentrations, and the neutral phenol at low amine concentrations. Since rates were determined by observing the change in absorbance at only one wavelength (for the production of p-nitrophenol or p-nitrophenoxide), the correct rates [d(product)/d(time)] could only be evaluated by knowing the total phenol concentration at any given instant in time. The simplest method to achieve this would be to determine the p-nitrophenol-p-nitrophenoxide equilibrium constant, in 95.3 mole % dioxane-water in the presence of TBAT.

Since tetra-n-butylammonium-p-nitrophenoxide has a single absorbance maximum in the visible region (λ_{max}= 408 nm) in 95.3 mole % dioxane-water, a spectrophotometric determination of the equilibrium constant was undertaken.

TABLE 2 Experimental Data and Equilibrium Constant (a,b) Evaluations at 25 °C

Set	Run	C_i (M) PNP (10^5)	C_i (M) TBAT (10^4)	C_e (M) (A/E) (10^5)	K^a (M^{-1})	K^b ($M^{-1/2}$)
1	E1	8.6946	3.3573	0.78693	303	3.81
1	E2	8.6946	8.3933	1.8503	329	3.85
1	E3	8.6946	16.787	3.2116	355	3.73
1	E4	8.6946	41.967	5.7809	479	3.66
2	E5	17.389	3.3573	1.2143	232	4.17
2	E6	17.389	8.3933	2.5885	214	3.69
2	E7	17.389	16.787	4.9197	242	3.82
2	E8	17.389	41.967	9.6093	301	3.76
3	E9	9.9993	3.7445	1.0089	308	4.12
3	E10	9.9993	9.3612	2.2271	313	3.91
3	E11	9.9993	18.722	3.9034	349	3.61
3	E12	9.9993	46.806	6.9993	506	3.92
4	E13	19.998	3.7445	1.4850	223	4.27
4	E14	19.998	9.3612	3.1967	210	3.86
4	E15	19.998	18.722	5.8346	227	3.82
4	E16	19.998	46.806	11.115	274	3.65

(a) $$K = \frac{(A/E)}{(ArOH_{stoi}-A/E)(TBAT_{stoi}-A/E)}$$

(b) $$K = \frac{(A/E)}{(\frac{ArOH_{stoi}-A/E}{2})^{1/2}(TBAT_{stoi}-A/E)}$$

c) C_i = initial conc. ; C_e = equilibrium conc.

d) PNP = p-nitrophenol

e) TBAT = tetra-n-butylammonium taurinate

The Associative Behavior of p-Nitrophenol in 95.3 Mole % Dioxane-Water

Acid-base reactions (between 2,4-dinitrophenol and various amines) were previously found (3) to conform to the general equations 1 and 2 in aqueous dioxane (studied up to 5.52 mole % water).

$$HA + B \overset{K}{<===>} BH^+---A^- \qquad \text{(eqn 1)}$$

$$K = \frac{[BH^+---A^-]}{[HA][B]} \qquad \text{(eqn 2)}$$

The associative behavior of p-nitrophenol molecules in 95.3 mole % dioxane-water became evident after attempts to calculate the simple equilibrium constant given by equation 4 (for p-nitrophenol (ArOH) and TBAT) showed an increase in equilibrium constant as the amine concentration was increased.

$$ArOH + Bu_4N^+---^-O_3SCH_2CH_2NH_2 \overset{K}{<===>}$$

$$ArO^----H_3^+NCH_2CH_2SO_3^----N^+(Bu)_4 \qquad \text{(eqn 3)}$$

$$K = \frac{ArO^----H_3^+NCH_2CH_2SO_3^----N^+(Bu)_4}{[ArOH][Bu_4N^+---^-O_3SCH_2CH_2NH_2]} \qquad \text{(eqn 4)}$$

From spectrophotometric analysis, the total p-nitrophenoxide concentration at equilibrium is simply the quotient of the total absorbance (A) at 408 nm (λ_{max}) and its molar absorptivity (E). The equilibrium concentrations

of p-nitrophenol (ArOH) and TBAT can therefore be expressed as:

$$(ArOH) = (ArOH)_{stoi} - A/E \qquad \text{(eqn 5)}$$

$$(TBAT) = (TBAT)_{stoi} - A/E \qquad \text{(eqn 6)}$$

where the subscript "stoi" is an abbreviation for stoichiometric.

Table 2 (column 6) contains values calculated for this equilibrium constant (equation 4) from my experimental data. Within each set of runs the initial p-nitrophenol concentration was varied by a factor of approximately twelve. One should note the fairly large inconsistencies among values within each set. A comparison of runs in sets 1 and 2 (or 3 and 4) at similar initial amine concentrations (ie. E1 and E5) and different initial p-nitrophenol concentrations shows that the values obtained for the equilibrium constant are approximately one-third higher at the lower p-nitrophenol concentration. Since a change in either p-nitrophenol or TBAT concentration causes a significant change in the value obtained for the equilibrium constant, the molecularity of one or more species in equation 4 must be incorrect.

The self association in phenols is a very important reaction in aprotic solvents (even when wet). The simplest way to express this phenomenon for p-nitrophenol is

$$n\ ArOH \ <===> \ (ArOH)_n \qquad \text{(eqn 7)}$$

where "n" is equal to the aggregation number. The self association of p-nitrophenol can now be included into equation 3, and the mass balanced to yield equations 8 and 9.

$$1/n(ArOH)_n + Bu_4N^+ \cdots {}^-O_3SCH_2CH_2NH_2 \ <=\overset{K}{=}=> \ ArO^- \cdots H_3^+NCH_2CH_2SO_3^- \cdots N^+(Bu)_4 \qquad \text{(eqn 8)}$$

$$K = \frac{ArO^- \cdots H_3^+NCH_2CH_2SO_3^- \cdots N^+(Bu)_4}{[(ArOH)_n]^{1/n}[Bu_4N^+ \cdots {}^-O_3SCH_2CH_2NH_2]} \qquad \text{(eqn 9)}$$

The equilibrium concentration of self associated p-nitrophenol can be derived from the total p-nitrophenoxide concentration (A/E) and the stoichiometric concentration of p-nitrophenol [$ArOH_{stoi}$] as in equations 10 and 11.

$$n(ArOH)_n + A/E = (ArOH)_{stoi} \qquad \text{(eqn 10)}$$

$$(ArOH)_n = (ArOH_{stoi} - A/E)/n \qquad \text{(eqn 11)}$$

An analogous derivation can be used to determine the equilibrium concentration of TBAT.

$$(TBAT) + (A/E) = (TBAT)_{stoi} \qquad \text{(eqn 12)}$$

$$(TBAT) = (TBAT)_{stoi} - (A/E) \qquad \text{(eqn 13)}$$

Substitution of equations 11 and 13 into equation 9, affords an expression for the equilibrium constant which

can be evaluated from my data.

$$K = \frac{[ArO^{-}---H_3^{+}NCH_2CH_2SO_3^{-}---Bu_4N^{+}]}{[\frac{ArOH_{stoi}-A/E}{n}]^{1/n}[Bu_4N^{+}---^{-}O_3SCH_2CH_2NH_2-A/E]} \quad \text{(eqn 14)}$$

Table 2 (column 7) contains values for this equilibrium constant (equation 14) assuming that n = 2 (later proven to be correct). Inconsistencies(approx. 10%) still exist within each set of runs, however, a comparison of sets no longer shows any disparity in equilibrium constant at different p-nitrophenol concentrations. These results indicate that the dimer of p-nitrophenol is probably the species undergoing ionization.

Determination of Coexisting Equilibria

The general expression for the equilibrium between phenols and amines contains a hydrogen bonded ion pair $BH^{+}---A^{-}$. The reaction of p-nitrophenol and TBAT has an added feature not previously studied in the literature, in that the base itself is a salt. When TBAT is the base the equilibrium product now contains four centers of charge in a single kinetic species, as in ion aggregate(I).

$$ArO^{-}---H_3^{+}NCH_2CH_2SO_3^{-}---N^{+}(Bu)_4$$

(I)

Since two positive charge centers coexist in the ion aggregate(I), one may speculate that two types of p-

nitrophenoxide ion aggregates are possible. One such ion aggregate is the p-nitrophenoxide-taurinate-quaternary ammonium found in ion aggregate(I), while the other is the p-nitrophenoxide-quaternary ammonium ion pair(II).

$$ArO^{-}---^{+}N(Bu)_4$$

(II)

$$^{-}O_3SCH_2CH_2NH_3^{+}$$

(III)

The formation of (II) comes about from the dissociation of the ion aggregate(I) into an ion pair(II) and a zwitterion(III) according to the following equilibrium equation.

$$ArO^{-}---H_3^{+}NCH_2CH_2SO_3^{-}---N^{+}(Bu)_4 \overset{K_d}{<===>}$$

$$ArO^{-}---^{+}N(Bu)_4 + {}^{-}O_3SCH_2CH_2NH_3^{+} \qquad \text{(eqn 15)}$$

Once the ion aggregate (I) dissociates into species (II) and (III), there is no reason to assume that they will continue to be associated to one another. Therefore, they can be treated as two distinct kinetic species.

This second equilibrium (equation 15) may explain the inconsistencies in the values of the equilibrium constants found in Table 2 (column 7) at various amine concentrations.

TABLE 3 Log K for Ion Pair Dissociation of Quaternary and Other Ammonium Picrates in Several Organic Solvents (25°C)[a]

Solvent (D)[b]	Cation[c]	log K	ref
Benzene (2.27)	$i\text{-Am}_4N^+$	-17.05	14
	$i\text{-Am}_3NH^+$	-20.60	14
Chlorobenzene (5.63)	Bu_4N^+	-7.73	15
	Bu_3NH^+	-12.68	15
Ethylene chloride (10.23)	Bu_4N^+	-3.64	16
	Bu_3NH^+	-7.68	16
Nitrobenzene (24.8)	Me_4N^+	-1.40	17
	Me_3NH^+	-3.82	17

a) Log K corresponds to the reaction $R_4N^+Pi^-$ <===> $R_4N^+ + Pi^-$

b) dielectric constant of the solvent

c) Bu signifies n-butyl

Determination of the Overall Equilibrium Expression

The overall equilibrium equation for the reaction of p-nitrophenol and TBAT in 95.3 mole % dioxane-water can be determined by combining equations 8 and 15. The equilibrium equation contains two coexisting equilibria, K and K_d.

$$1/n\ (ArOH)_n + Bu_4N^+ \cdots O_3^-SCH_2CH_2NH_2 \overset{K}{\langle ==== \rangle}$$

$$ArO^- \cdots H_3^+NCH_2CH_2SO_3^- \cdots {}^+N(Bu)_4 \overset{K_d}{\langle ==== \rangle}$$

$$ArO^- \cdots {}^+N(Bu)_4 + H_3^+NCH_2CH_2SO_3^- \qquad \text{(eqn 16)}$$

Dissociation constants of various ammonium and quaternary ammonium picrates in a variety of solvents are listed in Table 3. A reasonable prediction that can be made from values in Table 3, is that the amount of ion pair (II) will be quite small as compared to ion aggregate (I) in 95.3 mole % dioxane-water (D= 2.53). This assumption is justified by the fact that in any given solvent the ammonium picrate has a much lower dissociation constant than its quaternary ammonium analog(Table 3).

The Evaluation of Equilibrium Constants

Each equilibrium constant found in equation 16 can now be expressed separately in the form of equations 17 and 18.

$$K = \frac{[ArO^{-}---H_3^{+}NCH_2CH_2SO_3^{-}---Bu_4N^{+}]}{[\frac{ArOH_{stoi}-A/E}{n}]^{1/n}[Bu_4N^{+}---^{-}O_3SCH_2CH_2NH_2]}$$

(eqn 17)

$$K_d = \frac{[ArO^{-}---^{+}N(Bu)_4]\ [H_3N^{+}CH_2CH_2SO_3^{-}]}{[ArO^{-}---H_3N^{+}CH_2CH_2SO_3^{-}---^{+}N(Bu)_4]}$$

(eqn 18)

I will use n for the aggregation number of p-nitrophenol throughout the following derivation.

The ion aggregate (I) concentration can be written (equation 18) as a function of the concentration of ion pair (II) and K_d, assuming that $[ArO^{-}---^{+}N(Bu)_4]$ equals $[H_3N^{+}CH_2CH_2SO_3^{-}]$.

$$[ArO^{-}---H_3N^{+}CH_2CH_2SO_3^{-}---^{+}N(Pu)_4] = \frac{[ArO^{-}---^{+}N(Bu)_4]^2}{K_d}$$

(eqn 19)

A single expression containing both K and K_d can be written by substituting equation 19 into equation 17.

$$K = \frac{[ArO^{-}---^{+}N(Bu)_4]^2}{K_d\ [\frac{ArOH_{stoi}-A/E}{n}]^{1/n}\ [(Bu)_4N^{+}O_3^{-}SCH_2CH_2NH_2-A/E]}$$

(eqn 20)

Since the total p-nitrophenoxide concentration (A/E)

is merely the sum of the concentrations of the ion aggregate (I) and the ion pair (II),

$$A/E = [ArO^{-}---H_3^{+}NCH_2CH_2SO_3^{-}---{}^{+}N(Bu)_4] + [ArO^{-}---{}^{+}N(Bu)_4]$$

(eqn 21)

equation 18 can be rewritten whereby K_d is a function of only the ion aggregate (II) concentration and A/E.

$$K_d = \frac{[ArO^{-}---{}^{+}N(Bu)_4]^2}{[A/E - (ArO^{-}---{}^{+}N(Bu)_4)]} \qquad \text{(eqn 22)}$$

An expression can now be derived for the concentration of ion pair (II), by rearranging equation 22 and using the quadratic formula.

$$[ArO^{-}---{}^{+}N(Bu)_4] = \frac{-K_d \pm \sqrt{(K_d^2 + 4K_d(A/E))}}{2}$$

(eqn 23)

On substituting equation 23 into equation 20, an expression can now be written where K and K_d are functions of only the stoichiometric concentrations of reactants and the total p-nitrophenoxide concentration (A/E).

$$K = \frac{\left(-K_d \pm \sqrt{K_d^2 + 4K_d(A/E)} \right)^2}{4K_d \left(\frac{ArOH_{stoi} - A/E}{n}\right)^{1/n} (TBAT_{stoi} - A/E)}$$

(eqn 24)

At this point in the derivation to help simplify future mathematical manipulations, I will make the following replacement.

$$(C) = \left(\frac{(ArOH_{stoi} - A/E)}{n} \right)^{1/n} \qquad \text{(eqn 25)}$$

$$(B) = (TBAT_{stoi} - A/E) \qquad \text{(eqn 26)}$$

Equation 24 can now be written as in equation 27.

$$K = \frac{\left(-K_d \pm \sqrt{K_d^2 + 4K_d(A/E)} \right)^2}{4K_d\ (C)\ (B)} \qquad \text{(eqn 27)}$$

The numerator of equation 27 was expanded and like terms combined.

$$K = \frac{K_d^2 \pm 2K_d \sqrt{K_d^2 + 4K_d(A/E)} + K_d^2 + 4K_d(A/E)}{4K_d\ (C)\ (B)}$$

(eqn 28)

$$K = \frac{2K_d^2 \pm 2K_d \sqrt{K_d^2 + 4K_d(A/E)} + 4K_d(A/E)}{4K_d\ (C)\ (B)}$$

(eqn 29)

Cancellation of the $2K_d$ term from the numerator and denominator of equation 29 yields

$$K = \frac{K_d \pm \sqrt{K_d^2 + 4K_d(A/E)} + 2(A/E)}{2\ (C)\ (B)}$$

(eqn 30)

Equation 30 can now be rearranged into the form of

$$K - \frac{A/E}{(C)(B)} = \frac{K_d \pm \sqrt{K_d^2 + 4K_d(A/E)}}{2(C)(B)} \qquad \text{(eqn 31)}$$

and both sides multiplied by 2(C)(B).

$$2K(C)(B) - 2(A/E) = K_d \pm \sqrt{K_d^2 + 4K_d(A/E)} \qquad \text{(eqn 32)}$$

Equation 32 can now be rearranged as in equation 33, and each side squared.

$$2K(C)(B) - 2(A/E) - K_d = \pm \sqrt{K_d^2 + 4K_d(A/E)} \qquad \text{(eqn 33)}$$

$$(2K(C)(B) - 2(A/E) - K_d)^2 = (\pm \sqrt{K_d + 4K_d(A/E)})^2$$

(eqn 34)

Expansion of equation 34 and cancellation of like terms yields equation 37.

$$\left.\begin{array}{l} 4K^2(C)^2(B)^2 - 4K(C)(B)(A/E) - 2KK_d(C)(B) \\ -4K(C)(B)(A/E) + 4(A/E)^2 + 2K_d(A/E) \\ -2KK_d(C)(B) + 2K_d(A/E) + K_d^2 \end{array}\right\} = K_d^2 + 4K_d(A/E)$$

(eqn 35)

$$4K^2(C)^2(B)^2 - 8K(C)(B)(A/E) - 4KK_d(C)(B) + 4(A/E)^2 + 4K_d(A/E) + K_d^2 = K_d^2 + 4K_d(A/E)$$

(eqn 36)

$$4K^2(C)^2(B)^2 - 8K(C)(B)(A/E) - 4KK_d(C)(B) + 4(A/E)^2 = 0$$

(eqn 37)

An equation can now be derived for (A/E), by dividing equation 37 by 4 and using the quadratic formula.

$$K^2(C)^2(B)^2 - 2K(C)(B)(A/E) - KK_d(C)(B) + (A/E)^2 = 0$$

(eqn 38)

$$(A/E)^2 - 2K(C)(B)(A/E) + (K^2(C)^2(B)^2 - KK_d(C)(B)) = 0$$

(eqn 39)

$$(A/E) = \frac{2K(C)(B) \pm \sqrt{4K^2(C)^2(B)^2 - 4(K^2(C)^2(B)^2 - KK_d(C)(B))}}{2}$$

(eqn 40)

$$(A/E) = \frac{2K(C)(B) \pm \sqrt{4KK_d(C)(B)}}{2} \qquad \text{(eqn 41)}$$

$$(A/E) = K(C)(B) \pm \sqrt{KK_d(C)(B)} \qquad \text{(eqn 42)}$$

If I now divide both sides of equation 42 by $\sqrt{(C)(B)}$, an equation of the form y = mx + b results.

$$\frac{(A/E)}{\sqrt{(C)(B)}} = \frac{K(C)(B)}{\sqrt{(C)(B)}} \pm\sqrt{KK_d}$$

(eqn 43)

The values of the slope (m) and the y-intercept (b) are K and $\pm\sqrt{KK_d}$, respectively. The x and y coordinates for each run (E1 - E16) can be evaluated from the following equations.

$$x = \frac{(\frac{ArOH_{stoi} - A/E}{n})^{1/n} (TBAT_{stoi} - A/E)}{\sqrt{(\frac{ArOH_{stoi} - A/E}{n})^{1/n} (TBAT_{stoi} - A/E)}}$$

(eqn 44)

$$y = \frac{(A/E)}{\sqrt{(\frac{ArOH_{stoi} - A/E}{n})^{1/n} (TBAT_{stoi} - A/E)}}$$

(eqn 45)

Evaluation of Aggregation Number

With the aid of a computer program, I was able to evaluate an x,y pair (equations 44 and 45) for each of my sixteen data points for values of n from n = 1 to 3 (by 0.1 increments). For each separate value of n, the least square slope and y-intercept were evaluated, along with the standard deviation of the slope and y-intercept for all my data points. A plot of n versus % error in slope ($\frac{\text{s.d. in slope}}{\text{slope}} \times 100\ \%$) is shown in Graph I and listed in Table 4. The curve clearly shows a minimum at n equals 2. Therefore it was decided that the average aggregation state of p-nitrophenol in 95.3 mole % dioxane-water can best be depicted as the dimer.

TABLE 4 Percent Error in Slope[a] at Various Values of n

n	%Error in Slope	n	%Error in Slope
1.0	24.15	2.00	2.08
1.1	18.74	2.02	2.11
1.2	14.78	2.04	2.14
1.3	11.72	2.06	2.19
1.4	9.26	2.08	2.26
1.5	7.23	2.1	2.34
1.6	5.55	2.2	2.85
1.7	4.16	2.3	3.47
1.8	3.06	2.4	4.10
1.9	2.33	2.5	4.72
1.92	2.24	2.6	5.31
1.94	2.17	2.7	5.87
1.96	2.12	2.8	6.41
1.98	2.09	2.9	6.92
		3.0	7.40

a) %Error = (standard deviation of slope/slope) x 100%

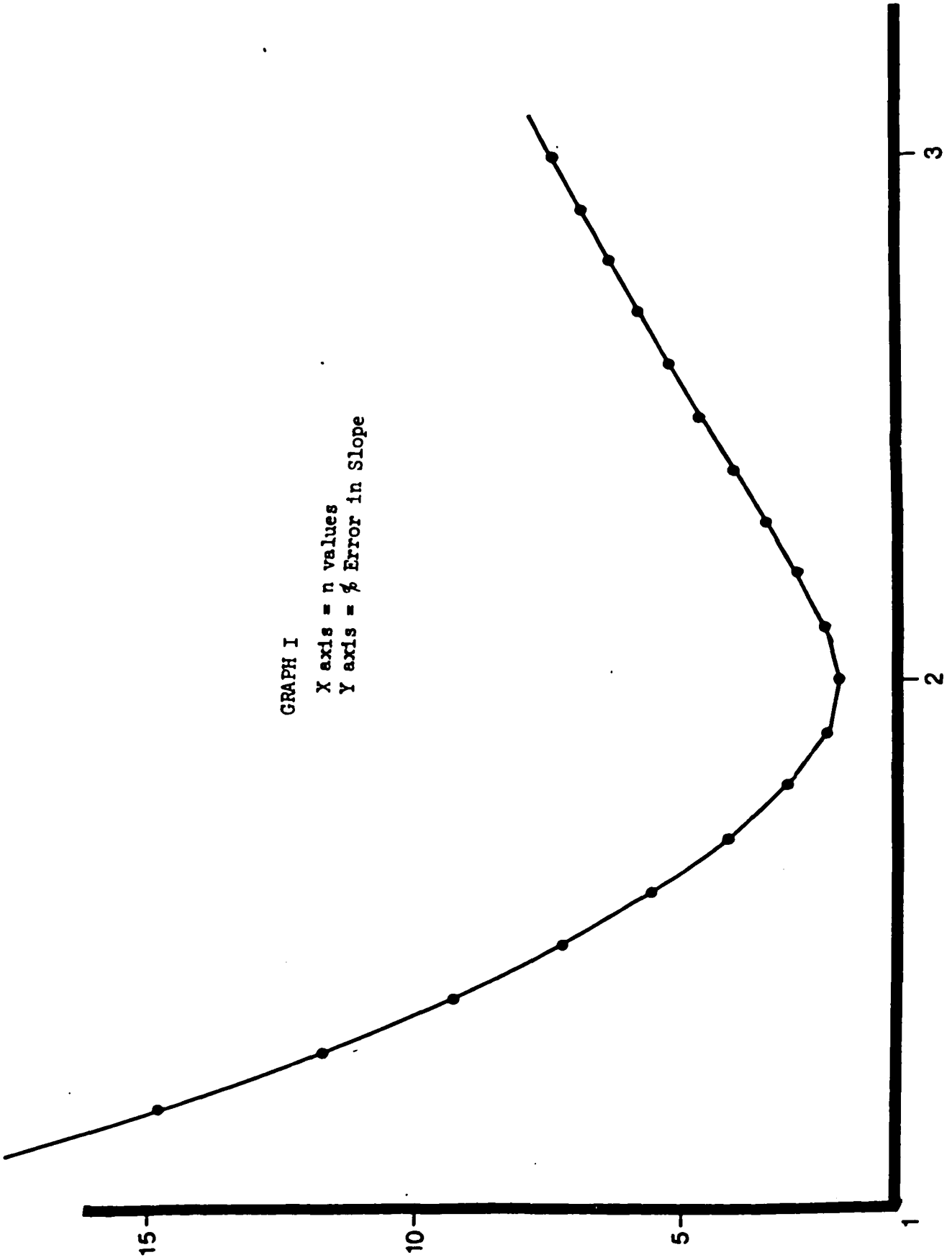
GRAPH I
X axis = n values
Y axis = % Error in Slope
15
10
5
1
2
3

TABLE 5: Values of X^a and Y^b Used in the Determination of Slope when n = 2.

Run#	$X^a(10^3)$	$Y^b(10^3)$
E1	1.4358	5.4807
E2	2.1913	8.4438
E3	2.9362	10.938
E4	3.9745	14.5447
E5	1.7059	7.1186
E6	2.6453	9.7851
E7	3.5870	13.715
E8	5.0572	19.001
E9	1.5630	6.4550
E10	2.3868	9.3311
E11	3.1813	12.270
E12	4.2257	16.564
E13	1.8600	7.9838
E14	2.8787	11.104
E15	3.9070	14.934
E16	5.5185	20.142

a) $$X = \sqrt{\left(\frac{ArOH_{stoi} - A/E}{2}\right)^{1/2} (TBAT_{stoi} - A/E)}$$

b) $$Y = \frac{A/E}{\sqrt{\left(\frac{ArOH_{stoi} - A/E}{2}\right)^{1/2} (TBAT_{stoi} - A/E)}}$$

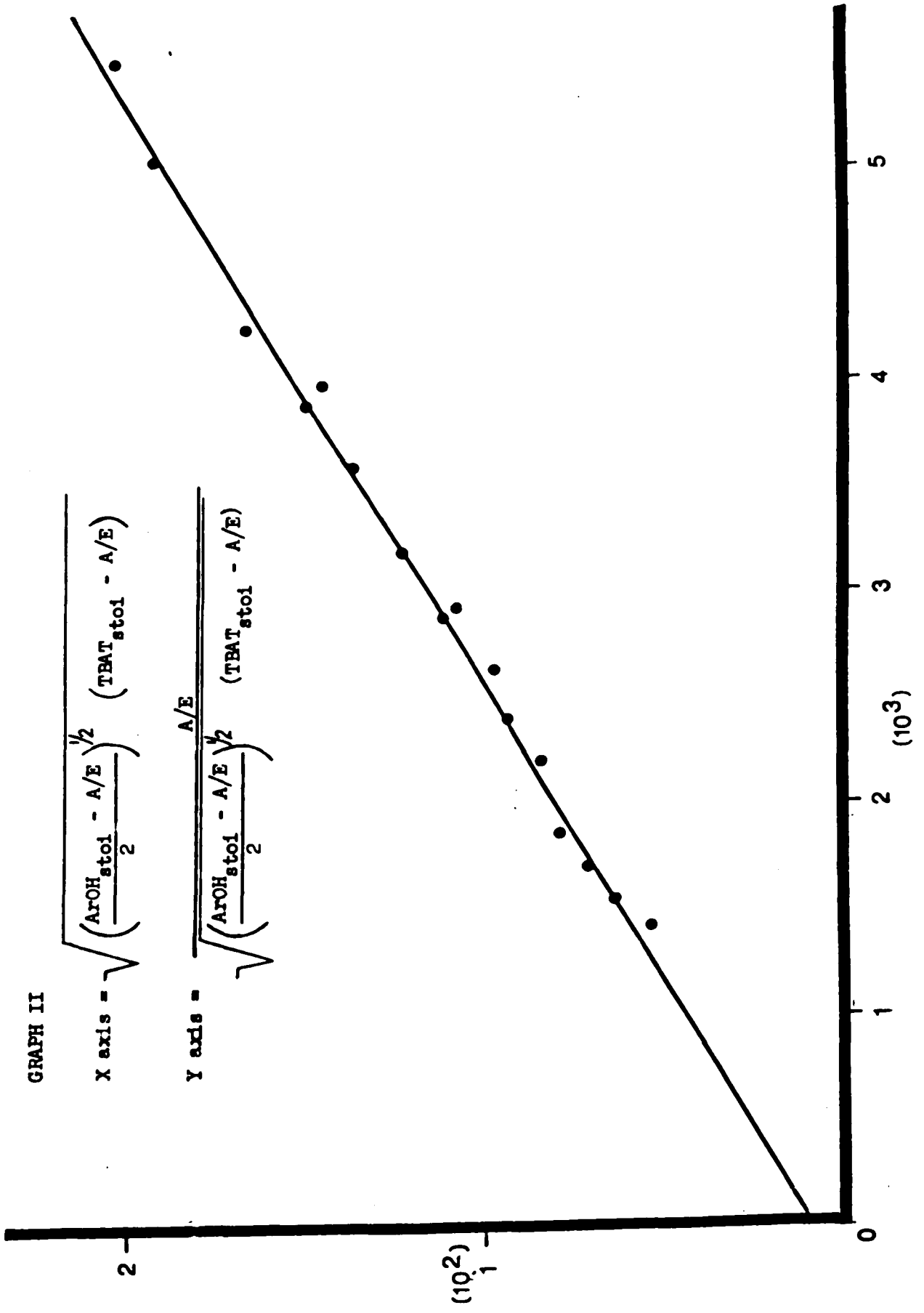
GRAPH II
X axis = $\sqrt{\left(\frac{ArOH_{stoi} - A/E}{2}\right)^{1/2} (TBAT_{stoi} - A/E)}$
Y axis = $\frac{A/E}{\sqrt{\left(\frac{ArOH_{stoi} - A/E}{2}\right)^{1/2} (TBAT_{stoi} - A/E)}}$
2
1
0
(10^2)
1
2
3
4
5
(10^3)

Evaluation of Equilibrium Constants (K and K_d)

Table 5 lists x and y values for all sixteen data points when n equals 2. A plot of x verses y for the 16 runs can be found in Graph II. The values of the slope (K) was determined to be 3.5722 $\pm$ 0.0746 l $mole^{-1}$. The value of the y-intercept ($\pm\sqrt{KK_d}$) was 7.8621 $\pm$ 2.45 x 10^{-4}, which yields a value of K_d of 1.7304 $\pm$ 0.168 x 10^{-7} M.

Since K and K_d do not have the same dimensions, the influence of each on the equilibrium can be seen more clearly by calculating the concentration of tetra-n-butylammonium-p-nitrophenoxide ion pair (formed by K_d), and can be calculated by rearranging equation 20 in the form of equation 46.

$$[ArO^-\text{---}{}^+N(Bu)_4] = (KK_d\ (\frac{ArOH_{stoi} - A/E}{2})^{1/2}\ x\ (TBAT_{stoi} - (A/E))^{1/2}$$

(eqn 46)

TABLE 6: The Percentage of ArO^----Bu_4N^+ Ion Pair in the Product Mixture

Run#	total p-nitrophenoxide (10^5)	percent as ArO^----Bu_4N^{+a}
E1	0.78693	14.35
E2	1.8503	9.31
E3	3.2116	7.19
E4	5.7809	5.41
E5	1.2143	11.04
E6	2.5885	8.04
E7	4.9197	5.73
E8	9.6093	4.14
E9	1.0089	12.18
E10	2.2271	8.43
E11	3.9034	6.41
E12	6.9993	4.75
E13	1.4850	9.85
E14	3.1967	7.08
E15	5.8346	5.26
E16	11.115	3.90

a) % of ArO^----$^+N(Bu)_4$ as a fraction of total p-nitrophenoxide ion present at equilibrium.

Table 6 lists the percentage of tetra-n-butylammonium-p-nitrophenoxide ion pair (as a fraction of the total p-nitrophenoxide concentration (A/E)) for each of my data points. The percentage of ion pair in a product mixture shows a steady decrease as the total p-nitrophenoxide concentration (A/E) increases. This phenomena is typical of equilibrium reactions of the form

$$A \overset{K}{\Longleftrightarrow} B + C$$

where

$$K = \frac{[B]\,[C]}{[A]} = \frac{[B]^2}{[A]}$$

It can be shown mathematically that at any given equilibrium constant K, as the equilibrium concentration of A increases, the percentage of B (or C) in the equilibrium mixture decreases (Table 6.1).

TABLE 6.1 Percentage of B in the Equilibrium Mixture at Increasing Equilibrium Concentrations of A

K	[A]^a	[B]^a	Percent B in Equil mixture
.1	5	0.707	12.4
.1	20	1.414	6.6
.1	64	2.53	3.8

a) equilibrium concentrations

Therefore, the results in Table 6 are compatible with our assumption that the ion aggregate (I) dissociates into two distinct kinetic species (II and III).

Spectra of Ion Pairs

On observing the spectrum of 2,4-dinitrophenol in chloroform, Pearson (3) found that in the presence of excess triethyl or diethylamine, two absorption peaks were apparent (360 and 400nm). He assumed that these peaks were due to the ammonium-2,4-dinitrophenolate ion pair. However, both peaks in the spectrum of tetraethylammonium-2,4-dinitrophenolate ion pair in chloroform, were shifted to higher wavelengths (370 and 429nm). He proposed that this effect was due to the fact that there was no proton coordinated to the anion in the tetraethylammonium-2,4-dinitrophenolate ion pair.

The results I obtained in 95.3 mole % dioxane-water

indicate that the tetra-n-butylammonium-4-nitrophenolate ion pair (Bu_4N^+---$^-$OAr) and the tetra-n-butylammonium-2-ammonium ethanesulfonate-4-nitrophenolate ion aggregate [ArO^----$H_3^+NCH_2CH_2SO_3^-$---Bu_4N^+] have the same absorbance maximum (λ_{max}= 408nm) and molar absorptivity (2.5073 x 10^4 l $mole^{-1}$). The identical spectra obtained for the ion pair and ion aggregate are probably due to the small amount of water in my solvent which allows protons to be H-bonded to the 4-nitrophenoxide ion in both species. The solvent is therefore exerting a "leveling effect" by forming hydrogen bonds to the p-nitrophenoxide ion which should not occur in aprotic solvent systems.

Association Between p-Nitrophenol and TBAT in 95.3 Mole % Dioxane-Water

Rivetti (5) found that in benzene the λ_{max} of p-nitrophenol shifts from 305 to 320nm on addition of excess imidazole. This observation was taken as an indication (6) of association through rather strong N---HOAr bonds of the solute molecules.

My observations in 95.3 mole % dioxane-water show no apparent association between amine and p-nitrophenol in the experimental concentration range. A 9.999 x 10^{-4} M solution of p-nitrophenol has a λ_{max} at 308nm in 95.3 mole % dioxane-water. On addition of tetra-n-butylammonium taurinate (TBAT) up to 4.6806 x 10^{-3} M the absorption peak of un-ionized p-nitrophenol showed no shift to longer

wavelength (Table 6.2).

In an analogous experiment in which benzylamine was used as the base, small shifts in the p-nitrophenol absorption peak were detected. At benzylamine concentrations of 1.68×10^{-1} M and 3.34×10^{-1} M, the λ_{max} of p-nitrophenol shifted to 312 and 314nm respectively (Table 6.3). These small shifts observed at higher benzylamine concentrations may be due to either a change in the character of the solvent system, or the formation of hydrogen bonds between p-nitrophenol and benzylamine ($ArOH---H_2NCH_2Ar$).

TABLE 6.2 Absorption Bands[a] of p-Nitrophenol (ArOH) and p-Nitrophenoxide (ArO^-) ion[b] in the presence of TBAT (V)

C_i (10^5) ArOH	C_i (10^3) TBAT	λ_{max} (nm) ArOH	λ_{max} (nm) ArO^-
4.999		308.5	
9.999	4.6806	308	408
9.999	1.8722	308	408
9.999	.93612	308	408
9.999	.37444	308	408

a) determined on a Perkin-Elmer model 402 U.V.-Vis Spectrophotometer

b) λ_{max} of Bu_4N^+---ArO^- ion pair (2.00 x 10^{-3} M) is 408nm.

C_i = Initial Concentration

TAPLE 6.3 Absorption Band[a] of p-Nitrophenol (ArOH) in the presence of High Concentrations of Benzylamine [b] (VII)

C_i (10^4) ArOH	C_i (10^1) Benzylamine	λ_{max} (nm.) ArOH
1.0833	3.3404	314
1.0833	1.6823	312
1.0833	.16824	308

a) determined on a Perkin-Elmer model 402 U.V.-Vis Spectrophotometer

b) No p-nitrophenoxide ion (λ_{max}= 408nm) was detected

C_i = Initial Concentration

Other Equilibrium Expressions

I have also considered the possibility that the initial state may, in fact, consist of a hydrogen bonded complex between p-nitrophenol and TBAT. Ionization schemes leading from the hydrogen bonded complex to ion pairs are represented by equations 47, 48, and 49 and calculated from equations 47.1, 48.1, and 49.1.

$$ArOH\text{---}TBAT \overset{K'}{<===>} ArO^-\text{---}H_3^+NCH_2CH_2SO_3^-\text{---}N^+(Bu)_4 \qquad \text{(eqn 47)}$$

$$K' = \frac{[ArO^-\text{---}H_3^+NCH_2CH_2SO_3^-\text{---}N^+(Bu)_4]}{[ArOH\text{---}TBAT]} \qquad \text{(eqn 47.1)}$$

$$ArOH\text{---}TBAT \overset{K''}{<===>} Bu_4N^+\text{---}^-OAr + H_3^+NCH_2CH_2SO_3^- \qquad \text{(eqn 48)}$$

$$K'' = \frac{[Bu_4N^+ \cdots {}^-OAr]\ [H_3^+NCH_2CH_2SO_3^-]}{[ArOH \cdots TBAT]} \qquad \text{(eqn 48.1)}$$

$$ArOH\cdots TBAT \overset{K'''}{\Longleftrightarrow} ArO^-\cdots H_3^+NCH_2CH_2SO_3^-\cdots Bu_4N^+ \overset{K_d}{\Longleftrightarrow}$$
$$(Bu)_4N^+\cdots {}^-OAr + H_3^+NCH_2CH_2SO_3^- \qquad \text{(eqn 49)}$$

$$\frac{A/E}{(ArOH_{stoi}-A/E)^{1/2}} = K''' \frac{(ArOH_{stoi}-A/E)}{(ArOH_{stoi}-A/E)^{1/2}} \pm (K'''K_d)^{1/2}$$

(eqn 49.1)

Comparison of equilibrium constants obtained for both K' (eqn 47.1) and K'' (eqn 48.1) showed substantial inconsistancies at different concentrations (Table 7). The slope (K''') determined from equation 49.1 was found to be negative, and have an extremely poor correlation coefficient (Table 7.1).

My data lead me to conclude that a hydrogen bonded complex between p-nitrophenol and TBAT can not be considered an important kinetic species in 95.3 mole % dioxane-water.

TABLE 7: Equilibrium Constants Determined from Equations 47.1 (K'') and 48.1 (K')

Run	K' (10^7)	K'' (10^2)
E1	7.83	9.95
E2	50.0	27.0
E3	188	58.5
E4	1147	198
E5	9.12	7.51
E6	45.3	17.5
E7	194	39.4
E8	1186	123

TABLE 7.1 Slope and Correlation Coeff Evaluations[c] from Equation 49.1.

Run	Y axis (10^4)[a]	X axis (10^3)[b]
E1	8.849	8.892
E2	22.37	8.273
E3	43.37	7.405
E4	107.1	5.398
E5	9.548	12.72
E6	21.28	12.16
E7	44.06	11.17
E8	108.9	8.820

a) Y axis = $A/E \;/\; (ArOH_{stoi}-A/E)^{1/2}$

b) X axis = $(ArOH_{stoi}-A/E) / (ArOH_{stoi}-A/E)^{1/2}$

c) slope = -9.71×10^{-1} ; correlation coefficient = 0.60

Conclusion

The following conclusions can be drawn from the experimental results for the ionization of p-nitrophenol by tetra-n-butylammonium taurinate (TBAT) in 95.3 mole % dioxane-water.

1.) p-Nitrophenol exists as a dimer in 95.3 mole % dioxane-water.

2.) The formation of an ion aggregate (formed by association of two ions and a zwitterion) is found to be an important kinetic species in this equilibrium.

3.) This ion aggregate can dissociate into two separate kinetic species (an ion pair and a zwitterion).

4.) Equilibrium constants for formation and dissociation of the ion aggregate have been calculated.

Experimental

Solvents.

Water was deionized and filtered through a Milli-Q water purification system (Millipore Corp.). Purification of 1,4-dioxane (Baker Analyzed Reagent) was accomplished by passing solvent through a 40 cm. (height) by 4 cm. (diameter) column of activated alumina (Alcoa), and collecting under nitrogen. The dioxane was tested at one liter intervals for peroxides (2% aq. KI), n_D^{20} = 1.4229 (lit(18): n_D^{20} = 1.4224). The 95.3 mole % dioxane-water was prepared by weight and deaerated for twenty minutes with CO_2 free nitrogen. the dioxane and 95.3 mole % dioxane-water, were stored in brown glass containers under nitrogen, and used within three days.

Materials.

Melting and boiling points are uncorrected. Taurine (Aldrich), was recrystallized from water and dried at 100 °C in vacuo. Benzylamine (Eastman) was purified by drying over KOH pellets and then distilled from KOH in an all glass apparatus under nitrogen, b.p. 180-81 °C (lit(19): bp 184.6-185.2 °C (771 torr)), n_D^{20} = 1.5441 (lit(20): n_D^{20} = 1.5438). p-Nitrophenol (Fisher) was recrystallized from 2% aqueous HCL and dried at 78 °C in vacuo, mp 113-114 °C (lit(21): mp 115-115.6 °C). Crystals were stored in the dark under nitrogen. Tetra-n-butylammonium bromide (East-

man) was recrystallized twice from a 3:1 by volume ethylacetate-ether solution, and dried at 78 °C in vacuo, mp 118-119 °C (lit(22): mp 118.5 °C). Tetra-n-butylammonium hydroxide (Eartman), 0.4 M solution in water, and silver(I) oxide (Baker Analyzed Reagent) were used without further purification. Tetra-n-butylammonium taurinate (TBAT) was prepared as in Part I of this work. (see Experimental pp 72).

Spectra.

Absorbance measurements were made with a Cary 17 and Perkin-Elmer Model 402 U.V.-Visible spectrophotometer. Each was equipped with a thermostatted cuvette holder through which water was circulated at 25.0 ± 0.1 °C.

Computations.

Calculations were carried out on an IBM 360-50 computer and PL/C compiler.

Evaluation of p-Nitrophenol-p-Nitrophenoxide Equilibrium Constants in 95.3 mole % Dioxane-Water at 25 °C.

The fcllowing procedure is typical of that used throughout my experimental runs. A 4.000×10^{-4} M solution of p-nitrophenol and 3.7444×10^{-3} M solution of tetra-n-butylammonium taurinate (TBAT, V) were prepared by weight and successive dilution in 95.3 mole % dioxane-water. Separate solutions of p-nitrophenol and amine were equili-

brated at 25.0 °C in a thermostatted bath. The spectrophotometer was adjusted to zero absorbance at 408 nm (visible region) with solvent. Ten milliliter aliquots of each solution were mixed in a 50 ml Erlenmeyer flask. The spectrophotometer cell was rinsed with this solution, and the filled cell was stoppered and placed in the thermostatted spectrophotometer cell compartment. The solution was allowed to equilibrate at 25 °C, until a horizontal absorbance plot versus time was achieved at 408 nm (Table 8).

The molar absorptivity of the tetra-n-butylammonium-p-nitrophenoxide ion pair in 95.3 mole % dioxane-water was determined in a separate experiment. A twenty milliliter aliquot of 2.3952 x 10^{-4} M p-nitrophenol (prepared by weight) was diluted to 100 milliliters with a 4.0 x 10^{-3} M solution of tetra-n-butylammonium hydroxide (prepared by dilution of a 0.4 M aqueous $BU_4N^+OH^-$ with dioxane). The molar absorptivity of the ion pair in 95.3 mole % dioxane-water at 408 nm (λ_{max}) was 25,092 l mole^{-1}.

The molar absorptivity of the tetra-n-butylammonium-2-ammoniumethylsulfonate-p-nitrophenoxide ion aggregate was determined by dilution of a 2 ml aliquot of 1.2171 x 10^{-4} M p-nitrophenol (prepared by weight) with successively higher concentrations of tetra-n-butylammonium taurinate, until a maximum absorbance at 408 nm (λ_{max}) was achieved. The highest concentration of tetra-n-butylammonium taurinate used was 2.8795 x 10^{-2} M (prepared

by weight), which gave a molar absorptivity for the ion aggregate of 25,048 l $mole^{-1}$ (a 0.17% difference from the molar absorptivity of the tetra-n-butylammonium-p-nitrophenoxide ion pair).

TABLE 8: Absorbance of p-Nitrophenoxide[a] (at 408 nm) in 95.3 Mole % Dioxane-Water at 25°C

Run	C_i (M) PNP (10^5)	C_i (M) TBAT (10^4)	Absorbance (408 nm)
E1	8.6946	3.3573	0.1945
E2	"	8.3933	0.4573
E3	"	16.787	0.7938
E4	"	41.967	1.429
E5	17.389	3.3573	0.3002
E6	"	8.3933	0.6398
E7	"	16.787	1.216
E8	"	41.967	2.375
E9	9.9993	3.7445	0.2532
E10	"	9.3612	0.5588
E11	"	18.722	0.9795
E12	"	46.806	1.756
E13	19.998	3.7445	0.3726
E14	"	9.3612	0.8021
E15	"	18.722	1.464
E16	"	46.806	2.789

a) Runs E1-E8 and E9-E16 were run on separate occasions. The molar absorptivities of p-nitrophenoxide at 408 nm were 24,717.7 M^{-1} and 25,092.6 M^{-1}, respectively

b) C_i = initial conc. ; PNP = p-nitrophenol

TABLE 1

Run[a] K142 Solvent Water Ester[d] PNPB Amine Sodium Taurinate

Ester conc 4.0581×10^{-5} M

Amine conc 3.7249×10^{-4} M

Time (sec)	Absorbance[b,c]	conc of Phenoxide (10^5)	% Reaction
60.0	0.1401	0.7665	18.9
68.0	0.1573	0.8604	21.2
78.0	0.1786	0.9770	24.1
88.0	0.1971	1.079	26.6
102.0	0.2226	1.218	30.0
116.0	0.2459	1.345	33.1
132.0	0.2703	1.479	36.4
150.0	0.2956	1.617	39.9
170.0	0.3210	1.756	43.3
192.0	0.3453	1.889	46.6
216.0	0.3710	2.030	50.0
242.0	0.3962	2.168	53.4
270.0	0.4211	2.304	56.8
302.0	0.4470	2.445	60.3
338.0	0.4716	2.580	63.6
374.0	0.4937	2.701	66.6
422.0	0.5209	2.850	70.2
476.0	0.5464	2.990	73.7
538.0	0.5706	3.122	76.9

a) second order aminolysis rate constant equals 1.61 $\pm$ 0.06

b) Kinetic analysis performed on a Cary 17 U.V.-Visible spectrophotometer absorbance range 0.5

c) $E_{phenoxide} = 1.8278 \times 10^4\ M^{-1}$

d) PNPB = charged ester IV

TABLE 2

Run[a] K143 Solvent Water Ester[d] PNPP Amine Sodium Taurinate

Ester conc 4.0581×10^{-5} M

Amine conc 1.8624×10^{-3} M

Time (sec)	Absorbance[b,c]	conc of Phenoxide (10^5)	% Reaction
42.0	0.2622	1.435	35.4
46.0	0.2806	1.535	37.8
50.0	0.3001	1.642	40.5
55.0	0.3212	1.758	43.3
60.0	0.3423	1.873	46.2
65.0	0.3607	1.973	48.6
70.0	0.3788	2.073	51.1
75.0	0.3948	2.160	53.2
80.0	0.4108	2.248	55.4
85.0	0.4270	2.336	57.6
91.0	0.4436	2.427	59.8
98.0	0.4621	2.528	62.3
105.0	0.4795	2.623	64.6
114.0	0.4992	2.731	67.3
133.0	0.5377	2.942	72.5
145.0	0.5564	3.044	75.0
158.0	0.5754	3.148	77.6
177.0	0.6008	3.287	81.0

a) second order aminolysis rate constant equals 1.67 $\pm$ 0.06

b) Kinetic analysis performed on a Cary 17 U.V.-Visible spectrophotometer absorbance range 0.5

c) $\varepsilon_{phenoxide} = 1.8278 \times 10^4\ M^{-1}$

d) PNPB = charged ester IV

TABLE 3

Run[a] K150 Solvent Water Ester[d] PNPT Amine Sodium Taurinate

Ester conc 4.4386×10^{-5} M

Amine conc 2.1219×10^{-3} M

Time (sec)	Absorbance[b,c]	conc of Phenoxide (10^5)	% Reaction
45.0	0.3266	1.787	40.3
49.0	0.3463	1.895	42.7
53.0	0.3654	1.999	45.0
57.0	0.3856	2.109	47.5
62.0	0.4081	2.232	50.3
67.0	0.4282	2.343	52.8
72.0	0.4495	2.459	55.4
78.0	0.4704	2.574	58.0
84.0	0.4917	2.690	60.6
100.0	0.5377	2.942	66.3
109.0	0.5592	3.059	68.9
117.0	0.5781	3.163	71.3
125.0	0.5965	3.264	73.5
136.0	0.6164	3.373	76.0
149.0	0.6407	3.504	79.0

a) second order aminolysis rate constant equals 1.44 $\pm$ 0.06

b) Kinetic analysis performed on a Cary 17 U.V.-Visible spectrophotometer absorbance range 0.5

c) $E_{phenoxide} = 1.8278 \times 10^4\ M^{-1}$

d) PNPB = charged ester IV

TABLE 4

Run[a]	Solvent	Ester[d]	Amine
K148	Water	PNPP	Sodium Taurinate

Ester conc 4.4386×10^{-5} M

Amine conc 3.1829×10^{-4} M

Time (sec)	Absorbance[b,c]	conc of Phenoxide (10^5)	% Reaction
70.0	0.1628	0.8906	20.1
84.0	0.1886	1.032	23.3
98.0	0.2147	1.175	26.5
114.0	0.2409	1.318	29.7
130.0	0.2656	1.453	32.7
148.0	0.2902	1.588	35.8
170.0	0.3177	1.738	39.2
190.0	0.3416	1.869	42.1
214.0	0.3672	2.009	45.3
240.0	0.3927	2.148	48.4
270.0	0.4199	2.297	51.8
302.0	0.4451	2.435	54.9
338.0	0.4732	2.589	58.3
405.0	0.5154	2.820	63.5
455.0	0.5412	2.961	66.7
509.0	0.5659	3.096	69.8
575.0	0.5912	3.234	72.9
681.0	0.6261	3.425	77.2

a) second order aminolysis rate constant equals 1.42 $\pm$ 0.05

b) Kinetic analysis performed on a Cary 17 U.V.-Visible spectrophotometer absorbance range 0.5

c) $E_{phenoxide} = 1.8278 \times 10^4\ M^{-1}$

d) PNPB = charged ester IV

TABLE 5

Run[a]	Solvent	Ester[d]	Amine
K91	Water	PNPB	Benzylamine

Ester conc 6.6547×10^{-5} M

Amine conc 3.2865×10^{-4} M

Time (sec)	Absorbance[b,c]	conc of Phenoxide (10^5)	% Reaction
70.0	0.301	1.907	28.7
88.2	0.350	2.217	33.3
106.3	0.402	2.546	38.3
124.5	0.441	2.793	42.0
148.7	0.495	3.136	47.1
178.9	0.552	3.497	52.5
212.1	0.603	3.820	57.4
242.4	0.645	4.086	61.4
296.8	0.704	4.459	67.0
342.1	0.748	4.738	71.2
438.9	0.821	5.200	78.1

a) second order aminolysis rate constant equals 2.80 $\pm$ 0.17

b) Kinetic analysis performed on a Perkin-Elmer Model 202 U.V.-Visible spectrophotometer

c) $E_{phenoxide} = 1.5787 \times 10^4\ M^{-1}$

d) PNPB = charged ester IV

TABLE 6

Run[a] K92	Solvent Water	Ester[d] PNPB	Amine Benzylamine

Ester conc 6.6547×10^{-5} M

Amine conc 6.5730×10^{-4} M

Time (sec)	Absorbance[b,c]	conc of Phenoxide (10^5)	% Reaction
65.0	0.427	2.705	40.6
83.2	0.500	3.167	47.6
101.3	0.572	3.623	54.4
113.4	0.602	3.813	57.3
131.6	0.648	4.105	61.7
149.0	0.689	4.364	65.6
173.9	0.740	4.687	70.4
207.1	0.801	5.074	76.2
231.3	0.831	5.264	79.1
337.1	0.930	5.891	88.5

a) second order aminolysis rate constant equals 2.95 $\pm$ 0.20

b) Kinetic analysis performed on a Perkin-Elmer Model 202 U.V.-Visible spectrophotometer

c) $E_{phenoxide} = 1.5787 \times 10^4\ M^{-1}$

d) PNPB = charged ester IV

TABLE 7

Run[a]	Solvent	Ester[d]	Amine
K138	Water	PNPB	Benzylamine

Ester conc 4.0496×10^{-5} M

Amine conc 2.2716×10^{-4} M

Time (sec)	Absorbance[b,c]	conc of Phenoxide (10^5)	% Reaction
55.0	0.1389	0.7611	18.8
69.0	0.1657	0.9079	22.4
81.0	0.1889	1.035	25.6
97.0	0.2151	1.179	29.1
113.0	0.2417	1.325	32.7
129.0	0.2650	1.452	35.9
147.0	0.2894	1.586	39.2
169.0	0.3152	1.727	42.7
191.0	0.3408	1.868	46.1
215.0	0.3647	1.998	49.3
243.0	0.3901	2.138	52.8
273.0	0.4157	2.278	56.2
307.0	0.4393	2.407	59.4
345.0	0.4647	2.547	62.9
389.0	0.4901	2.686	66.3
440.0	0.5164	2.830	69.9
498.0	0.5408	2.963	73.2
576.0	0.5672	3.108	76.7

a) second order aminolysis rate constant equals 2.76 $\pm$ 0.10

b) Kinetic analysis performed on a Cary 17 U.V.-Visible spectrophotometer absorbance range 0.5

c) $E_{phenoxide} = 1.8278 \times 10^4\ M^{-1}$

d) PNPB = charged ester IV

TABLE 8

Run[a] K139	Solvent Water	Ester[d] PNPB	Amine Benzylamine

Ester conc 4.0496×10^{-5} M

Amine conc 1.1358×10^{-3} M

Time (sec)	Absorbance[b,c]	conc of Phenoxide (10^5)	% Reaction
51.0	0.3094	1.693	41.8
55.0	0.3272	1.790	44.2
58.0	0.3398	1.859	45.9
62.0	0.3571	1.954	48.3
66.0	0.3731	2.041	50.4
71.0	0.3927	2.148	53.0
76.0	0.4104	2.245	55.4
81.0	0.4264	2.333	57.6
87.0	0.4451	2.435	60.1
94.0	0.4657	2.548	62.9
102.0	0.4864	2.661	65.7
110.0	0.5061	2.769	68.4
126.0	0.5403	2.956	73.0
135.0	0.5564	3.044	75.2
147.0	0.5758	3.150	77.8
161.0	0.5955	3.258	80.4
177.0	0.6156	3.368	83.2

a) second order aminolysis rate constant equals 2.62 $\pm$ 0.10

b) Kinetic analysis performed on a Cary 17 U.V.-Visible

spectrophotometer absorbance range 0.5

c) $E_{phenoxide} = 1.8278 \times 10^4\ M^{-1}$

d) PNPB = charged ester IV

TABLE 9

Run[a] K153	Solvent Water	Ester[d] PNPB	Amine Benzylamine
Ester conc 4.2416×10^{-5} M		Amine conc 2.0080×10^{-4} M	

Time (sec)	Absorbance[b,c]	conc of Phenoxide (10^5)	% Reaction
55.0	0.1519	0.8313	19.6
67.0	0.1756	0.9608	22.7
81.0	0.2030	1.111	26.2
95.0	0.2259	1.236	29.1
111.0	0.2520	1.379	32.5
127.0	0.2764	1.512	35.7
145.0	0.3005	1.644	38.8
165.0	0.3254	1.780	42.0
187.0	0.3498	1.914	45.1
213.0	0.3769	2.062	48.6
241.0	0.4017	2.198	51.8
269.0	0.4260	2.331	54.9
301.0	0.4503	2.464	58.1
339.0	0.4759	2.604	61.4
405.0	0.5154	2.820	66.5
457.0	0.5403	2.956	69.7
517.0	0.5657	3.095	73.0
589.0	0.5912	3.234	76.3
671.0	0.6152	3.366	79.4

a) second order aminolysis rate constant equals 2.95 $\pm$

0.11

b) Kinetic analysis performed on a Cary 17 U.V.-Visible spectrophotometer absorbance range 0.5

c) $E_{phenoxide} = 1.8278 \times 10^4\ M^{-1}$

d) PNPB = charged ester IV

TABLE 10

Run[a] K155	Solvent Water	Ester[d] PNPB	Amine Benzylamine
Ester conc 4.2416×10^{-5} M		Amine conc 1.0040×10^{-3} M	
Time (sec)	Absorbance[b,c]	conc of Phenoxide (10^5)	% Reaction
48.0	0.3098	1.695	40.0
52.0	0.3297	1.804	42.5
57.0	0.3520	1.926	45.4
61.0	0.3690	2.019	47.6
67.0	0.3921	2.145	50.6
73.0	0.4161	2.277	53.7
79.0	0.4363	2.387	56.3
85.0	0.4558	2.494	58.8
91.0	0.4738	2.592	61.1
115.0	0.5371	2.939	69.3
124.0	0.5556	3.040	71.7
134.0	0.5756	3.149	74.2
146.0	0.5955	3.258	76.8
160.0	0.6152	3.366	79.4

a) second order aminolysis rate constant equals 2.97 $\pm$ 0.10

b) Kinetic analysis performed on a Cary 17 U.V.-Visible spectrophotometer absorbance range 0.5

c) $E_{phenoxide} = 1.8278 \times 10^4\ M^{-1}$

d) PNPB = charged ester IV

TABLE 11

Run[a]	Solvent	Ester[d]	Amine
K93	Water	PNPH	Benzylamine

Ester conc 6.2456×10^{-5} M

Amine conc 6.5730×10^{-4} M

Time (sec)	Absorbance[b,c]	conc of Phenoxide (10^5)	% Reaction
146.5	0.144	0.9121	14.6
195.0	0.185	1.172	18.7
258.4	0.240	1.520	24.3
318.9	0.287	1.818	29.1
400.5	0.345	2.185	35.0
492.1	0.400	2.534	40.6
570.8	0.442	2.800	44.8
678.4	0.495	3.135	50.2
810.3	0.550	3.484	55.8
1062.1	0.634	4.016	64.3
1296.3	0.698	4.421	70.8
1566.3	0.758	4.801	76.9

a) second order aminolysis rate constant equals 1.23 $\pm$ 0.04

b) Kinetic analysis performed on a Perkin-Elmer Model 202 U.V.-Visible spectrophotometer

c) $E_{phenoxide} = 1.5787 \times 10^4\ M^{-1}$

d) PNPH = p-nitrophenyl hexanoate (VI)

TABLE 12

Run[a]	Solvent	Ester[d]	Amine
K95	Water	PNPH	Benzylamine

Ester conc: 6.2456×10^{-5} M

Amine conc: 3.2865×10^{-3} M

Time (sec)	Absorbance[b,c]	conc of Phenoxide (10^5)	% Reaction
62.0	0.262	1.660	26.6
80.2	0.318	2.014	32.3
98.3	0.380	2.407	38.5
116.5	0.429	2.717	43.5
134.6	0.470	2.977	47.7
152.8	0.513	3.250	52.0
177.0	0.562	3.560	57.0
202.1	0.608	3.851	61.7
238.4	0.661	4.187	67.0
274.7	0.705	4.466	71.5
326.1	0.762	4.827	77.3

a) second order aminolysis rate constant equals 1.27 $\pm$ 0.08

b) Kinetic analysis performed on a Perkin-Elmer Model 202 U.V.-Visible spectrophotometer

c) $E_{phenoxide} = 1.5787 \times 10^4\ M^{-1}$

d) PNPH = p-nitrophenyl hexanoate (VI)

TABLE 13

Run[a] K140 Solvent Water Ester[d] PNPH Amine Benzylamine

Ester conc 3.2526×10^{-5} M Amine conc 5.6790×10^{-4} M

Time (sec)	Absorbance[b,c]	conc of Phenoxide (10^5)	% Reaction
189.0	0.1042	0.5700	17.5
229.0	0.1239	0.6780	20.8
285.0	0.1500	0.8204	25.2
345.0	0.1758	0.9619	29.6
405.0	0.1995	1.091	33.6
473.0	0.2253	1.233	37.9
549.0	0.2506	1.371	42.2
633.0	0.2760	1.510	46.4
717.0	0.3003	1.643	50.5
813.0	0.3258	1.782	54.8
925.0	0.3508	1.919	59.0
1048.0	0.3753	2.053	63.1
1176.0	0.4007	2.193	67.4
1348.0	0.4260	2.331	71.7
1556.0	0.4509	2.467	75.8
1794.0	0.4757	2.603	80.0

a) second order aminolysis rate constant equals 1.22 $\pm$ 0.04

b) Kinetic analysis performed on a Cary 17 U.V.-Visible spectrophotometer absorbance range 0.5

c) $E_{phenoxide} = 1.8278 \times 10^4\ M^{-1}$

d) PNPH = p-nitrophenyl hexanoate (VI)

TABLE 14

Run[a] K141 Solvent Water Ester[d] PNPH Amine Benzylamine

Ester conc 3.2526×10^{-5} M Amine conc 4.5432×10^{-3} M

Time (sec)	Absorbance[b,c]	conc of Phenoxide (10^5)	% Reaction
62.0	0.1504	0.8226	25.3
69.0	0.1719	0.9403	28.9
76.0	0.1914	1.047	32.2
84.0	0.2111	1.155	35.5
92.0	0.2309	1.263	38.8
101.0	0.2516	1.376	42.3
110.0	0.2703	1.479	45.5
120.0	0.2910	1.592	49.0
131.0	0.3110	1.701	52.3
143.0	0.3311	1.812	55.7
155.0	0.3512	1.922	59.1
169.0	0.3710	2.030	62.4
184.0	0.3907	2.138	65.7
201.0	0.4104	2.245	69.0
220.0	0.4305	2.356	72.4
241.0	0.4515	2.470	75.9
265.0	0.4702	2.573	79.1
297.0	0.4910	2.686	82.6

a) second order aminolysis rate constant equals 1.28 $\pm$ 0.05

b) Kinetic analysis performed on a Cary 17 U.V.-Visible spectrophotometer absorbance range 0.5

c) $E_{phenoxide} = 1.8278 \times 10^4\ M^{-1}$

d) PNPH = p-nitrophenyl hexanoate (VI)

TABLE 15

Run[a] K156	Solvent Water	Ester[d] PNPH	Amine Benzylamine

Ester conc 3.7737×10^{-5} M

Amine conc 1.0040×10^{-3} M

Time (sec)	Absorbance[b,c]	conc of Phenoxide (10^5)	% Reaction
142.0	0.1513	0.8280	21.9
170.0	0.1762	0.9640	25.5
200.0	0.2011	1.100	29.2
230.0	0.2257	1.235	32.7
262.0	0.2506	1.371	36.3
298.0	0.2760	1.510	40.0
338.0	0.3005	1.644	43.6
382.0	0.3260	1.783	47.3
435.0	0.3554	1.944	51.5
479.0	0.3753	2.053	54.4
535.0	0.4006	2.192	58.1
599.0	0.4262	2.332	61.8
667.0	0.4509	2.467	65.4
747.0	0.4759	2.604	69.0
880.0	0.5110	2.796	74.1
1000.0	0.5363	2.934	77.8
1152.0	0.5629	3.080	81.6

a) second order aminolysis rate constant equals 1.34 $\pm$ 0.05

b) Kinetic analysis performed on a Cary 17 U.V.-Visible

spectrophotometer absorbance range 0.5

c) $E_{phenoxide} = 1.8278 \times 10^4\ M^{-1}$

d) PNPH = p-nitrophenyl hexanoate (VI)

TABLE 16

Run[a] K157	Solvent Water	Ester[d] PNPH	Amine Benzylamine

Ester conc 3.7737×10^{-5} M

Amine conc 5.0201×10^{-3} M

Time (sec)	Absorbance[b,c]	conc of Phenoxide (10^5)	% Reaction
57.0	0.2289	1.252	33.2
64.0	0.2516	1.376	36.5
70.0	0.2701	1.478	39.2
77.0	0.2901	1.587	42.1
84.0	0.3102	1.697	45.0
92.0	0.3313	1.813	48.0
101.0	0.3518	1.925	51.0
110.0	0.3727	2.039	54.0
119.0	0.3913	2.141	56.7
128.0	0.4104	2.245	59.5
139.0	0.4303	2.355	62.4
151.0	0.4503	2.464	65.3
163.0	0.4706	2.575	68.2
200.0	0.5195	2.842	75.3
225.0	0.5418	2.964	78.6
250.0	0.5612	3.070	81.4

a) second order aminolysis rate constant equals 1.23 $\pm$ 0.05

b) Kinetic analysis performed on a Cary 17 U.V.-Visible spectrophotometer absorbance range 0.5

c) $E_{phenoxide} = 1.8278 \times 10^4\ M^{-1}$

d) PNPH = p-nitrophenyl hexanoate (VI)

TABLE 17

Run[a] K146	Solvent Water	Ester[d] PNPH	Amine Sodium Taurinate

Ester conc 3.2526×10^{-5} M

Amine conc 1.8624×10^{-3} M

Time (sec)	Absorbance[b,c]	conc of Phenoxide (10^5)	% Reaction
134.0	0.1048	0.5732	17.6
206.0	0.1503	0.8226	25.3
246.0	0.1748	0.9565	29.4
298.0	0.2010	1.100	33.8
346.0	0.2253	1.233	37.9
406.0	0.2510	1.373	42.2
462.0	0.2758	1.509	46.4
530.0	0.3010	1.646	50.6
606.0	0.3256	1.781	54.7
690.0	0.3522	1.927	59.2
778.0	0.3757	2.055	63.2
886.0	0.4007	2.193	67.4
998.0	0.4256	2.329	71.6
1134.0	0.4511	2.468	75.9
1298.0	0.4757	2.603	80.0

a) second order aminolysis rate constant equals 0.378 $\pm$ 0.035

b) Kinetic analysis performed on a Cary 17 U.V.-Visible spectrophotometer absorbance range 0.5

c) $E_{phenoxide} = 1.8278 \times 10^4\ M^{-1}$

d) PNPH = p-nitrophenyl hexanoate (VI)

TABLE 18

Run[a] K147 Solvent Water Ester[d] PNPH Amine Sodium Taurinate

Ester conc 3.2526×10^{-5} M Amine conc 9.3123×10^{-3} M

Time (sec)	Absorbance[b,c]	conc of Phenoxide (10^5)	% Reaction
50.0	0.1316	0.7201	22.1
60.0	0.1540	0.8420	25.9
70.0	0.1766	0.9662	29.7
80.0	0.1963	1.074	33.0
90.0	0.2154	1.179	36.2
102.0	0.2368	1.295	39.8
114.0	0.2569	1.406	43.2
128.0	0.2802	1.533	47.1
142.0	0.2999	1.641	50.4
156.0	0.3206	1.754	53.9
176.0	0.3443	1.884	57.9
194.0	0.3656	2.000	61.5
218.0	0.3907	2.138	65.7
246.0	0.4153	2.272	69.9
282.0	0.4412	2.414	74.2
318.0	0.4657	2.548	78.3
368.0	0.4909	2.686	82.6

a) second order aminolysis rate constant equals 0.383 $\pm$ 0.015

b) Kinetic analysis performed on a Cary 17 U.V.-Visible

spectrophotometer absorbance range 0.5

c) $E_{phenoxide} = 1.8278 \times 10^4\ M^{-1}$

d) PNPH = p-nitrophenyl hexanoate (VI)

TABLE 19

Run[a]	Solvent	Ester[d]	Amine
K151	Water	PNPH	Sodium Taurinate

Ester conc: 3.8745×10^{-5} M

Amine conc: 2.1219×10^{-3} M

Time (sec)	Absorbance[b,c]	conc of Phenoxide (10^5)	% Reaction
149.0	0.1444	0.7902	20.4
181.0	0.1699	0.9295	24.0
217.0	0.1957	1.071	27.6
253.0	0.2220	1.215	31.3
289.0	0.2459	1.345	34.7
333.0	0.2723	1.490	38.5
377.0	0.2976	1.628	42.0
429.0	0.3254	1.780	45.9
481.0	0.3494	1.912	49.3
541.0	0.3761	2.058	53.1
597.0	0.4003	2.190	56.5
669.0	0.4266	2.334	60.2
741.0	0.4509	2.467	63.7
829.0	0.4771	2.610	67.4
929.0	0.5028	2.751	71.0
1125.0	0.5446	2.980	76.9
1317.0	0.5760	3.151	81.3

a) second order aminolysis rate constant equals 0.384 $\pm$ 0.015

b) Kinetic analysis performed on a Cary 17 U.V.-Visible

spectrophotometer absorbance range 0.5

c) $E_{phenoxide} = 1.8278 \times 10^4\ M^{-1}$

d) PNPH = p-nitrophenyl hexanoate (VI)

TABLE 20

Run[a]	Solvent	Ester[d]	Amine
K152	Water	PNPH	Sodium Taurinate

Ester conc 3.8745×10^{-5} M

Amine conc 1.0610×10^{-2} M

Time (sec)	Absorbance[b,c]	conc of Phenoxide (10^5)	% Reaction
50.0	0.1677	0.9176	23.7
60.0	0.1971	1.079	27.8
70.0	0.2240	1.225	31.6
80.0	0.2496	1.366	35.2
90.0	0.2747	1.503	38.8
102.0	0.3019	1.652	42.6
114.0	0.3277	1.793	46.3
126.0	0.3516	1.924	49.7
140.0	0.3788	2.073	53.5
156.0	0.4049	2.215	57.2
172.0	0.4303	2.355	60.8
192.0	0.4574	2.502	64.6
212.0	0.4807	2.630	67.9
250.0	0.5185	2.837	73.2
284.0	0.5456	2.985	77.0
322.0	0.5712	3.125	80.7

a) second order aminolysis rate constant equals 0.387 $\pm$ 0.012

b) Kinetic analysis performed on a Cary 17 U.V.-Visible spectrophotometer absorbance range 0.5

c) $E_{phenoxide} = 1.8278 \times 10^4\ M^{-1}$

d) PNPH = p-nitrophenyl hexanoate (VI)

TABLE 21

Run[a] K54 Solvent[d] D-W Ester[b] PNPB Amine Benzylamine

Ester conc 1.0055×10^{-4} M Amine conc 2.9996×10^{-3} M

Time (sec)	Absorbance[c,e]	conc of Phenol (10^5)	% Reaction
223.2	0.211	1.267	12.6
353.2	0.273	1.995	19.8
483.2	0.331	2.675	26.6
573.9	0.370	3.133	31.2
672.6	0.410	3.602	35.8
822.6	0.460	4.189	41.6
972.6	0.511	4.787	47.6
1122.6	0.557	5.327	53.0
1308.9	0.604	5.878	58.5
1548.2	0.654	6.465	64.3
1782.6	0.700	7.005	69.7
2208.2	0.768	7.803	77.6

a) Second order aminolysis rate constant equals 0.232 $\pm$ 0.001

b) PNPB = charged ester IV

c) $E_{ArOH} = 9.547 \times 10^3\ M^{-1}$; $E_{ester} = 1.024 \times 10^3\ M^{-1}$

d) D-W = 95.3 mole% dioxane-water

e) Kinetic analysis performed on a Perkin-Elmer Model 202 UV-Visible spectrophotometer

TABLE 22

Run[a] K56 Solvent[d] D-W Ester[b] PNPB Amine Benzylamine

Ester conc 1.0055×10^{-4} M Amine conc 2.9996×10^{-2} M

Time (sec)	Absorbance[c,e]	conc of Phenol (10^5)	% Reaction
54.0	0.349	2.886	28.7
72.2	0.420	3.719	37.0
84.3	0.467	4.271	42.5
96.4	0.507	4.740	47.1
108.5	0.550	5.245	52.2
126.6	0.598	5.808	57.8
144.8	0.642	6.324	62.9
175.0	0.705	7.063	70.2
198.2	0.749	7.580	75.4
228.4	0.795	8.119	80.7

a) Second order aminolysis rate constant equals 0.249 $\pm$ 0.003

b) PNPB = charged ester IV

c) $E_{ArOH} = 9.547 \times 10^3\ M^{-1}$; $E_{ester} = 1.024 \times 10^3\ M^{-1}$

d) D-W = 95.3 mole% dioxane-water

e) Kinetic analysis performed on a Perkin-Elmer Model 202 UV-Visible spectrophotometer

TABLE 23

Run[a]	Solvent[d]	Ester[b]	Amine
K72	D-W	PNPB	Benzylamine

Ester conc 9.9716×10^{-5} M

Amine conc 2.9945×10^{-3} M

Time (sec)	Absorbance[c,e]	conc of Phenol (10^5)	% Reaction
153.6	0.187	0.9547	9.6
258.4	0.242	1.603	16.1
318.9	0.271	1.945	19.5
423.7	0.322	2.546	25.5
528.4	0.367	3.076	30.9
627.1	0.408	3.560	35.7
762.1	0.455	4.114	41.3
858.9	0.486	4.479	44.9
978.7	0.528	4.974	49.9
1188.9	0.579	5.575	55.9
1488.4	0.652	6.436	64.5
1758.7	0.702	7.025	70.4

a) Second order aminolysis rate constant equals 0.236 $\pm$ 0.001

b) PNPB = charged ester IV

c) $E_{ArOH} = 9.547 \times 10^3\ M^{-1}$; $E_{ester} = 1.063 \times 10^3\ M^{-1}$

d) D-W = 95.3 mole% dioxane-water

e) Kinetic analysis performed on a Perkin-Elmer Model 202 UV-Visible spectrophotometer

TABLE 24

Run[a] K73 Solvent[d] D-W Ester[b] PNPB Amine Benzylamine

Ester conc 9.9716×10^{-5} M Amine conc 2.9945×10^{-2} M

Time (sec)	Absorbance[c,e]	conc of Phenol (10^5)	% Reaction
70.0	0.392	3.371	33.8
82.1	0.435	3.878	38.9
94.2	0.477	4.373	43.9
106.3	0.523	4.915	49.3
124.5	0.575	5.528	55.4
142.6	0.622	6.082	61.0
166.8	0.669	6.636	66.5
185.0	0.704	7.048	70.7
206.1	0.748	7.567	75.9
236.3	0.788	8.039	80.6

a) Second order aminolysis rate constant equals 0.246 $\pm$ 0.003

b) PNPB = charged ester IV

c) $E_{ArOH} = 9.547 \times 10^3\ M^{-1}$; $E_{ester} = 1.063 \times 10^3\ M^{-1}$

d) D-W = 95.3 mole% dioxane-water

e) Kinetic analysis performed on a Perkin-Elmer Model 202 UV-Visible spectrophotometer

TABLE 25

Run[a] K128	Solvent[d] D-W	Ester[b] PNPB	Amine Benzylamine

Ester conc 1.1360×10^{-4} M

Amine conc 2.5208×10^{-3} M

Time (sec)	Absorbance[c,e]	conc of Phenol (10^5)	% Reaction
118.0	0.2206	0.9530	8.4
198.0	0.2506	1.267	11.2
286.0	0.3000	1.784	15.7
378.0	0.3512	2.322	20.4
482.0	0.4013	2.847	25.1
586.0	0.4515	3.372	29.7
690.0	0.5008	3.889	34.2
822.0	0.5525	4.430	39.0
958.0	0.6006	4.935	43.4
1102.0	0.6511	5.464	48.1
1290.0	0.7111	6.092	53.6
1474.0	0.7616	6.621	58.3
1662.0	0.8110	7.138	62.8
1890.0	0.8611	7.663	67.5
2174.0	0.9152	8.230	72.4

a) Second order aminolysis rate constant equals 0.239 $\pm$ 0.001

b) PNPB = charged ester IV

c) $E_{ArOH} = 1.0686 \times 10^4\ M^{-1}$; $E_{ester} = 1.1412 \times 10^3\ M^{-1}$

d) D-W = 95.3 mole% dioxane-water

e) Kinetic analysis performed on a Cary 17 UV-Visible spectrophotometer absorbance range 1.0

TABLE 26

Run[a]	Solvent[d]	Ester[b]	Amine
K129	D-W	PNPB	Benzylamine

Ester conc 1.1360×10^{-4} M

Amine conc 2.5208×10^{-2} M

Time (sec)	Absorbance[c,e]	conc of Phenol (10^5)	% Reaction
57.0	0.4349	3.198	28.2
67.0	0.4799	3.669	32.3
76.0	0.5209	4.099	36.1
85.0	0.5608	4.517	39.8
96.0	0.6034	4.963	43.7
106.0	0.6393	5.340	47.0
117.0	0.6803	5.770	50.8
130.0	0.7222	6.208	54.6
143.0	0.7609	6.613	58.2
158.0	0.8011	7.035	61.9
179.0	0.8524	7.572	66.7
197.0	0.8923	7.990	70.3
218.0	0.9313	8.400	73.9
242.0	0.9704	8.809	77.5

a) Second order aminolysis rate constant equals 0.251 $\pm$ 0.001

b) PNPB = charged ester IV

c) $E_{ArOH} = 1.0686 \times 10^4\ M^{-1}$; $E_{ester} = 1.1412 \times 10^3\ M^{-1}$

d) D-W = 95.3 mole% dioxane-water

e) Kinetic analysis performed on a Cary 17 UV-Visible

spectrophotometer absorbance range 1.0

TABLE 27

Run[a] K75 Solvent[d] D-W Ester[b] PNPH Amine Benzylamine

Ester conc 1.4417×10^{-4} M Amine conc 2.9945×10^{-2} M

Time (sec)	Absorbance[c,e]	conc of Phenol (10^5)	% Reaction
276.1	0.244	0.5156	3.6
756.1	0.317	1.412	9.8
1074.7	0.361	1.952	13.5
1326.8	0.396	2.382	16.5
1722.1	0.450	3.044	21.1
2046.8	0.489	3.523	24.4
2442.1	0.542	4.174	29.0
2982.6	0.601	4.898	34.0
3402.1	0.642	5.401	37.5

a) Second order aminolysis rate constant equals $4.59 \pm 0.03 \times 10^{-3}$

b) PNPH = p-nitrophenyl hexanoate (VI)

c) $E_{ArOH} = 9.547 \times 10^3\ M^{-1}$; $E_{ester} = 1.4011 \times 10^3\ M^{-1}$

d) D-W = 95.3 mole% dioxane-water

e) Kinetic analysis performed on a Perkin-Elmer Model 202 UV-Visible spectrophotometer

TABLE 28

Run[a] K126 Solvent[d] D-W Ester[b] PNPH Amine Benzylamine

Ester conc 7.7208×10^{-5} M Amine conc 4.8063×10^{-2} M

Time (sec)	Absorbance[c,e]	conc of Phenol (10^5)	% Reaction
60.0	0.1156	0.0889	1.2
152.0	0.1300	0.2434	3.2
252.0	0.1452	0.4063	5.3
364.0	0.1604	0.5693	7.4
468.0	0.1750	0.7258	9.4
580.0	0.1902	0.8889	11.5
720.0	0.2086	1.086	14.1
860.0	0.2255	1.268	16.4
988.0	0.2403	1.426	18.5
1116.0	0.2555	1.589	20.6
1244.0	0.2705	1.750	22.7
1380.0	0.2863	1.919	24.9
1520.0	0.3005	2.072	26.8
1660.0	0.3151	2.228	28.9
1812.0	0.3305	2.393	31.0

a) Second order aminolysis rate constant equals $4.25 \pm 0.02 \times 10^{-3}$

b) PNPH = p-nitrophenyl hexanoate (VI)

c) $E_{ArOH} = 1.0714 \times 10^4\ M^{-1}$; $E_{ester} = 1.3903 \times 10^3\ M^{-1}$

d) D-W = 95.3 mole% dioxane-water

e) Kinetic analysis performed on a Cary 17 UV-Visible spectrophotometer absorbance range 0.5

TABLE 29

Run[a]	Solvent[d]	Ester[b]	Amine
K127	D-W	PNPH	Benzylamine

Ester conc: 7.7208×10^{-5} M

Amine conc: 9.6127×10^{-3} M

Time (sec)	Absorbance[c,e]	conc of Phenol (10^6)	% Reaction
90.0	0.1137	0.6856	0.9
202.0	0.1182	1.168	1.5
338.0	0.1223	1.608	2.1
470.0	0.1262	2.023	2.6
638.0	0.1303	2.463	3.2
798.0	0.1341	2.869	3.7
926.0	0.1382	3.310	4.3
1078.0	0.1421	3.733	4.8
1238.0	0.1462	4.165	5.4
1456.0	0.1522	4.816	6.2
1624.0	0.1562	5.240	6.8
1776.0	0.1602	5.671	7.4
1968.0	0.1650	6.188	8.0

a) Second order aminolysis rate constant equals $3.98 \pm 0.02 \times 10^{-3}$

b) PNPH = p-nitrophenyl hexanoate (VI)

c) $E_{ArOH} = 1.07144 \times 10^4\ M^{-1}$; $E_{ester} = 1.3903 \times 10^3\ M^{-1}$

d) D-W = 95.3 mole% dioxane-water

e) Kinetic analysis performed on a Cary 17 UV-Visible spectrophotometer absorbance range 0.2

TABLE 30

Run[a]	Solvent[d]	Ester[b]	Amine
K131	D-W	PNPH	Benzylamine

Ester conc: 8.5931×10^{-5} M

Amine conc: 5.0415×10^{-2} M

Time (sec)	Absorbance[c,e]	conc of Phenol (10^5)	% Reaction
430.0	0.1932	0.7822	9.1
594.0	0.2184	1.054	12.3
766.0	0.2437	1.326	15.4
930.0	0.2680	1.588	18.5
1126.0	0.2934	1.862	21.7
1318.0	0.3183	2.130	24.8
1550.0	0.3483	2.453	28.5
1754.0	0.3727	2.716	31.6
1986.0	0.3984	2.993	34.8
2214.0	0.4234	3.263	38.0
2448.0	0.4489	3.537	41.2
2704.0	0.4738	3.805	44.3
3075.0	0.5083	4.177	48.6
3267.0	0.5239	4.345	50.6
3575.0	0.5487	4.612	53.7
3972.0	0.5783	4.931	57.4
4260.0	0.5989	5.152	60.0

a) Second order aminolysis rate constant equals $4.25 \pm 0.01 \times 10^{-3}$

b) PNPH = p-nitrophenyl hexanoate (VI)

c) $E_{ArOH} = 1.0686 \times 10^4\ M^{-1}$; $E_{ester} = 1.4030 \times 10^3\ M^{-1}$

d) D-W = 95.3 mole% dioxane-water

e) Kinetic analysis performed on a Cary 17 UV-Visible spectrophotometer absorbance range 0.5

TABLE 31

Run[a]	Solvent[d]	Ester[b]	Amine
K132	D-W	PNPH	Benzylamine

Ester conc 8.5931×10^{-5} M

Amine conc 5.0415×10^{-3} M

Time (sec)	Absorbance[c,e]	conc of Phenol (10^5)	% Reaction
5370.0	0.2032	0.8906	10.4
5690.0	0.2082	0.9442	11.0
5990.0	0.2123	0.9884	11.5
6270.0	0.2162	1.030	12.0
6570.0	0.2204	1.076	12.5
6835.0	0.2244	1.118	13.0
7115.0	0.2283	1.161	13.5
7425.0	0.2323	1.203	14.0
7725.0	0.2366	1.250	14.5
8145.0	0.2422	1.311	15.3
8445.0	0.2463	1.354	15.8

a) Second order aminolysis rate constant equals $4.00 \pm 0.01 \times 10^{-3}$

b) PNPH = p-nitrophenyl hexanoate (VI)

c) $E_{ArOH} = 1.0686 \times 10^4\ M^{-1}$; $E_{ester} = 1.4030 \times 10^3\ M^{-1}$

d) D-W = 95.3 mole% dioxane-water

e) Kinetic analysis performed on a Cary 17 UV-Visible spectrophotometer absorbance range 0.2

TABLE 32

Run[a] K164 Solvent Water Ester[b] PNPH

Ester conc 3.3539×10^{-5} M Na_2CO_3 conc 4.4495×10^{-3} M

Time (sec)	Absorbance[c,e]	conc of Phenoxide (10^5)	% Reaction
60.0	0.1449	0.7942	23.7
72.0	0.1696	0.9292	27.7
84.0	0.1936	1.061	31.6
100.0	0.2240	1.227	36.6
116.0	0.2535	1.390	41.4
132.0	0.2780	1.524	45.4
152.0	0.3084	1.690	50.4
172.0	0.3332	1.826	54.4
192.0	0.3588	1.966	58.6
216.0	0.3847	2.108	62.9
244.0	0.4121	2.258	67.3
272.0	0.4361	2.390	71.3
304.0	0.4586	2.513	74.9
348.0	0.4850	2.658	79.3
437.0	0.5250	2.877	85.8

a) Second order hydrolysis rate constant equals 5.64 $\pm$ 0.15

b) PNPH = p-nitrophenyl hexanoate (VI)

c) $E_{ArO^-} = 1.8247 \times 10^4\ M^{-1}$

d) Kinetic analysis performed on a Cary 17 UV-Visible

spectrophotometer absorbance range 0.5

TABLE 33

Run[a] K165 Solvent Water Ester[b] PNPH

Ester conc 3.3539×10^{-5} M Na_2CO_3 conc 4.4495×10^{-3} M

Time (sec)	Absorbance[c,e]	conc of Phenoxide (10^5)	% Reaction
60.0	0.1510	0.8277	24.7
72.0	0.1759	0.9638	28.7
84.0	0.2011	1.102	32.9
96.0	0.2247	1.232	36.7
110.0	0.2504	1.372	40.9
126.0	0.2760	1.513	45.1
142.0	0.3009	1.649	49.2
160.0	0.3259	1.786	53.3
178.0	0.3494	1.915	57.1
200.0	0.3746	2.053	61.2
224.0	0.3991	2.187	65.2
252.0	0.4239	2.323	69.3
284.0	0.4485	2.458	73.3
322.0	0.4734	2.594	77.4
392.0	0.5095	2.792	83.3

a) Second order hydrolysis rate constant equals 5.64 $\pm$ 0.15

b) PNPH = p-nitrophenyl hexanoate (VI)

c) $E_{ArO^-} = 1.8247 \times 10^4\ M^{-1}$

d) Kinetic analysis performed on a Cary 17 UV-Visible

spectrophotometer absorbance range 0.5

TABLE 34

Run[a] K166 Solvent Water Ester[b] PNPH

Ester conc 3.3539×10^{-5} M Na_2CO_3 conc 4.4495×10^{-2} M

Time (sec)	Absorbance[c,e]	conc of Phenoxide (10^5)	% Reaction
40.0	0.2455	1.345	40.1
46.0	0.2723	1.492	44.5
52.0	0.2997	1.642	49.0
58.0	0.3233	1.772	52.8
65.0	0.3490	1.912	57.0
72.0	0.3726	2.042	60.9
80.0	0.3965	2.173	64.8
90.0	0.4239	2.323	69.3
100.0	0.4476	2.452	73.1
113.0	0.4740	2.597	77.4
150.0	0.5288	2.898	86.4
173.0	0.5485	3.006	89.6

a) Second order hydrolysis rate constant equals 5.30 $\pm$ 0.26

b) PNPH = p-nitrophenyl hexanoate (VI)

c) $E_{ArO^-} = 1.8247 \times 10^4\ M^{-1}$

d) Kinetic analysis performed on a Cary 17 UV-Visible spectrophotometer absorbance range 0.5

TABLE 35

Run[a] K168 Solvent Water Ester[b] PNPB

Ester conc 3.8660×10^{-5} M Na_2CO_3 conc 4.4495×10^{-4} M

Time (sec)	Absorbance[c,d]	conc of Phenoxide (10^5)	% Reaction
40.0	0.2606	1.428	36.9
44.0	0.2804	1.536	39.7
48.0	0.3003	1.646	42.6
53.0	0.3216	1.762	45.6
58.0	0.3431	1.880	48.6
65.0	0.3697	2.026	52.4
72.0	0.3949	2.164	56.0
80.0	0.4203	2.304	59.6
88.0	0.4450	2.439	63.1
97.0	0.4692	2.572	66.5
108.0	0.4949	2.712	70.1
125.0	0.5302	2.905	75.1
138.0	0.5507	3.018	78.1
155.0	0.5751	3.152	81.5
176.0	0.5900	3.288	85.0

a) Second order hydrolysis rate constant equals 58.3 $\pm$ 1.5

b) PNPB = charged ester IV

c) $E_{ArO^-} = 1.8247 \times 10^4\ M^{-1}$

d) Kinetic analysis performed on a Cary 17 UV-Visible spectrophotometer absorbance range 0.5

TABLE 36

Run[a] K169 Solvent Water Ester[b] PNPB

Ester conc 3.8185×10^{-5} M

Na_2CO_3 conc 4.4495×10^{-3} M

Time (sec)	Absorbance[c,d]	conc of Phenoxide (10^5)	% Reaction
11.2	0.3036	1.664	43.6
12.4	0.3271	1.793	46.9
13.2	0.3413	1.870	49.0
14.4	0.3620	1.984	52.0
15.6	0.3813	2.090	54.7
16.8	0.3993	2.188	57.3
18.4	0.4211	2.308	60.4
19.6	0.4377	2.399	62.8
21.2	0.4568	2.504	65.6
22.8	0.4752	2.604	68.2
24.8	0.4953	2.714	71.1

a) Second order hydrolysis rate constant equals 60.9 $\pm$ 1.5

b) PNPB = charged ester IV

c) $E_{ArO^-} = 1.8247 \times 10^4\ M^{-1}$

d) Kinetic analysis performed on a Cary 17 UV-Visible spectrophotometer absorbance range 0.5

TABLE 37

Run[a] K170 Solvent Water Ester[b] PNPB

Ester conc 3.8185×10^{-5} M Na_2CO_3 conc 4.4495×10^{-3} M

Time (sec)	Absorbance[c,d]	conc of Phenoxide (10^5)	% Reaction
12.8	0.3545	1.943	50.9
13.6	0.3685	2.019	52.9
14.4	0.3823	2.095	54.9
15.2	0.3947	2.163	56.6
16.4	0.4131	2.264	59.3
17.2	0.4251	2.330	61.0
18.4	0.4418	2.421	63.4
19.6	0.4568	2.504	65.6
20.8	0.4726	2.590	67.8
22.4	0.4897	2.684	70.3
24.0	0.5067	2.777	72.7

a) Second order hydrolysis rate constant equals 63.0 $\pm$ 2.3

b) PNPB = charged ester IV

c) $E_{ArO^-} = 1.8247 \times 10^4\ M^{-1}$

d) Kinetic analysis performed on a Cary 17 UV-Visible spectrophotometer absorbance range 0.5

TABLE 38

Run[a]	Solvent[d]	Ester[b]	Amine
K122	D-W	PNPB	TBAT(V)

Ester conc: 1.9457×10^{-5} M

Amine conc: 2.0686×10^{-5} M

Time (sec)	Absorbance[c,e]	conc of Product (10^5)	% Reaction
71.0	0.07070	0.5374	27.6
81.0	0.07658	0.5999	30.8
92.0	0.08297	0.6680	34.3
102.0	0.08904	0.7327	37.7
117.0	0.09511	0.7973	41.0
131.0	0.1007	0.8568	44.0
150.0	0.1070	0.9237	47.5
168.0	0.1129	0.9864	50.7
191.0	0.1191	1.051	54.0
250.0	0.1312	1.178	60.6
280.0	0.1370	1.241	63.8
351.0	0.1438	1.313	67.5
440.0	0.1498	1.376	70.7
498.0	0.1558	1.438	73.9
568.0	0.1609	1.492	76.7

a) Observed rate over the first twenty-seven percent reaction was found to be 7.570×10^{-8} Msec^{-1} (dp/dt), in the presence of 6.77×10^{-5} M N-Benzyl-γ-Trimethylammonium Butyramide Fluoborate (XVI). Product concentration corrected for p-nitrophenol-p-nitrophenoxide equilibrium

in presence of TBAT(V).

b) PNPB = charged ester IV

c) $E_{ArOH} = 1.0517 \times 10^4\ M^{-1}$; $E_{ester} = 1.1450 \times 10^3\ M^{-1}$

d) D-W = 95.3 mole% dioxane-water

e) Kinetic analysis performed on a Cary 17 UV-Visible spectrophotometer absorbance range 0.2

TABLE 39 Initial Rates of Reaction of Charged Ester IV and TBAT(V) in 95.3 Mole % Dioxane-Water (25°C)

Run #	$C_I(10^5)$ Ester	$C_I(10^3)$ Amine	Time (sec)	conc (10^6)[a] product	Initial[b,c] rate(10^6)	# of determ.
SF1	4.9206	5.5322	0.3	3.5840	11.947	3
SF2	"	2.7662	0.4	2.5109	6.2773	2
SF3	"	1.1064	0.6	1.7979	2.9964	2
SF4	"	0.5532	2.0	3.7740	1.8870	3
SF5	5.3332	5.9957	0.3	4.1791	13.930	2
SF6	"	0.5996	2.0	4.3886	2.1943	3
SF7	5.2269	2.2877	0.3	1.7943	5.9809	2
SF8	"	3.8222	0.3	2.6361	8.7871	3
SF9	"	1.1438	0.6	2.1306	3.5511	2
SF10	"	1.9111	0.3	1.5726	5.2420	2
SF11	"	0.7644	1.5	3.0716	2.0477	2
SF12	"	0.5719	1.5	2.1316	1.4211	3
K174	1.1463	0.01154	19	2.1825	0.1149	2
K163	1.6160	0.02127	19	4.0983	0.2157	1

a) Corrected for p-nitrophenol-p-nitrophenoxide equilibrium in presence of TBAT(V).

b) Determined at 400 nm by stopped-flow technique. Experimental error in determination of initial rates is approximately 2.7 %.

c) Initial rates determined from initial slope (dp/dt) in units of $Msec^{-1}$.

TABLE 40 Initial Rates of Reaction of p-Nitrophenyl Hexanoate and TBAT(V) in 95.3 Mole % Dioxane-Water (25°C)

Run#	$C_I(10^5)$ Ester	$C_I(10^3)$ Amine	Time (sec)	Conc(10^8)[a] product	Initial rate(10^6)	# of determ.
SF13[b,c]	6.5280	7.0221	15	4.4554	29.702	2
SF14[b,d]	"	1.4044	75	4.7391	6.3188	2
K123[e,h]	7.7208	7.6602	50	20.279	40.557	1
K124[f,h]	"	"	55	21.827	39.686	1
K125[g,h]	"	1.5320	65	5.4896	8.4455	1

a) Corrected for p-nitrophenol-p-nitrophenoxide equilibrium in the presence of TBAT(V).

b) Determined at 400 nm by stopped-flow technique. Experimental error in initial rates is approx. 2.7%. Initial rates determined from initial slope (dp/dt), in units of $M sec^{-1}$.

c) Second order aminolysis rate constant equals 0.648

d) Second order aminolysis rate constant equals 0.689

e) Second order aminolysis rate constant equals 0.686

f) Second order aminolysis rate constant equals 0.671

g) Second order aminolysis rate constant equals 0.714

h) Initial rates determined on Cary 17 U.V.-Visible spectrophotometer at 400 nm.

TABLE 41 Initial Rates of Hydrolysis of Charged Ester (IV) in Aqueous Na_2CO_3 Buffer Solution (25°C)

Run#	$C_I(10^5)$ Ester	$C_I(10^2)$ Na_2CO_3	Time (sec)	Conc(10^6) product	Initial[a,b] rate(10^6)	# of determ.
SF15[c]	3.9387	9.323	0.4	3.9873	9.9682	2
SF16[d]	"	0.9323	1.0	2.7741	2.7741	2

a) Determined at 400 nm by stopped-flow technique. Experimental error in determination of initial rates is approx. 2.7%.

b) Initial rates determined from initial slope (dp/dt) in units of $Msec^{-1}$.

c) Second order hydrolysis rate constant equals 63.4

d) Second order hydrolysis rate constant equals 58.6

References to Part I

1) Fife,T.H. in "Biooganic Chemistry." Van Tamelan,E.E., ed.; Acamedic Press, New York, 1978, Vol I, pg 93-116.

2) Bender,M.L., Chem. Revs., 1960, 60, 53.

3) Koshland,D.E., J. Cell. Compt. Physiol. Suppl. 1, 1956, 47, 217.

4) Koshland,D.E., J. Theor. Biol., 1962, 2 75.

5) Lumry,R. in "The Enzymes.",Vol I. 2nd ed., Bayer,P.D., Lardy,H.,and Myrback,K.,eds., Academic Press, Inc. New York, 1959 Ch.4.

6) Bruice,T.C., "Enzyme Models and Enzyme Structure.", Symposium No.15, Biology Dept. Broohaven Natl. Laboratories,1962.

7) Bruice,T.C.;Benkovic,S.J., J. Am. Chem. Soc., 1963, 85 1.

8) Bruice,T.C.;Benkovic,S.J., "Biooganic Mechanisms." Benjamin, New York, 1966.

9) Jencks,W.P., "Catalysis in Chemistry and Enzymology." McGraw-Hill, New York, 1969.

10) Bender,M.L., "Mechanisms of Homogeneous Catalysis from Protons to Proteins." Wiley(Interscience), New York, 1971.

11) Bruice,T.C., in "The Enzymes." Boyer,P.D. ed., 3rd ed., Vol 2, Chapter 4, Academic Press, New York, 1970.

12) Kirby,A.J.;Fersht,A., Prog. Bioorg. Chem., 1971, 1, 1.

13) Fife,T.H., Adv. Phys. Org. Chem., 1975, 11, 1.

14) Bruice,T.C.;Turner,A., J. Am. Chem. Soc., 1970, 92, 3422.

15) Fife,T.H.;Hutchins,J.E.C.;Wang,M.S., J. Am. Chem. Soc., 1975, 97, 5878.

16) Fife,T.H.;Przystas,T.J., J. Am. Chem. Soc., 1979, 101, 1202.

17) Breslow,R.;McClure,D.E., J. Am. Chem. Soc., 1976, 98, 258.

18) Scott,A.I.;Wiesner,C.J.;Yoo,S.;Chung,S., J. Am. Chem. Soc., 1975, 97, 6277.

19) Letsinger,R.L.;Savereide,T.J., J. Am. Chem. Soc., 1962, 84, 314;3122.

20) Overberger,C.G.;Salamone,J.C., Acc. Chem. Res., 1969, 2, 217.

21) Overberger,C.G.;Smith,W.S., Macromolec., 1975, 8, 401.

22) Kitano,H.;Tanaka,M.;Okubo,T., J. Chem. Soc. Perkin 2, 1976, 1074.

23) Letsinger,R.L.;Klaus,I., J. Am. Chem. Soc., 1964, 86, 3884.

24) Meyers,W.E.;Royer,G.P., J.Am. Chem. Soc., 1977, 99, 6141.

25) Klotz,I.M.;Royer,G.P.;Scarpa,I.S., Proc. Natl. Acad. Sci. USA, 1971, 68, 263.

26) Moravetz,H.;Overberger,C.G.;Salamone,T.C.; Yaroslavsky,S., J. Am. Chem. Soc., 1968, 90, 651.

27) Kunitake,T.;Okahata,Y., J. Am. Chem. Soc., 1976, 98, 7793.

28) Overberger,C.G.;Sitaramaiah,R.;St. Pierre,T.; Yaroslavsky,S., J.Am. Chem. Soc., 1965, 87, 3270

29) Aso,C.;Kunitake,T.;Shimada,F., J. Pol. Sci. B, 1968, 6, 467.

30) Overberger,C.G.;Yuen,P.S., J. Am. Chem. Soc., 1970, 92, 1667.

31) Overberger,C.G.;St.Pierre,T.;Vorchheimer,N.;Lee,J.; Yaroslavsky,S., J. Am. Chem. Soc., 1965, 87, 296.

32) Pecht,I.;Levitzki,A.;Anbar,M., J. Am. Chem. Soc., 1967, 89, 1587.

33) Overberger,C.G.;Salamone,J.C.;Yaroslavsky,S., J. Am. Chem. Soc., 1967, 89, 6231.

34) Overberger,C.G.;St. Pierre,T.;Yaroslavsky,S., J. Am. Chem. Soc., 1965, 87, 4310.

35) Ise,N.;Okubo,T.;Kitano,H.;Kunugi,S., J. Am. Chem. Soc., 1975, 97, 2882 and references found therein.

36) Bender,M.L. in "Biooganic Chemistry." Van Tamelen,E.E.,ed.; Academic Press, New York, 1978, Vol I, pg 19-57.

37) Verheij,H.M.;Volwerk,J.J.;Jansen,E.H.J.;Puyk,W.C.; Dijkstra, B.S.;Drennth,J.;deHass,G.J., Biochemistry, 1980, 19, 743.

38) Koshland,D.E.;Neet,K.E., Annu. Rev. Biochem., 1968, 37, 359.

39) Menger,F.M.;Smith,J.H., J. Am. Chem. Soc., 1972, 94, 3824 and references quoted therein.

40) Menger,F.M.;Vitale,A.C., J. Am. Chem. Soc., 1973, 95, 4931.

41) Su,C.W.;Watson,J.W., J. Am. Chem. Soc., 1974, 96, 1854.

42) Singh,T.D.;Taft,R.W., J. Am. Chem. Soc., 1975, 97, 3867.

43) Pocker,Y.;Ellsworth,D.L., J. Am. Chem. Soc., 1977, 99, 2284.

44) Satchell,D.P.N.;Secemski,I.I., J. Chem. Soc.(R), 1969, 130; 1970, 1013.

45) Wallenberg,G.;Boger,J.;Haake,P., J. Am. Chem. Soc., 1971, 93, 4938.

46) Rivetti,F.;Tonellato,U., J. Chem. Soc. Perkin 2, 1977, 1176.

47) Menger,F.M., J. Am. Chem. Soc., 1966, 88, 3081.

48) Fuoss,R.M.;Kraus,C.A., J. Am. Chem. Soc., 1933, 55, 21.

49) Robinson,R.A.;Kiang,A.K., Trans. Faraday Soc., 1956, 52, 327.

50) King,E.J., J. Am. Chem. Soc., 1953, 75, 2204.

51) Hansen,B., Acta. Chem. Scand., 1962, 16, 1927.

52) Lazarus,R.A.;Benkovic,S.J., J. Am. Chem. Soc., 1979, 101, 4300.

53) Fuchs,R.;Caputo,J.A., J. Org. Chem., 1966, 31, 1524.

54) Bruice,P.Y.;Mautner,H., J. Am. Chem. Soc., 1972, 95, 1582.

55) Hajdu,J.;Smith,G.M., J. Am. Chem. Soc., 1981, 103, 6192.

56) Powell,A.L.;Martell,A.E., J. Am. Chem. Soc., 1957, 79, 2118.

57) Mead,D.J.;Ramsey,J.B.;Rothrock,D.A.;Kraus,C.A., J. Am. Chem. Soc., 1947, 69, 528.

58) Mead,D.J.;Fuoss,R.M.;Kraus,C.A., Trans. Faraday Soc., 1936, 32, 594.

59) Tucker,L.M.;Kraus,C.A., J. Am. Chem. Soc., 1947, 69, 454.

60) Curry,H.L.;Gilkerson,W.R., J. Am. Chem. Soc., 1957, 79, 4021.

61) McDowell,M.J.;Kraus,C.A., J. Am. Chem. Soc., 1951, 73, 3293.

62) Reynolds,M.B.;Kraus,C.A., J. Am. Chem. Soc., 1948, 70, 1709.

63) Taylor,E.G.;Kraus,C.A., J. Am. Chem. Soc., 1947, 69, 1731.

64) French,C.M.;Tomlinson,R.C.B., J. Chem. Soc., 1961, 311.

65) White,A.;Handler,P.;Smith,E., "Principles of Biochemistry.", Mcgraw-Hill, New York, 1968, pgs. 866-870.

66) Froede,H.C.;Wilson,I.B., "The Enzymes.", 3rd. ed., Academic Press, New York, 1971, pgs. 87-114.

67) Wilson,I.B.;Bergmann,F., J. Biol. Chem., 1950, 185, 479; 186, 683.

68) Wilson,I.B.;Quan,C., Arch. Biochim. Biophys., 1958, 73, 131.

69) Bender,M.L., J. Am. Chem. Soc., 1953, 75, 5986.

70) Rogers,G.A.;Bruice,T.C., J. Am. Chem. Soc., 1973, 95, 4452.

71) Gravitz,N.;Jencks,W.P., J. Am. Chem. Soc., 1974, 96, 489, 499, 507.

72) Bamford,C.H.;Tipper,C.F.H., Eds., "Ester Formation and Hydrolysis (Comprehensive Chemical Kinetics, Vol. 10).", American Elsevier, New York, 1972 Chapters 2 and 3.

73) Fox,J.P.;Page,M.I.;Satterthwaith,A.;Jencks,W.P., J. Am. Chem. Soc., 1972, 94, 4729.

74) Jencks,W.P., J. Am. Chem. Soc., 1972, 94, 4731.

75) Fox,J.P.;Jencks,W.P., J. Am. Chem. Soc., 1974, 96, 1436.

76) Satterthwaith,A.;Jencks,W.P., J. Am. Chem. Soc., 1974, 96, 7018.

77) Su,C.;Watson,J.H., J. Am. Chem. Soc., 1974, 96, 1854.

78) Singh,T.D.;Taft,R.W., J. Am. Chem. Soc., 1975, 97, 3867.

79) Hess,K.;Frahm,H., Ber., 1938, 71B, 2632.

80) Grimm,F.V.;Patrick,W.A., J. Am. Chem. Soc., 1923, 45, 2799.

81) McVicker,W.H.;Marsh,J.K.;Stewart,A.W., J. Chem. Soc., 1926, 18.

82) Vogel,A.I., J. Chem. Soc.(London), 1948, 1825, 1830.

83) Carrick,L.L., J. Phys. Chem., 1921, 25, 633.

84) Reynolds,M.B.;Kraus,C.A., J. Am. Chem. Soc., 1948, 70, 1709.

85) Yathiraja,A.R.;Sudborough,J.J., J. Indian Inst. Sci., 1925, 8A, 55.

86) Sah,P.;Anderson,H., J. Am. Chem. Soc., 1941, 63, 3164.

87) McKinley,C.;Copes,J.P., J. Am. Chem. Soc., 1950, 72, 5331.

88) Conant,J.B.;Kirner,W.R., J. Am. Chem. Soc., 1924, 46, 244.

89) Kutscher,F.;Ackerman,D., Z. Physiol. Chem., 1933, 221.

90) Simon,I., Bl. Soc. Chim. Belg., 1929, 38, 51.

91) Blyth,C.A.;Knowles,J.P., J. Am. Chem. Soc., 1971, 93, 3020.

92) Engeland,R., Ber., 1921, 54, 2208.

93) Simon,I., Bl. Soc. Chim. Belg., 1929, 38, 56.

94) Bruice,T.C.;Benkovic,J., J. Am. Chem. Soc., 1963, 85, 1.

95) Albert,A.;Serjeant,E.P., in "Ioniz. Const. of Acids and Bases.", John Wiley Inc., New York, 1962.

References to Part II

1) Davis, M.M., National Bureau of Standards Monograph 105, U.S. Government Printing Office, Washington, D.C. (1968).

2) King, E.J. "Acid-Base Behavior.",Macmillan, New York (1965).

3) Pearson, R.G.; Vogelsong, D.C., J.Am.Chem.Soc., 1958, 80, 1038.

4) Davis, M.M., J.Am.Chem.Soc., 1962, 84, 3623.

5) Rivetti, F.; Tonellato, U., J.Chem.Soc.Perkin II, 1977, 1176.

6) Steigman, J.; Lorenz,P.M., J.Am.Chem.Soc., 1966, 88, 2083 and references therein.

7) Philbrick, F.A., J.Am.Chem.Soc., 1934, 56, 2581.

8) Lassettre, E.N.; Dickinson, R.G., J.Am.Chem.Soc., 1939, 61, 54.

9) Ito, M., J.Mol.Spetry., 1960, 4, 125.

10) Dearden, J.C., Can.J.Chem., 1963, 41, 2683.

11) Davison, J.A., J.Am.Chem.Soc., 1945, 67, 228.

12) Jaffe, H.H., J.Am.Chem.Soc., 1957, 79, 2373.

13) Cardinaud, R., Bull.Soc.Chim.France, 1960, 634.

14) Fuoss,R.M.;Kraus,C.A., J. Am. Chem. Soc., 1933, 55, 3614.

15) McIntosh,R.L.;Mead,D.J.;Fuoss,R.M., J. Am. Chem. Soc., 1940, 62, 506.

16) Mead,D.J.;Kraus,C.A.;Fuoss,R.M., J. Am. Chem. Soc., 1939, 61, 3257.

17) Taylor,E.G.;Kraus,C.A., J. Am. Chem. Soc., 1947, 69, 1731.

18) Hess,K.;Frahm,H., Ber., 1938, 71B, 2632.

19) McVicker,W.H.;Marsh,J.K.;Stewart,A.W., J. Chem. Soc., 1926, 18.

20) Vogel,A.I., J. Chem. Soc.(London), 1948, 1825, 1830.

21) Carrick,L.L., J. Phys. Chem., 1921, 25, 633.

22) Reynolds,M.B.;Kraus,C.A., J. Am. Chem. Soc., 1948, 70, 1709.